

c 165

yr 2

PL ISSN 0028-3894

ASSOCIATION OF POLISH
NEUROPATHOLOGISTS
and
MEDICAL RESEARCH CENTRE
POLISH ACADEMY OF SCIENCES

NEUROPATHOLOGIA POLSKA

358, Dworakowa - polska

VOLUME 31

1993

NUMBER 1-2

WROCLAW · WARSZAWA · KRAKÓW
ZAKŁAD NARODOWY IM. OSSOLIŃSKICH
WYDAWNICTWO POLSKIEJ AKADEMII NAUK

<http://rcin.org.pl>

NEUROPATHOLOGIA POLSKA

QUARTERLY

Volume 31

1993

Number 1–2

EDITORIAL COUNCIL

Maria Dąbbska, Jerzy Dymecki, Krystyna Honczarenko, Danuta Maślińska,
Mirosław J. Mossakowski, Halina Weinrauder

EDITORS

Editor-in-Chief: Maria Dąbbska

Co-editors: Wiesława Biczyskova, Halina Kroh, Mirosław J. Mossakowski,
Mieczysław Wender, Irmina B. Zelman

Secretary: Anna Taraszewska

Technical secretary: Teresa Miodowska

EDITORIAL OFFICE

Medical Research Centre

ul. Dworkowa 3, 00-784 Warszawa, Poland

Phone: 49-54-10

The typescript of the present issue was delivered to the publisher 05.08.1993 r.



PAWEŁ P. LIBERSKI^{1, 2}, RICHARD YANAGIHARA¹,
GERALD A. H. WELLS³, D. CARLETON GAJDUSEK²

BOVINE SPONGIFORM ENCEPHALOPATHY IN CATTLE MIMICS ULTRASTRUCTURALLY EXPERIMENTAL SCRAPIE AND CREUTZFELDT-JAKOB DISEASE IN RODENTS

¹ Laboratory of Central Nervous System Studies, National Institute of Neurological Disorders and Stroke, National Institutes of Health Bethesda, Maryland, U.S.A.; ² Electron Microscopic Laboratory, Department of Oncology, School of Medicine, Łódź, Poland; ³ Central Veterinary Laboratory, Ministry of Agriculture, Fisheries and Food, New Haw, Addlestone, Surrey, U.K.

We report a comparison of the ultrastructural pathology of bovine spongiform encephalopathy, experimental scrapie in hamsters and a panencephalopathic model of Creutzfeldt-Jakob disease (CJD) in mice. Vacuoles in dendrites, intramyelinic vacuoles (myelin ballooning), dystrophic axons, phagocytic astrocytes and macrophages, differing in extent, were found in all three models.

We conclude, that this axonal and myelin pathology is a phenomenon common to the three models of SSVE studied, and the differences between panencephalopathic CJD and prionencephalopathic BSE and scrapie are only quantitative.

Key words: *Bovine spongiform encephalopathy, Creutzfeldt-Jakob disease, prion diseases, scrapie, slow viruses.*

Bovine spongiform encephalopathy (BSE), a novel transmissible disease recently discovered among domestic cattle in England (Wells et al. 1987), resembles clinically, neuropathologically and molecularly (Hope et al. 1988, 1989; Scott et al. 1990), and by the results of transmission studies (Fraser et al. 1988; Barlow, Middleton 1990; Dawson et al. 1990) other slow unconventional virus disorders of animals and man (for review see: Kimberlin 1992; Liberski 1992). Only limited reports on the ultrastructure of BSE have been published to date (Liberski 1990; Liberski et al. 1992a, b). We report here further ultrastructural similarities between naturally occurring BSE, and experimentally induced scrapie and Creutzfeldt-Jakob disease (CJD).

MATERIAL AND METHODS

The source of bovine material was a 6-year-old Fresian/Holstein cow from the U.K. affected with bovine spongiform encephalopathy (Liberski 1990; Liberski et al. 1992a, b). The animal had developed clinical signs of BSE consisting

of changes in behaviour, hyperreflexia to touch and sound, excessive ear movement and teeth grinding. The disease progressed rapidly with weight loss and wasting, and the animal was killed three weeks after the onset of disease. A total of twenty samples of the solitary tract nucleus and the spinal tract nucleus of the trigeminal nerve from the medulla at the obex level, central gray matter of the mesencephalon and frontal cortex of the gyrus marginalis were obtained within maximally 10 min of postmortem. Corresponding samples were taken from a normal cow and served as control material.

Two other models were explored: NIH Swiss mice inoculated with the Fujisaki strain of CJD virus (Tateishi et al. 1978; Kingsbury et al. 1982; Liberski et al. 1990a, b) and Syrian hamsters inoculated with the 263K strain of scrapie virus (Kimberlin, Walker 1977, 1978; Liberski et al. 1989b).

Electron microscopy

Mice and hamsters were killed by intracardiac perfusion as previously reported (Liberski et al. 1989b, 1990a, b). This report is confined only to animals with advanced disease. Samples taken from the BSE-affected and control cows were immersion fixed (perfusion fixation in such large animals was considered to be impracticable) for approximately 3 h in 3% glutaraldehyde freshly prepared in phosphate buffer, then transferred to the same buffer before transshipment to the National Institutes of Health. Samples were postfixed in 1% osmium tetroxide, dehydrated through graded ethanols and propylene oxide and embedded in Epon 812 or Embed. Semithin sections were stained with methyl blue. Ultrathin sections stained with lead citrate and uranyl acetate, were examined with Hitachi 11A, Philips 300 and Zeiss (Opton) EM109 transmission electron microscopes.

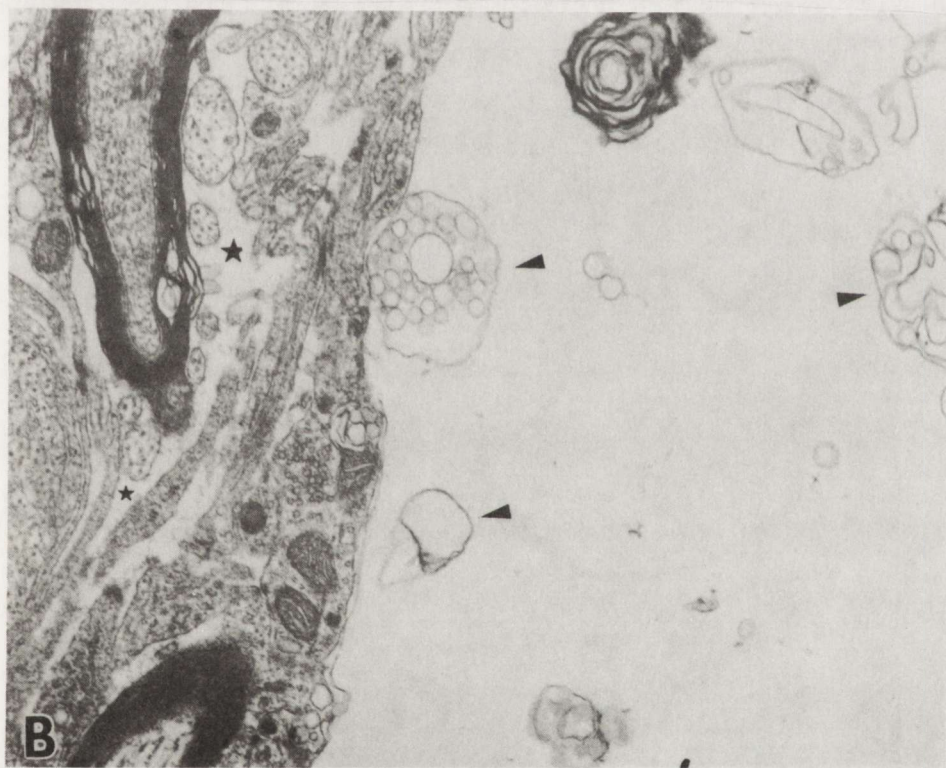
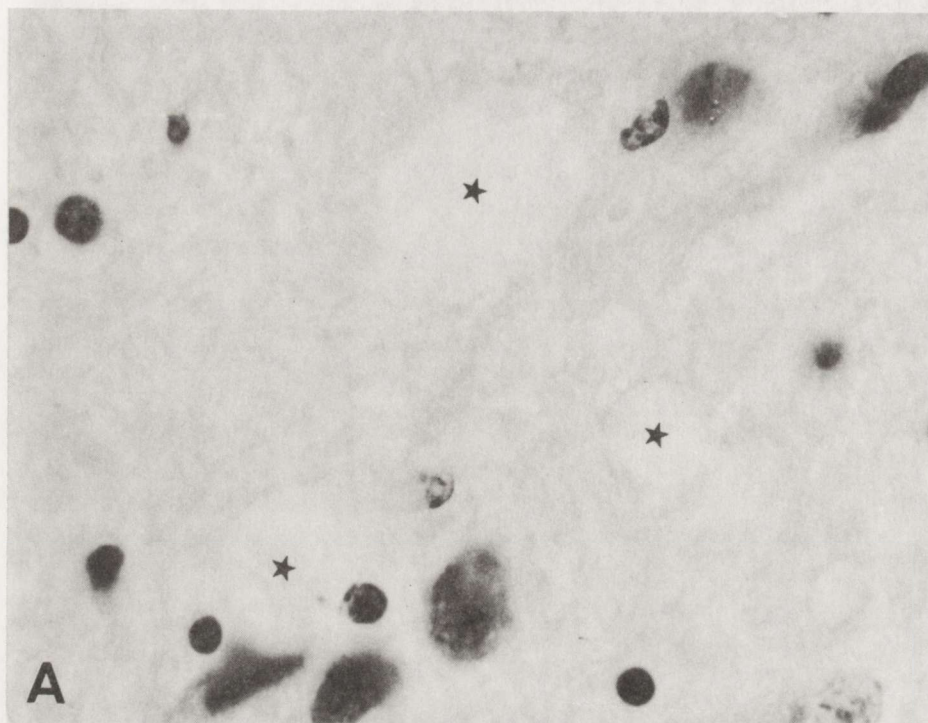
RESULTS

The ultrastructural neuropathology of hamsters infected with the 263K strain of scrapie virus, the BSE-affected cow and mice infected with the Fujisaki strain of CJD was basically similar and consisted of spongiform changes, astrocytic hypertrophy and hyperplasia, neuronal dystrophy and neuronal degeneration as described previously (Liberski et al. 1989b, 1990a, b, 1992a, b). In the BSE affected cow, numerous membrane-bound intracellular vacuoles (Fig. 1) were observed, predominantly in dendrites, but also in myelinated axons (*vide infra*). Some vacuoles, particularly in brain stem (Fig. 1B), were extremely large and involved several neuronal processes.

In hamsters infected with the 263K strain of scrapie, several myelinated fibers, particularly those traversing thalamic nuclei, showed vacuoles which greatly distended the myelin sheath (Fig. 2A). Axons were of apparently normal size

Fig. 1A. Spongiform changes in brain of a BSE-affected cow. Light macroscopic appearance of typical spongiform vacuoles (asterisks). HE. $\times 400$

Fig. 1B. Margin of a large vacuole in brain stem of BSE-affected cow. Note numerous curled membranes (arrowheads). The tissue surrounding vacuole seem to be edematous (asterisk). $\times 12000$



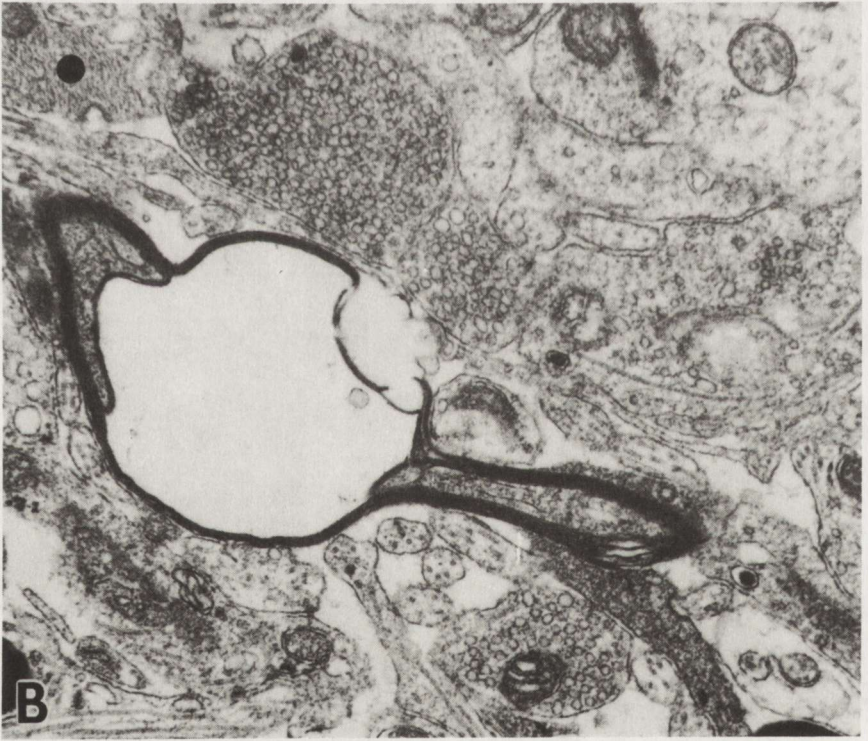
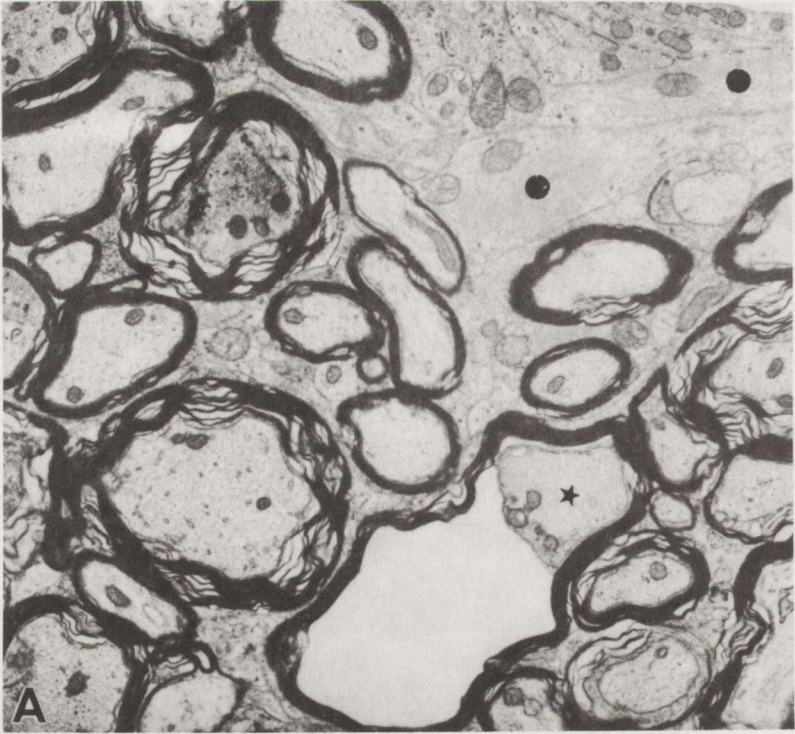




Fig. 3A. Astrocytic process filled with glial filaments in BSE-affected cattle brain. Circle indicates neuronal process containing mitochondria. $\times 12\ 000$

and contained a normal component of microtubules, neurofilaments and mitochondria. Some axons were shrunken and adherent to the innermost layer of the myelin. The attenuated myelin sheath bordering each vacuole was clearly continuous with that lining the associated axon and was of normal periodicity. In NIH Swiss mice infected with the Fujisaki strain of CJD virus which served as our „standard” for the panencephalopathic type of SSVE, intramyelin ballooning was a prominent finding in every area where myelinated fibers could be found. In the BSE-affected cow such myelin ballooning (Fig. 2B) was found only occasionally but was nevertheless unambiguous. Thus, while in the CJD-affected mice intramyelinic vacuoles formed the hallmark of the pathological process, in scrapie-affected hamsters and in the BSE-affected cow they were infrequent findings.

Formation of intramyelinic vacuoles and the widespread axonal damage were accompanied by a cellular reaction which consisted of a hyperplasia of astrocytes

Fig. 2A. Intramyelin vacuole in subcortical gray matter of scrapie-affected hamster brain. Note a shrunken axon (asterisk) adherent to the innermost layer of myelin and numerous astrocytic processes (circles). $\times 12\ 000$

Fig. 2B. Intramyelin vacuole in central gray matter of BSE-affected cattle brain. Circle indicates an astrocytic process. $\times 12\ 000$

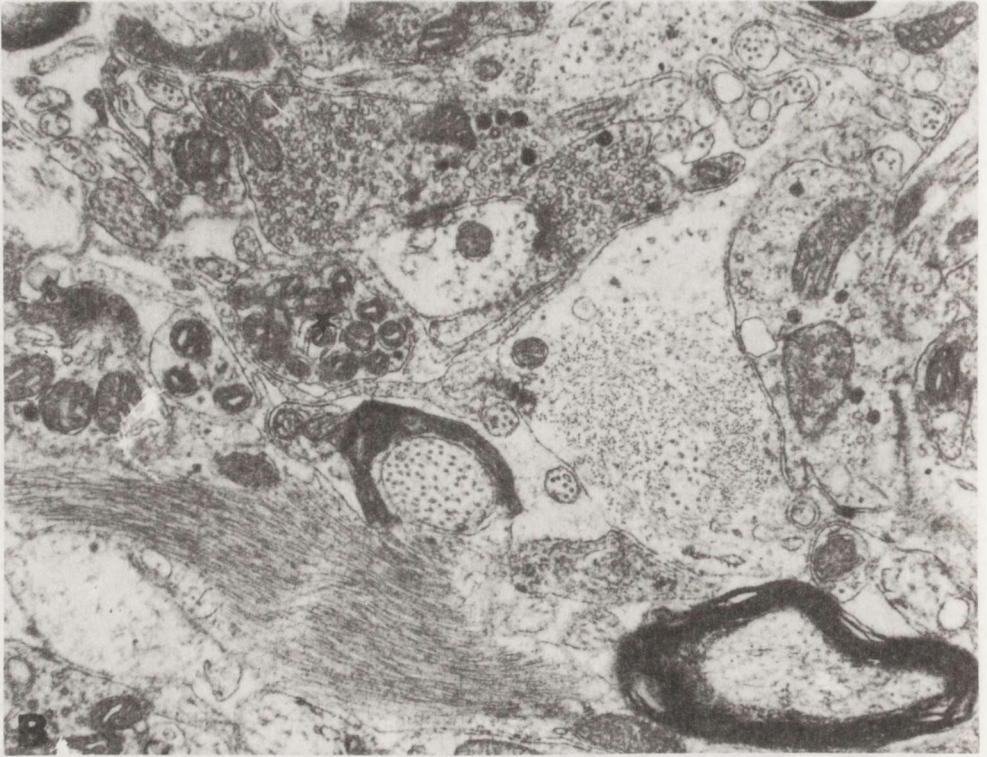


Fig. 3B. Astrocytic processes in BSE-affected cattle brain. Note neuronal process filled with mitochondria (asterisk). $\times 12\,000$

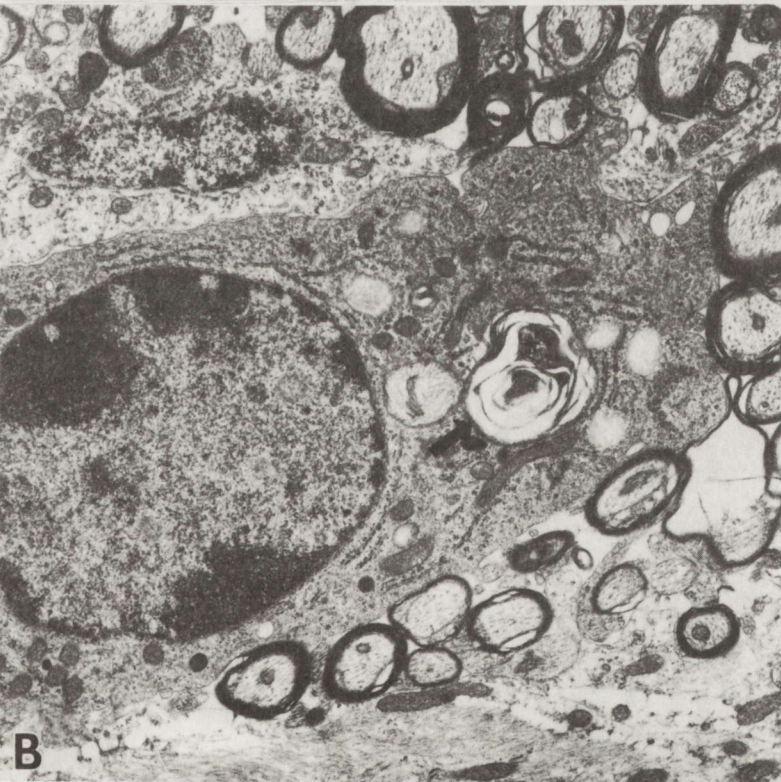
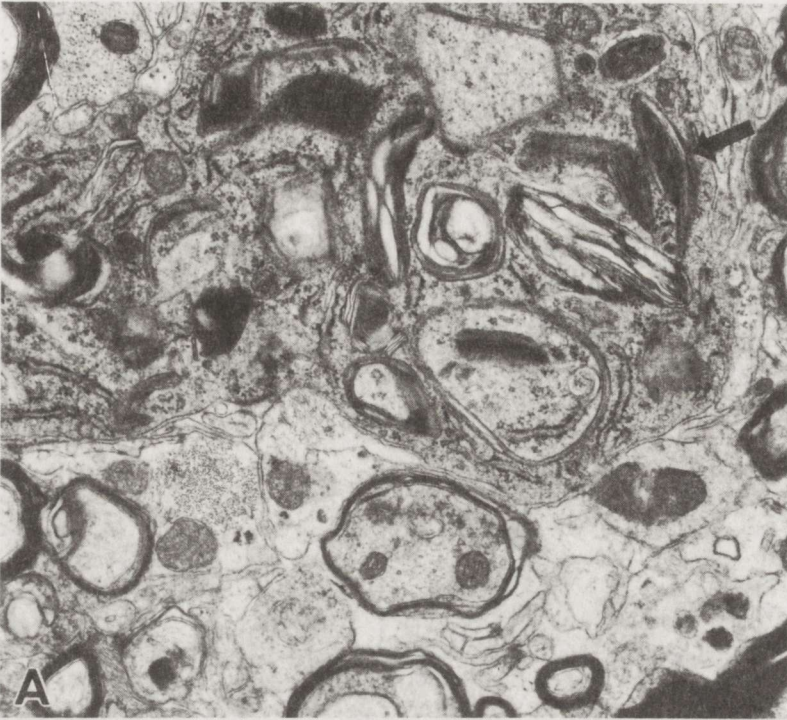
(Fig. 3) and macrophages (*vide infra*). Hypertrophic astrocytes, containing innumerable glial fibrils were numerous in all three models. In the areas most affected, adjacent astrocytic processes virtually replaced all other tissue elements.

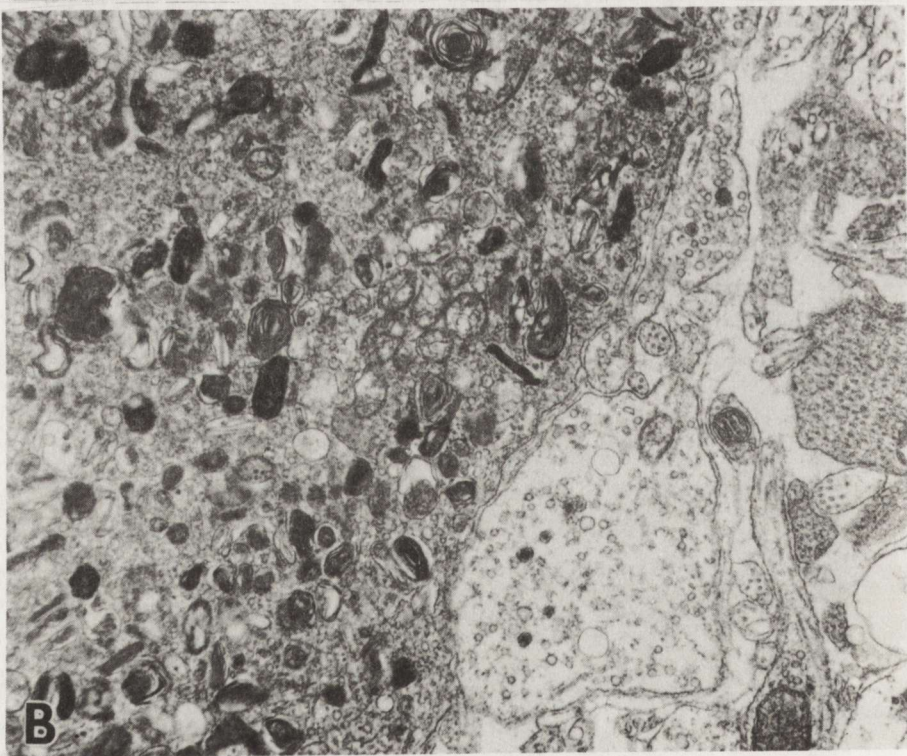
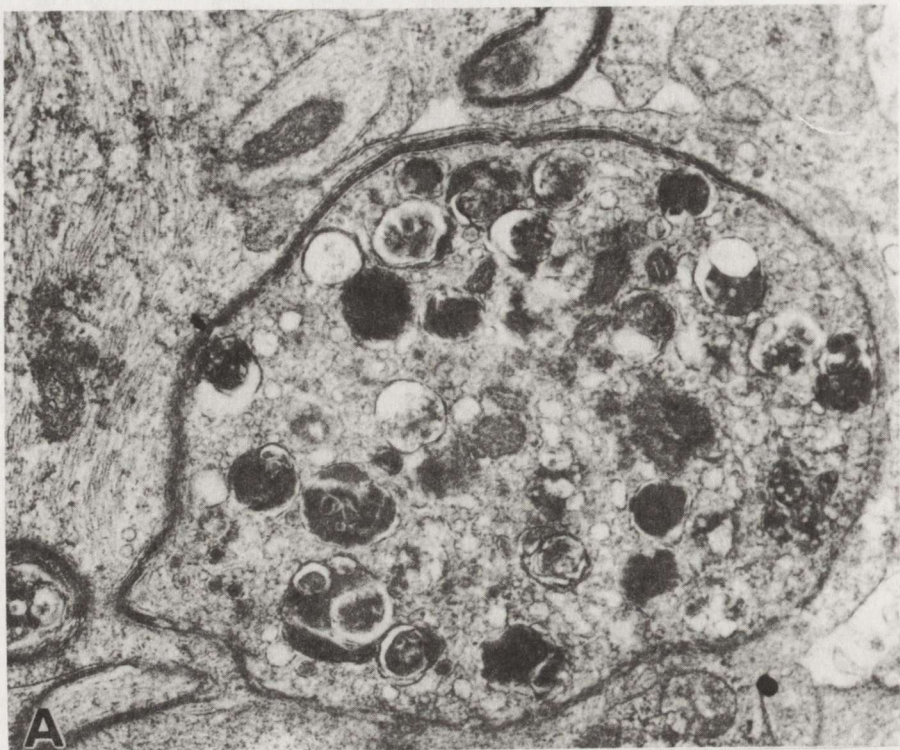
Macrophages, identified by darker cytoplasm, the absence of any intermediate filaments within the cytoplasm and numerous phagocytosed myelin fragments and, in CJD-affected mice electron-dense and lyre-like paracrystalline inclusions (Fig. 4A) (not encountered in scrapie-affected hamsters), were found in all of the models reported here. Macrophage prevalence correlated well with the degree of overall change in myelinated fibers. Thus, macrophages were abundant in CJD-affected mice, frequent in myelin-rich areas of scrapie infected hamsters and extremely rare in the BSE-affected cow (Fig. 4B).

Numerous myelinated axons undergoing degeneration in the form of neuroaxonal dystrophy (Fig. 5A-C) were found in all three models in this study. In

Fig. 4A. Fragment of cytoplasm of macrophage in corpus callosum of CJD virus-infected mouse brain. Note lyre-like inclusion (arrow) within macrophage. $\times 12\,000$

Fig. 4B. Macrophage in brain stem of BSE-affected cow. Note myelin debris within macrophage cytoplasm (arrow). $\times 12\,000$





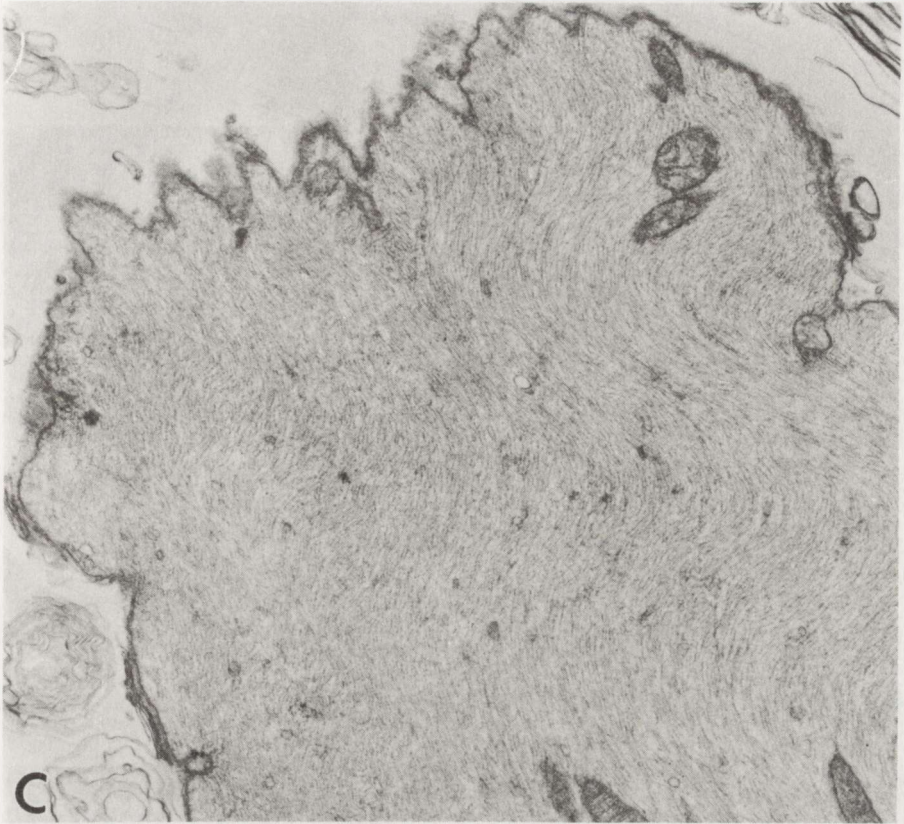


Fig. 5C. Axon filled with masses of neurofilaments in brain stem of BSE-affected cow. $\times 12\,000$

BSE (Fig. 5B) dystrophic neurites were generally much larger than those of scrapie-infected hamsters and CJD-affected mice (Fig. 5A). Surprisingly, the number of dystrophic axons did not seem to correlate with the extent of myelin damage in any of the models reported here. Both dendrites and axons accumulated masses of interwoven neurofilaments (Fig. 5C) with altered subcellular organelles entrapped within these accumulations. Other neurites showed accumulations of mitochondria and a plethora of electron-dense inclusions, and thus met the criteria of „reactive axonal swellings” (Liberki et al. 1989). Occasionally neurites contained a network of branching tubules and electron-lucent cisternae with entrapped mitochondria, vesicles and Golgi apparatus (Fig. 6). These accumulations of organelles most closely resembled those found predominantly in human neuroaxonal dystrophies (Jellinger 1973; Liberki et al. 1989a).

Fig. 5A. Typical dystrophic neurite containing mitochondria and electron-dense bodies in corpus callosum of CJD virus-infected mouse. $\times 12\,000$

Fig. 5B. Dystrophic neurite in BSE-affected cow. $\times 12\,000$

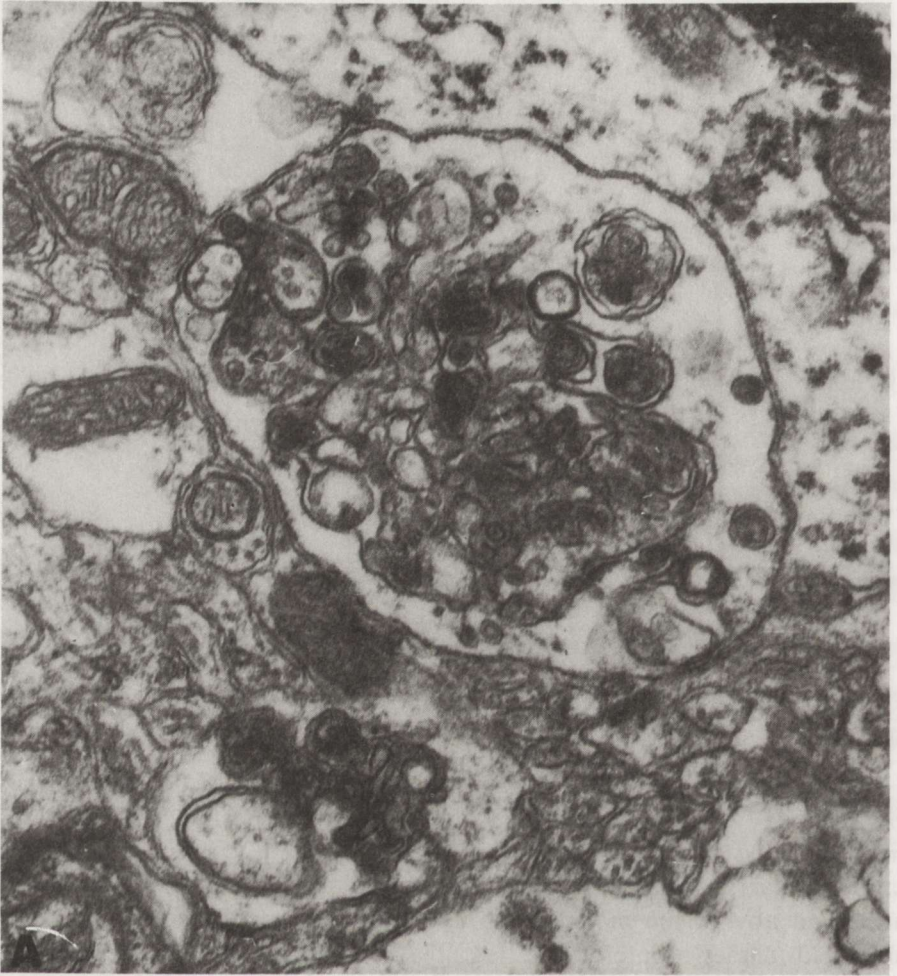


Fig. 6A. Neurite containing cisternae and vesicles in subcortical gray matter of scrapie-affected hamster. $\times 12\,000$

Several neuronal perikarya had accumulations of lipofuscin granules and numerous lamellated electron-dense lysosomal inclusions. Lysosomes were, however, also observed in control material. An unusual form of intraneuronal inclusions was composed of dense meshes of 10-nm tubules and circular profiles



Fig. 6B. Neurite containing cisternae and branching tubules in brain stem of BSE-affected cow. $\times 12\,000$

within a structureless matrix surrounded by a common membrane (Fig. 7). Neuritic degenerations and vacuolation were accompanied by a reaction composed of numerous hypertrophic astrocytes.

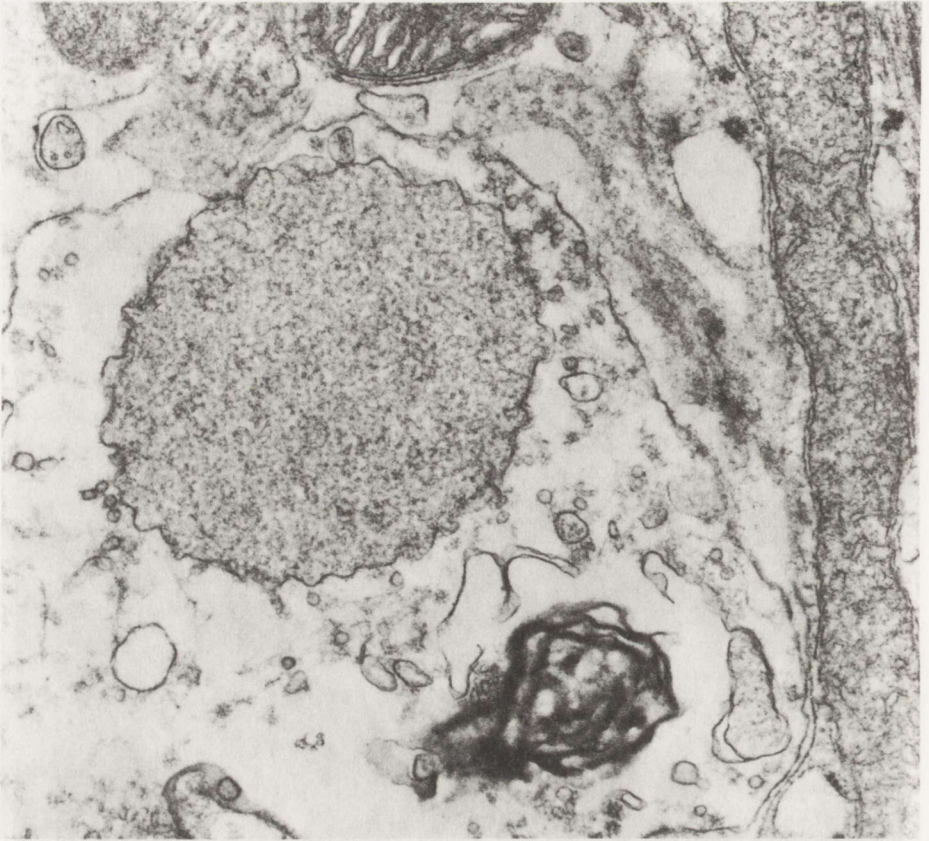


Fig. 7. Intraaxonal inclusion body in brain stem of BSE-affected cow. $\times 27\,000$

DISCUSSION

Spongiform change is regarded as the most disease-specific and even pathognomonic finding in subacute spongiform virus encephalopathies (SSVE) (Bignami, Parry 1972; Masters, Gajdusek 1982; Liberski 1992). However, in some cases of natural scrapie in sheep (Fraser 1976; Beck, Daniel 1988) and in a few cases of CJD (DeReuck et al. 1975; Kim et al. 1988) spongiform change is limited or conspicuously absent. Also, in transmissible mink encephalopathy passaged in mink of Chediak-Higashi genotype, spongiform change is minimal if any (Marsh et al. 1976). Furthermore, mutations within gene encoding PrP were found in human cases with dementia, but without any obvious pathology (Collinge et al. 1990). The latter phenomenon suggests the absence of correlation between the alteration of the PrP gene and pathology. Although spongiform change was easily detectable in the BSE-affected cow, the intensity of spongiosis was less than found in mice infected with the Fujisaki strain of CJD virus and was more comparable to that found in hamsters infected with the 263K strain of scrapie virus.

SSVE have been regarded by most investigators as polioencephalopathies – neurodegenerative disorders of the gray matter (Masters, Gajdusek 1982) despite the fact that infrequent axonal and myelin changes were reported twenty years ago in experimental kuru (Beck et al. 1973) and CJD (Beck et al. 1969) and thirty years ago in experimental scrapie in goats (Hadlow 1961). However, these changes were regarded as secondary phenomenon and indicative of Wallerian type of degeneration which has been reported in natural scrapie (Palmer 1968). Recently, several reports on CJD cases with severe involvement of white matter, particularly from Japan, have refocused the attention of neuropathologists to white matter changes and led to the nosological separation of the panencephalopathic type of CJD (Park et al. 1980; Mizutani et al. 1981; Kitagawa et al. 1983; Yamamoto et al. 1985). Furthermore, some scrapie isolates are characterized in mice by the same feature (Fraser 1979) and, analogously, panencephalopathic models of scrapie are, therefore, recognized.

The 263K strain of scrapie virus is “polioencephalopathic” in the sense that it does not produce light microscopically substantial myelin or axonal damage (Liberski et al. 1989b). In contrast, the Fujisaki strain of CJD virus, characterized by severe involvement of axons and myelin (Liberski et al. 1990a, b), clearly belongs to “the panencephalopathic” type of SSVE. The strain of scrapie virus responsible for the BSE epidemic is clearly different from those isolated from scrapie-affected sheep (Fraser et al. 1992) and the involvement of the white matter in mice infected with this strain is inconspicuous. Thus, BSE is rather a “polio-clastic” disorder.

The viruses of the SSVE are intimately associated with membranes (Gibbons, Hunter 1967). Curled membrane fragments may be the ultrastructural correlates of the pathology of the scrapie isoform of prion protein (PrP^{sc}), a membrane protein closely associated with infectivity (Bazan et al. 1987). Thus, the old hypothesis that membranes are the primary target of the virus (Lampert et al. 1971) is worth re-evaluation at the molecular level.

Branching tubules and cisternae and neuronal inclusions probably reflect the neurodegenerative nature of BSE and the limited repertoire of the central nervous system to degenerate. Various forms of tubules and cisternae, strikingly similar to those found in human neuroaxonal dystrophies, have been found in natural and experimental scrapie (Field, Narang 1972; Narang 1973; Liberski et al. 1989a). Membrane-bound inclusions composed of tubules and vesicles, measuring approximately 10 nm in diameter, vaguely resemble the type “D” inclusions found in rats experimentally infected with scrapie (Field, Narang 1972), but their nature is completely obscure.

It is clearly evident from the present study that, not unexpectedly, BSE mimics ultrastructurally all the other SSVE. Furthermore, the elements of axonal and myelin changes – intramyelinic vacuoles (myelin ballooning), intraaxonal vacuoles, neuroaxonal dystrophy and phagocytosis of myelin debris – were detectable in all three models, but differed in severity between the models. They dominated the ultrastructural pathology in mice infected with the Fujisaki strain of CJD

virus, were relatively easily detected in hamsters infected with the 263K strain of scrapie virus and were rather scanty in the BSE-affected cow. Quantitative differences of SSVE neuropathology have been elaborated in experimental scrapie at the light microscopy level and reflected by the "lesion profile" (Fraser, Dickinson 1968), a method which proved a useful tool for scrapie virus strain typefying. By the use of electron microscopy more detailed structural information is added to the light microscopic studies, suggesting that different "lesion profiles" may consist of a combination of the same basic elements interrelated in variable proportions.

Acknowledgements. Dr. P. P. Liberski was the recipient of a fellowship from the Fogarty International Center while in the USA, from the British Council while in the UK and a grant from the intramural research program of the School of Medicine Lodz. The skillful technical assistance of Mr. R. Kurczewski, Ms. E. Naganska, Ms. L. Romanska and Mr. K. Smoktunowicz is gratefully acknowledged.

ENCEFALOPATIA GĄBCZASTA U BYDŁA NAŚLADUJE W OBRAZIE ULTRASTRUKTURALNYM SCRAPIE I CHOROBY CREUTZFELDTA-JAKOBA

Streszczenie

Przedstawiono wyniki badań ultrastrukturalnych mózgów w terminalnym okresie encefalopatii gąbczastej bydła (BSE), nowo odkrytej choroby wywołanej przez tzw. niekonwencjonalne wirusy powolne, i porównano je z danymi uzyskanymi w doświadczalnej scrapie u chomików oraz chorobie Creutzfeldta-Jakoba u myszy. BSE charakteryzuje się obecnością wakuoli zarówno w dendrytach, jak i aksonach, odpowiedzią astrocytarną i makrofagową oraz dystrofią neuroaksonalną. W odróżnieniu od opisywanych modeli u gryzoni, w BSE występują charakterystyczne wtęty w zakończeniach synaptycznych. Są one oblonione i utworzone z masy przeplatających się tubul o średnicy 10 nm.

BSE wykazuje dotychczas opisane cechy ultrastrukturalne encefalopatii gąbczastych, a różnice stwierdzane między różnymi modelami są tylko ilościowe.

REFERENCES

1. Barlow RM, Middleton DJ: Dietary transmission of bovine spongiform encephalopathy to mice. *Vet Rec*, 1990, 126, 111–112.
2. Bazan JF, Fletterick RI, McKinley MP, Prusiner SB: Predicted secondary structure and membrane topology of the scrapie prion protein. *Protein Eng*, 1987, 1, 125–135.
3. Beck E, Daniel PM: Neuropathology of transmissible spongiform encephalopathy. In: *Prions. Novel Infectious Pathogens causing Scrapie and Creutzfeldt-Jakob Disease*. Eds: SB Prusiner, MP McKinley. Academic Press, New York, 1988, pp 331–385.
4. Beck E, Daniel PM, Asher DM, Gajdusek DC, Gibbs CJ, Jr: Experimental kuru in chimpanzee: a neuropathological study. *Brain*, 1973, 96, 441–462.
5. Beck E, Daniel PM, Matthews WB, Stevens DL, Alpers MP, Asher DM, Gajdusek DC, Gibbs CJ, Jr: Creutzfeldt-Jakob disease. The neuropathology of a transmission experiment. *Brain*, 1969, 92, 699–716.
6. Bignami A, Parry HB: Electron microscopic studies of the brain of sheep with natural scrapie. I. The fine structure of neuronal vacuolation. *Brain*, 1972, 95, 319–326.
7. Collinge J, Owen F, Poulter M, Leach M, Crow TJ, Rossor MN, Hardy J, Mullan MJ, Janota I, Lantos PL: Prion dementia without characteristic pathology. *Lancet*, 1990, 336, 7–9.

8. Dawson M, Wells GAH, Parker BNJ: Preliminary evidence of the experimental transmissibility of bovine spongiform encephalopathy to cattle. *Vet Rec*, 1990, 126, 112–113.
9. DeReuck J, DeCoster W, Vaan der Ecken H, Daneels P: Creutzfeldt-Jakob disease: a comparative light microscopic, histochemical and electron-microscopic study. *Europ Neurol*, 1975, 13, 154–166.
10. Dickinson AG, Fraser H: An assessment of the genetics of scrapie in sheep and mice. In: *Slow Transmissible Diseases of the Nervous System*, vol 1. Eds: SB Prusiner, WJ Hadlow. Academic Press, New York, 1979, pp 367–385.
11. Field EJ, Narang HK: An electron-microscopic study of scrapie in the rat: further observations on “inclusion bodies” and virus-like particles. *J Neurol Sci*, 1972, 17, 347–364.
12. Fraser H: The pathology of natural and experimental scrapie. In: *Slow Virus Diseases of Animals and Man*. Ed: R Kimberlin. North-Holland Publ Comp, Amsterdam, 1976, pp 267–406.
13. Fraser H: Neuropathology of scrapie: the precision of lesions and their significance. In: *Slow Transmissible Diseases of the Nervous System*, vol 1. Eds: SB Prusiner, WJ Hadlow. Academic Press, New York, 1979, pp 387–406.
14. Fraser H, Bruce M, Chree A, McConnell I, Wells GAH: Transmission of bovine spongiform encephalopathy and scrapie to mice. *J Gen Virol*, 1992, 73, 1891–1897.
15. Fraser H, McConnell I, Wells GAH, Dawson M: Transmission of bovine spongiform encephalopathy to mice. *Vet Rec*, 1988, 123, 472.
16. Gibbons RA, Hunter GD: Nature of scrapie agent. *Nature*, 1967, 210, 794–796.
17. Hadlow WJ: The pathology of experimental scrapie in the dairy goat. *Res Vet Sci*, 1961, 2, 289–314.
18. Hope J, Reekie LJ, Hunter N, Multhaup G, Beyreuther K, White K, Scott AC, Stack J, Dawson M, Wells GAH: Fibrils from brains of cows with new cattle disease contain scrapie-associated protein. *Nature*, 1988, 336, 390–392.
19. Hope J, Ritchie L, Farquar C, Hunter N: Bovine spongiform encephalopathy: a scrapie like disease of British cattle. In: *Alzheimer Disease and Related Disorders*. Eds: K Iqbal, HM Wisniewski, B Winblad. AL Liss Inc, New York, 1989, pp 659–667.
20. Jellinger K: Neuroaxonal dystrophy: its natural history and related disorders. In: *Progress in Neuropathology*, vol 2. Ed HM Zimmerman. Grune, Stratton, New York, 1973, pp 129–180.
21. Kim JH, Lach BM, Manuelidis EE: Creutzfeldt-Jakob disease with intranuclear inclusions: a biopsy case of negative light microscopic findings and successful animal transmission. *Acta Neuropathol (Berl)*, 1988, 76, 422–426.
22. Kimberlin RH: Bovine spongiform encephalopathy. *Rev Sci Tech Off Int Epiz*, 1992, 11, 347–390.
23. Kimberlin RH, Walker CA: Characteristic of short incubation model of scrapie in golden hamsters. *J Gen Virol*, 1977, 34, 295–304.
24. Kimberlin RH, Walker CA: Evidence that transmission of one source of the agent involves separation of the agent from the mixture. *J Gen Virol*, 1978, 39, 487–496.
25. Kingsbury DT, Smeltzer DA, Amyx HL, Gibbs CJ, Jr, Gajdusek DC: Evidence for an unconventional virus in mouse adapted strain of Creutzfeldt-Jakob disease. *Infect Immunity*, 1982, 37, 1050–1053.
26. Kitagawa Y, Gotoh F, Koto A, Ebihara S, Okayashu H, Ishii T, Matsuyama H: Creutzfeldt-Jakob disease: a case with extensive white matter degeneration and optic atrophy. *J Neurol Sci*, 1983, 229, 97–101.
27. Lampert PW, Hooks J, Gibbs CJ, Jr, Gajdusek DC: Altered plasma membranes in experimental scrapie. *Acta Neuropathol (Berl)*, 1971, 19, 81–93.
28. Liberski PP: *Light and Electron Microscopic Neuropathology of Slow Virus Disorders*. CRC Press, Boca Raton, 1992.
29. Liberski PP: The enigma of slow viruses: facts and artifacts. *Arch Virol*, 1993, suppl 6, pp 277.
30. Liberski PP: Ultrastructural neuropathologic features of bovine spongiform encephalopathy. *J Vet Med Ass*, 1990, 196, 1682–1683.
31. Liberski PP, Yanagihara R, Gibbs CJ, Gajdusek DC: Reevaluation of the ultrastructural pathology of experimental Creutzfeldt-Jakob disease. *Brain*, 1990a, 113, 121–137.

32. Liberski PP, Yanagihara R, Gibbs CJ, Jr, Gajdusek DC: White matter ultrastructural pathology of experimental Creutzfeldt-Jakob disease in mice. *Acta Neuropathol (Berl)*, 1990b, 79, 1–9.
33. Liberski PP, Yanagihara R, Gibbs CJ, Jr, Gajdusek DC: Scrapie as a model for neuroaxonal dystrophy. *Exp Neurol*, 1989a, 106, 133–141.
34. Liberski PP, Yanagihara R, Gibbs CJ, Jr, Gajdusek DC: Serial ultrastructural studies of scrapie in hamsters. *J Comp Pathol*, 1989b, 101, 429–442.
35. Liberski PP, Yanagihara R, Wells GAH, Gibbs CJ, Jr, Gajdusek DC: Comparative ultrastructural neuropathology of naturally occurring bovine spongiform encephalopathy and experimentally induced scrapie and Creutzfeldt-Jakob disease. *J Comp Pathol*, 1992a, 106, 361–381.
36. Liberski PP, Yanagihara R, Wells GAH, Gibbs CJ, Jr, Gajdusek DC: Ultrastructural pathology of axons and myelin in experimental scrapie in hamsters and bovine spongiform encephalopathy in cattle and a comparison with the panencephalopathic type of Creutzfeldt-Jakob disease. *J Comp Pathol*, 1992b, 106, 383–398.
37. Marsh RF, Sipe JC, Morse SS, Hanson RP: Transmissible mink encephalopathy reduced spongiform degeneration in aged mink of Chediak-Higashi genotype. *Lab Invest*, 1976, 34, 381–386.
38. Masters CL, Gajdusek DC: The spectrum of Creutzfeldt-Jakob disease and the virus-induced subacute spongiform encephalopathies. In: *Recent Advances in Neuropathology*. Eds: WT Smith, JB Cavanagh. Churchill Livingstone, Edinburgh, 1982, pp 139–163.
39. Mizutani T, Okumbra A, Oda M, Shiraki H: Panencephalopathic type of Creutzfeldt-Jakob disease: primary involvement of the cerebral white matter. *J Neurol Neurosurg Psychiatry*, 1981, 44, 103–115.
40. Narang HK: Virus-like particles in natural scrapie in sheep. *Res Vet Sci*, 1973, 14, 108–110.
41. Palmer AC: Wallerian type of degeneration in sheep scrapie. *Vet Rec*, 1968, 82, 729–731.
42. Park TS, Kleinman GM, Richardson EP: Creutzfeldt-Jakob disease with extensive degeneration of white matter. *Acta Neuropathol (Berl)*, 1980, 52, 239–242.
43. Scott AC, Wells GAH, Stack MJ, White H, Dawson M: Bovine spongiform encephalopathy: detection and quantitation of fibrils, fibril protein (PrP) and vacuolation in brain. *Vet Microbiol*, 1990, 23, 295–304.
44. Tateishi J, Ohta M, Koga M, Soto Y, Kuroiwa J: Transmission of chronic spongiform encephalopathy with kuru plaques from human to small rodents. *Ann Neurol*, 1978, 5, 581–584.
45. Wells GAH, Scott AC, Johnson CT, Gunning RF, Hancock RD, Jeffrey M, Dawson M, Bradley R: A novel progressive spongiform encephalopathy in cattle. *Vet Rec*, 1987, 121, 419–420.
46. Yamamoto T, Nagashima K, Tsubaki T, Oikawa K, Akai J: Familial Creutzfeldt-Jakob disease in Japan. Three cases in a family with white matter involvement. *J Neurol Sci*, 1985, 67, 119–130.

Correspondence address: Dr. P. P. Liberski, Department of Oncology, Electron Microscopic Laboratory, School of Medicine, Paderewskiego 4 Str., 93-509 Łódź, Poland

MIECZYŚLAW WENDER¹, JÓZEF SZCZECH¹, STANISŁAW HOFFMANN²

ANALYSIS OF HEAVY METALS CONTENT IN THE BRAIN WITH THE USE OF ELECTRON PARAMAGNETIC RESONANCE IN A CLINICALLY UNUSUAL CASE OF HEPATO-LENTICULAR DEGENERATION

¹ Department of Neurology School of Medicine, Poznań, Poland; ² Institute of Molecular Physics,
Polish Academy of Sciences, Poznań, Poland

An analysis of heavy metals content in the brain of a clinically unusual case of hepato-lenticular degeneration was performed with the use of paramagnetic resonance. The studies established a manifold increase of copper content in the brain in the form of free ions, and, less significant, also in the form of copper multiion clusters. The content of iron in the studied brain was lower than in controls. These results confirmed significantly the neuropathological diagnosis of hepato-lenticular degeneration.

Key words: *hepato-lenticular degeneration, histochemistry, electron paramagnetic resonance, cations.*

Electron paramagnetic resonance (EPR), a physical method introduced broadly in recent years in many scientific spheres, creates also new possibilities in the analysis of heavy metals content in the central nervous system. Studies of these compounds using EPR method are significant not only for diagnostic purposes, but also in analysis of the physico-chemical state of the metallic deposits in the nervous tissue. That is why we have performed studies of copper and iron content in the clinically atypical case of hepato-lenticular degeneration using EPR method.

CASE REPORT

Male, 24-year-old, felt ill 2 years before death with pseudoneurotic symptoms, diagnosed as hysteric neurosis. The patient was treated with sedative drugs and neuroleptics without improvement. One year later he was admitted to the Department of Psychiatry with affection of several psychic functions, with dominance of depression. Neurological examination revealed hypokinesia and speech disturbances. The disease progressed quickly. There appeared some difficulties in contact with the patient. One months later severe rigidity with contractures of upper and lower extremities was noticed. Body temperature was enhanced. There appeared bladder disturbances.

Computer tomography scan, performed in the initial period of the disease revealed moderate atrophy of the brain. CSF examination: cells $2.3/\text{mm}^3$, total protein 40 mg%. Routine blood and urine examination without any changes. Indirect immunofluorescence test for toxoplasmosis was positive (1:1024).

The patient died in the second year after appearance of the first symptoms, under progressing circulatory and respiratory insufficiency. Familial anamnesis was unevenful. General autopsy revealed liver cirrhosis, enlargement and intumescencia of spleen and peritoneal exudation (600 ml).

NEUROPATHOLOGICAL EXAMINATION

On frontal brain sections basal ganglia appeared smaller than normal. Bilaterally in upper poles of the putamen yellow-green foci of tissue necrosis were seen. Other regions of brain hemispheres, pons, medulla oblongata, cerebellum and spinal cord did not revealed any macroscopic changes.

Tissue blocks taken from frontal, parietal and temporal cortex, centrum semiovale, basal ganglia, pons, medulla, cerebellum and spinal cord (cervical, thoracic and lumbar segments) were fixed in formalin and embedded in paraffin. Tissue sections were stained with hematoxylin and eosin, Nissl and Kanzler methods.

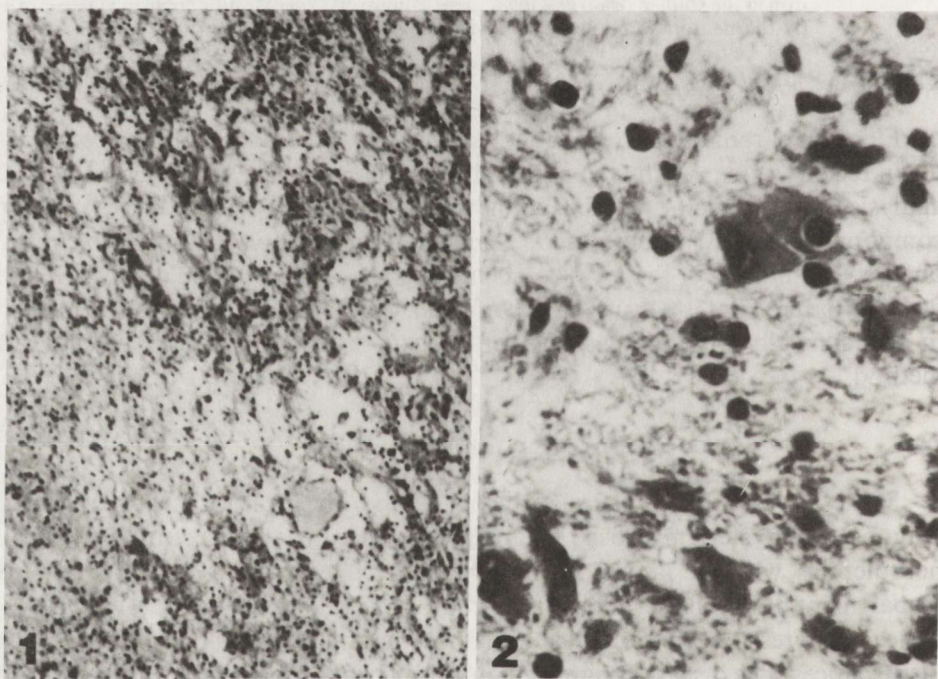


Fig. 1. Putamen of right hemisphere with spongy changes. HE. $\times 50$

Fig. 2. Alzheimer type I cells in the spongy region. HE. $\times 600$

The greatest microscopic changes were seen in basal ganglia, cerebral peduncles and pons. Yellow-green foci in basal ganglia observed during macroscopic examination, corresponded to incomplete necrosis with spongy tissue loosening (Fig. 1), scanty glial fibers and proliferating capillaries. Many hypertrophic glial cells, like Alzheimer type I cells (Fig. 2) and sometimes Opalski cells (Fig. 3) were seen in the glial-mesodermal network, more abundant at the borders of necrotic regions. In addition, spongy changes with enlarged glial nuclei, like Alzheimer type II cells, were visible in the central part of the pons (Fig. 4). A small fusiform hemorrhage in the substantia nigra was noted. Deposits of brown pigment were observed in neurons of the Vth cortical layer. In subcortical white matter astroglial nuclei were moderately enlarged. In other brain regions only changes related to subacute circulatory disturbances were seen.

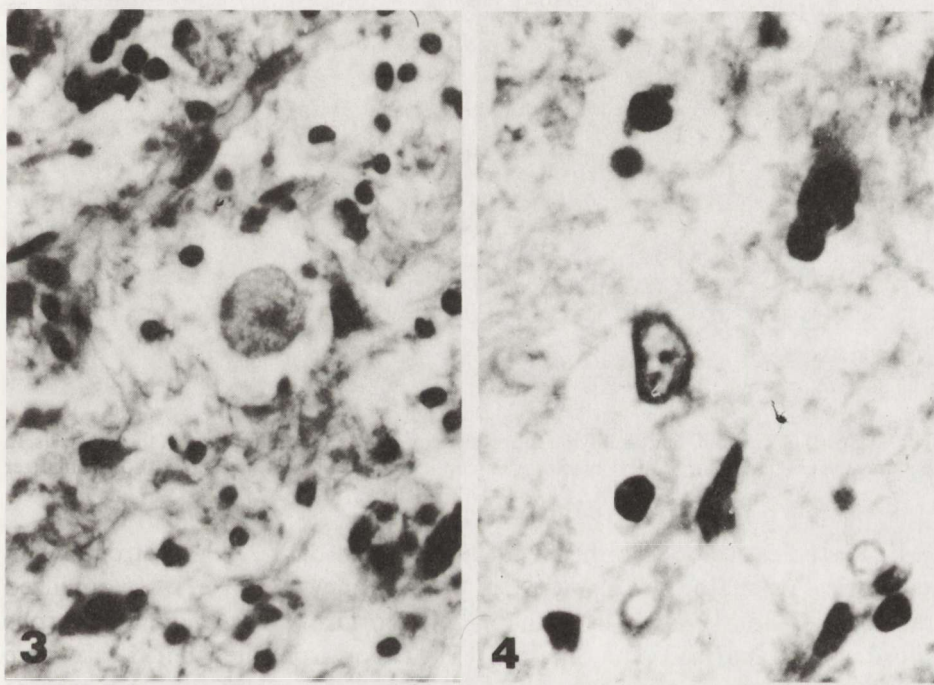


Fig. 3. Opalski cells in the focus of spongy degeneration. HE. $\times 600$

Fig. 4. Pale nuclei of Alzheimer type II cells in the spongy focus. HE. $\times 600$

Topography and type of the brain lesions and hepatic cirrhosis suggested hepato-lenticular degeneration as the cause of the illness. To verify this suggestion, histochemical and EPR investigations of Cu and Fe cations content were performed on pieces of tissue derived from various regions of the investigated brain.

In selected sections of basal ganglia, midbrain and centrum semiovale histochemical reactions were performed for detection of iron according to Tirmann and Schmalzer and for detection of copper using the method of Okamoto and

Utamura, as presented in monograph of Godlewski (1982). Reaction for iron was positive in substantia nigra in the form of Turnbull blue granules lying free and inside of glia cells (Fig. 5). The inhibition reaction with oxalic acid was confined to the presence of iron in this brain region. The reaction for iron was negative in basal ganglia and in medulla oblongata. The histochemical reaction for copper was only trace in the basal ganglia and the mesencephalon.

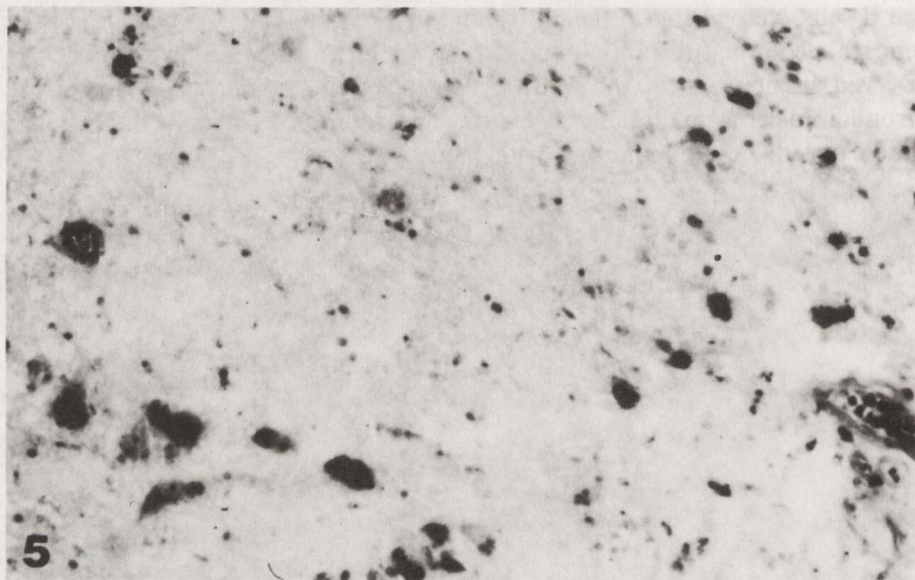


Fig. 5. Deposits of Turnbull blue, testifying the presence of iron extracellularly and in the glial cells. In the same region the histochemical reaction for copper was very faint. Tirmann and Schmalzter method. $\times 270$

EPR studies were performed with a Radiopan SEX-2543 spectrometer in a cylindrical resonator of TE_{011} type, at the frequency of 9.40 GHz. Lyophilized brain tissue (about 1 mm^3) from the parietal cortex, basal ganglia and corpus callosum were analysed. The obtained EPR curves from the studied case were compared with results established in topographically analogical brain regions obtained from 15 young (mean age — 29 years) persons who died from other neurological and nonneurological diseases.

The quantitative data concerning the content of ions and radicals were obtained by the method of double integration the whole EPR curves and their comparison with the standard curve of substances of known spin number (benzene DPPH solution and weak pitch Varian standard). Essential methodical information on the use and significance of EPR in biology may be found in the publication of Heckly (1972).

In all studied slices the EPR signals deriving from ions: Cu^{+2} , Fe^{+3} , clusters Cu^{+2} , and Fe^{+3} , as well as free radicals were noted. The pattern of EPR curves in the full range of the used strength of the magnetic field is presented in Fig. 6.

The EPR signal for copper Cu^{+2} deriving from ions is homogeneously dispersed in the whole volume of the studied material and is characteristic for ions coordinated in octahedral or square-planar configuration. The split, but relatively broad, lines of Cu^{+2} hyperfine structure suggest coordination of the nitrogen atom. The observed pattern of splitting is close to those of erythrocytorein and similar to the pattern of cytochrome oxidase or copper glycinate complexes.

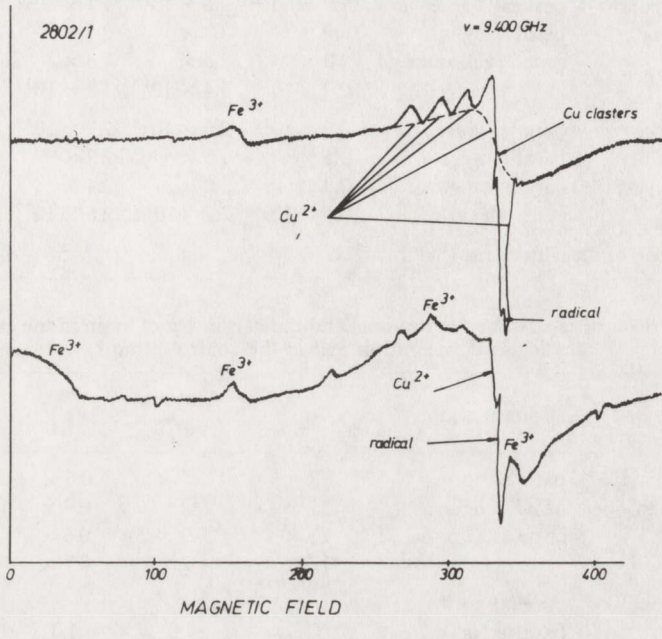


Fig. 6. EPR lines obtained in the sample of parietal cortex in the case of hepato-lenticular degeneration (upper curve) and in the control case (lower curve). Intensity of magnetic field expressed in millitesla

Iron Fe^{+3} is the source of three signals (Fig. 6), from which the signal in the field around 155 mT arises from the ions in the asymmetric surrounding, but distributed homogeneously in the studied slice. The signal is similar to those of transferrin. The remaining signals are connected with the isolated Fe^{+3} ions, their clusters and ferromagnetic aggregates. The fragment of pattern derived from clusters (multiion aggregates), depends mainly on Cu^{+2} ions and in the lower part from Fe^{+3} ions. Participation of iron was better visible when slices were studied in the liquid nitrogen (77°K). The shape of the curve derived from the free radicals does not allow to establish its definite origin. Lyophilization of the brain tissue and the influence of atmospheric oxygen on the dry sample may have some effect on the appearance of signals. It can only be said that, as generally known, an important role in raising this part of the curve is played by the radicals of ascorbic acid. The results of the quantitative studies of ions and radicals in the analyzed

material are presented in Table 1, and comparison of the relative number of ions and radicals in Table 2.

Table 1. Quantity of ions and radicals in 1 g of nervous tissue in the case of hepato-lenticular degeneration and in the control group, determined by the method of double integration of the whole EPR curves

Clinical diagnosis	Brain region	Cu^{+2}	Clusters of Cu	Fe^{+3}	Radicals
Hepato-lenticular degeneration	parietal cortex	7.8×10^{18}	9.6×10^{18}	1.7×10^{17}	10.0×10^{14}
	basal ganglia	$16.0 \times$	$3.7 \times$	$2.5 \times$	$4.2 \times$
	corpus callosum	$9.0 \times$	$2.8 \times$	$1.3 \times$	$2.5 \times$
	mean	10.9×10^{18}	5.4×10^{18}	1.8×10^{17}	5.6×10^{14}
Control group 15 cases mean age 29 years	parietal cortex	0.6×10^{18}	2.0×10^{18}	2.7×10^{17}	12.7×10^{14}
	basal ganglia	$0.6 \times$	$1.5 \times$	$2.9 \times$	$12.3 \times$
	corpus callosum	$0.8 \times$	$3.0 \times$	$2.4 \times$	$9.2 \times$
	mean	0.7×10^{18}	2.2×10^{18}	2.6×10^{17}	11.4×10^{14}
Relative error of measurements (%)		4	8	5	5

Table 2. Comparison of relative number of ions and radicals in 1 g of brain in the case of hepato-lenticular degeneration and in the control group*

Clinical diagnosis	Brain region	Cu^{+2}	Clusters of Cu	Fe^{+3}	Radicals
Hepato-lenticular degeneration	parietal cortex	$13 \times$	$5 \times$	$0.6 \times$	$0.8 \times$
	basal ganglia	$27 \times$	$2 \times$	$0.9 \times$	$0.3 \times$
	corpus callosum	$11 \times$	$0.9 \times$	$0.6 \times$	$0.3 \times$
	mean	$17 \times$	$2 \times$	$0.7 \times$	$0.5 \times$
Control group	parietal cortex				
	basal ganglia	1.0	1.0	1.0	1.0
	corpus callosum				

* Value of number of ions and radicals in the brain of control group as 1.0.

DISCUSSION

Positive histochemical reaction to iron in comparison with the only trace reaction to copper suggested a differentiation between hepato-lenticular degeneration and Hallervorden-Spatz disease. The course and clinical symptoms are similar in both illnesses and they are summarized in Table 3, according to Evrard et al. (1968) and Yanagizawa et al. (1966).

The results obtained by the use of the EPR method indicate an approximately 20-fold increase in the content of Cu^{+2} ions in the whole studied material in comparison with the control. The increase was the highest in the basal ganglia. In some brain regions an increase of Cu^{+2} ion aggregates (clusters) was also noticed, highest in the parietal cortex (5-fold). The mean value of all studied brain samples indicates a lower number of Fe^{+3} ions and radicals in comparison with the

Table 3. Summary of clinical and neuropathological characteristics of hepato-lenticular degeneration and Hallervorden-Spatz disease

	Hepato-lenticular degeneration (all variants)	Hallervorden-Spatz disease
Onset of the disease		
infantile form	5–10th year of life	3–6 years
juvenile form	15–20th year of life	7–15 years
late form	30–40th year of life	22–64 years
Occurrence	sporadic and familial	sporadic and familial
Clinical characteristics	progressing rigidity tremor progressing dementia	progressing rigidity extrapyramidal movements progressing dementia
Localisation and character of neuropathological changes	striatum, substantia nigra thalamus, n. ruber neurocytes, astroglia demyelination	pallidum substantia nigra neurocytes, astroglia, microglia demyelination
Histochemical reaction	not always positive histochemical reaction for copper Fe in phagocytes (substantia nigra, pallidum)	strong reaction for Fe positive PAS reaction
Life span	not treated 3–10 years	death before 30th year of life

control group (see Table 2). The content of iron in the studied brain was lower than in controls. These results confirmed significantly the neuropathological diagnosis of hepato-lenticular degeneration.

The studies of Mossakowski et al. (1970) and of Mossakowski and Weinrauder (1984a) have established that excessive accumulation of copper in the central nervous system, due to disturbances in the metabolism of the Krebs cycle, lead to a decrease of endogenic synthesis of alpha-ketoglutarate. This results in insufficiency of ammonium detoxication, and subsequently, in disturbances of many metabolic processes in the astroglia, and in its transformation into Opalski cells or, independently, into the cells of Alzheimer type I and type II (Mossakowski 1966; Mossakowski, Weinrauder 1984b).

Some comment is also necessary to the clinical picture of the observed patient. The clinical symptomatology of hepato-lenticular degeneration is highly variable, as is well documented in its division into three completely different forms in the neurological picture: the type with predominating symptomatology of trembling (type of Westphal-Strümpel), with overwhelming extrapyramidal rigidity (Wilson type) and the abdominal form. Our case belongs undoubtedly to the Wilson type. However, very unusual were the initial symptoms of the disease: lasting more than one year marked domination of subjective symptoms, even interpreted as hysterical neurosis. This indicates once more how much caution should be applied in concluding this diagnosis.

ANALIZA ZAWARTOŚCI CIĘŻKICH METALI W MÓZGU PRZY UŻYCIU
REZONANSU PARAMAGNETYCZNEGO W KLINICZNIE NIEZWYKŁYM PRZYPADKU
ZWYRODNIENIA WĄTROBOWO-SOCZEWKOWEGO

Streszczenie

Przeprowadzono analizę zawartości metali ciężkich w mózgu w klinicznie niezwykłym przypadku zwyrodnienia wątrobowo-soczewkowego za pomocą elektronowego rezonansu paramagnetycznego.

Wykonane badania wykazały wyraźny wielokrotny wzrost zawartości miedzi w mózgu i to w postaci wolnych jonów oraz mniej wyraźny także w postaci wielojonowych klastrów miedzi. Zawartość żelaza w badanym mózgu była niższa od stwierdzonej w przypadkach kontrolnych. Wyniki te potwierdzają w istotny sposób rozpoznanie histopatologiczne zwyrodnienia wątrobowo-soczewkowego.

REFERENCES

1. Evrard E, Hariga J, Martin J, Reznik M: Maladie de Hallervorden-Spatz tardive avec importante participation réticulaire et cérébelleuse. *Psych Neurol Neurochir*, 1968, 71, 243–254.
2. Godlewski HG: Składniki mineralne. In: *Topochemiczne metody badania komórek i tkanek*. PWN, Warszawa 1982, 279–328.
3. Heckly RJ: Biological applications of electron spin resonance. Eds. HM Schwartz, JR Bolton, DC Borg, Wiley, New York 1972.
4. Mossakowski M: Patomorfologia i histochemia spontanicznych i doświadczalnych encefalopatii pochodzenia wątrobowego. *Neuropatol Pol*, 1966, 4, 231–304.
5. Mossakowski M, Renkawek K, Kraśnicka Z, Śmiałek M, Pronaszko-Kurczyńska A: Morphology and histochemistry of Wilsonian and hepatogenic gliopathy in tissue culture. *Acta Neuropatol (Berl)*, 1970, 16, 1–16.
6. Mossakowski M, Weinrauder H: Historia naturalna komórek Opalskiego. *Neuropatol Pol*, 1984a, 22, 471–481.
7. Mossakowski M, Weinrauder H: Immunomorphology of Wilsonian and hepatic gliopathy in vitro. *Neuropatol Pol*, 1984b, 22, 161–178.
8. Yanagizawa N, Shiraki H, Minakawa M, Narabayashi H: Clinico-pathological and histochemical studies of Hallervorden-Spatz disease and torsion dystonia with special reference to diagnostic criteria of the disease from the clinico-pathological viewpoint. *Prog Brain Res*, 1966, 21, 373–381.

Authors' address: Department of Neurology, School of Medicine, 49 Przybyszewskiego Str., 60-355 Poznań, Poland

HANNA MIERZEWSKA-RZESZOT

ADRENAL MEDULLA GRAFTS INTO THE RAT STRIATUM – AN EVALUATION OF SURVIVAL AND DYNAMICS OF THE HOST BRAIN RESPONSE

Department of Neuropathology, Institute of Psychiatry and Neurology, Warsaw

Allogenic adrenal medullary tissue was implanted into the striatum of 68 rats. The material was evaluated by routine histological, histochemical, immunocytochemical as well as histofluorescence techniques 1, 3, 7, 14, 21 and 42 days after implantation. The viability of chromaffin cells continued through the 21st day after the implantation. The host brain tissue responded in two ways. First, by macrophagic resorption of the progressively necrotic graft in the experimental group and of the damaged area along the needle tract, noted both in experimental and control animals. This was accompanied by demarcation by proliferating reactive astrocytes and microglial cells. Second, by lymphocyte infiltration in the graft and around it, detected only in the experimental group which suggested immunological rejection.

Key words: brain transplant, adrenal medulla, immunological rejection, allograft, rat.

In the past decade several attempts have been made to implant adrenal medullary tissue into the brain and spinal cord with a view to experimental therapy of some neurological disorders. They were preceded by successful trials of intracerebral grafting in animals which proved that adrenal chromaffin cells survived and the implantation had positive functional effects (Fine 1990; Freed et al. 1990). This problem was also studied by Dymecki et al. (1986) and Jędrzejewska and Dymecki (1990) at our Department. To date over 400 transplantation of chromaffin tissue as a source of dopamine, have been made in patients with Parkinson's disease (Ząbek et al. 1993). In the majority of cases they were autografts of mature adrenal medulla. Only in the case of one patient an allograft of fetal adrenal tissue was implanted (Madrazo et al. 1987b). On several occasions adrenal medulla, as a source of endogenous opioids, was also implanted in patients with neoplastic diseases suffering chronic pain after the pharmacotherapy had failed (Sagen, Pappas 1992). Allogenic, cadaveric tissue was used as a graft. The results so far have not been clearcut. Considerable improvement was noted only in a very few parkinsonian patients (Madrazo et al. 1987a; Jiao et al. 1989). Short lasting and rather minor improvement in the majority of patients as well as few publications on autopsy results (Frank et al. 1988; Hurtig et al. 1989; Jankovic et al. 1989; Peterson et al. 1989; Hirsch et al.

1990; Forno, Langston 1991) seem to indicate that survival of the transplanted chromaffin tissue in humans is rather poor (Fine 1990; Freed et al. 1990). This may be due to a number of reasons. First, the chromaffin tissue is extremely sensitive to hypoxia. Secondly, it is heterogenic to the brain tissue despite the fact that from the ontogenic point of view it comes from the same germ layer. Thirdly, in the case of allogenic grafts, their poor survival may be due to immunological rejection.

Damage of the host tissue at the time of implantation may also account for poorer survival of the graft. The biological age of the transplanted tissue is also very important. In experiments the best results have so far been achieved when young, mainly fetal tissue was used (Nishino et al. 1988). Fine (1990) and Freed et al. (1990), who reviewed all the existing experimental and clinical data on adrenal tissue transplantations, found the method rather promising and suggested that further research should be carried out. Chromaffin tissue is more accessible than fetal brain tissue and its transplantations do not raise so many controversies of ethical and legal nature.

Still insufficiently studied is the host brain tissue response to the graft. In recent years some studies have been published on the immune response to neural tissue transplantation into the brain (Finsen et al. 1990, 1991a, b; Lawrance et al. 1990). However, no studies have so far been made on the reaction to heterotopically implanted chromaffin cells. This is the reason why the present study is an attempt at evaluating the survival of adrenal medullary graft and the host brain tissue response.

MATERIAL AND METHODS

The experiments were performed on 133 young, male Wistar rats, weighting 180–200 g. Implantations were made in 68 recipients divided into 6 groups (according to the survival time) of 10–12 animals, while the 25 control animals were divided into 6 groups of 4–5 each.

The adrenal medullary tissue for the transplantations and control stainings (Fig. 1) was taken from 40 animals under deep ether anesthesia and immersed in sterile 0.6% glucose in Ringer solution at 20°C. Next, the tissue was dissected into small pieces. The time which elapsed between dissection and implantation did not exceed 30 min.

Procedure of transplantation

The experimental animals were anesthetized with chloral hydrate and pentobarbital, and were grafted into the right striatum with a solid piece of adrenal tissue (ca 0.5 mm³) in a David Kopf stereotactic apparatus (coordinates to the bregma: R = 0.5 mm, L = 2.2 mm, V = 4.5 mm). After 1, 3, 7, 14, 21 and 42 days the recipients were sacrificed in deep ether anesthesia. The control animals received 0.5 mm³ of 0.6% glucose in Ringer solution instead of the graft. The survival was exactly the same as in experimental group. All procedures were

performed under sterile conditions. In order to examine an unmodified host's immune and brain tissue response, the animals were not treated with antibiotics or immunosuppression.

Histopathology and histochemistry

The material for routine techniques and immunocytochemistry was fixed by immersion in 4% buffered paraformaldehyde and embedded in paraffin. Tissue blocks were cut serially in sections 5 μm thick and one section in five was stained with hematoxylin and eosin (HE), by the Klüver-Barrera and van Gieson methods. For Schmorl's histochemical detection of chromaffin cells, the material was fixed in potassium dichromate solution by Pearce (1972).

Immunocytochemistry

The representative paraffin-embedded sections (containing grafts or needle track), adjacent to those stained by HE, were stained by the avidin-biotin-peroxidase technique (Hsu et al. 1981) using respective antibodies (Ab). Adrenal cells in the graft were visualized by Ab to tyrosine hydroxylase (TH), (Eugene, Tech.) and dopamine-hydroxylase (DBH), (Eugene Tech.). To examine the host selected tissue reaction Ab were applied to glial fibrillary acidic protein (GFAP), (Serva) for visualization of hypertrophic astrocytes, and to ferritin (Dakopatts) for visualisation of active microglial cells and macrophages. The sections were incubated in 0.3% hydrogen peroxide followed by 2% normal goat serum in PBS for 20 min and then incubated with the primary Ab to TH (diluted 1:1000), DBH (1:1000), GFAP (1:2000), or ferritin (1:1000) at 4°C overnight. The sections were then successively incubated with secondary antibody and the AB reagent (Vectastain ABC kit, Vector Lab.) for 1 h at room temperature. Then the sections were coloured with 0.05% diaminobenzidine (Sigma) and some of them were counter-stained with hematoxylin.

Histofluorescence technique

A modified De La Torre's (1980) method of sucrose-potassium sulfate-glyoxylic acid (SPG) for tissue monoamines was used. Fresh material was immersed in SPG solution for 24 h, then frozen and dissected into 10 μm sections in a cryostat chamber. The preparations were examined in a Fluoval (Zeiss) microscope with excitation filter BG-12 and barrier filter OG-4.

RESULTS

I. Graft

It was found that a heterotopically implanted allograft of adrenal medulla showed poor survival in the parenchyma of striatum. The viability of cells was detected by immunocytochemical (TH, DBH), Schmorl's and histofluorescence techniques mostly up to the 7th day (Fig. 2a, b). With time chromaffin cells gradually decreased in number and showed degenerative changes by way of shrunken or disintegrated cytoplasm. Only in one case a few disintegrated cells

were preserved in the graft after 21 days (Fig. 2c). No processes started to form in the adrenal cells.

Starting from the first days after implantation a gradually progressing necrotic area and hemorrhages were observed in the graft tissue. On the 1st day, at first peripherally and then in the graft, phagocytic cells were found, mainly macrophages and a few polynuclear leukocytes. On the 3rd day after implantation lymphocytes were discovered in the graft and their number gradually grew to reach a peak on the 21st day. After 42 days in the examined brains there was either no trace of the graft or remnants of graft connective tissue stroma.

II. Host brain tissue

Around the graft and in the central part of the cannula track necrotic tissue and hemorrhages were found. The area of destruction and effusions was slightly larger in the animals with implanted grafts than in the control groups. From the 1st postoperative day concretions of fibrin were observed. As late as the 7th

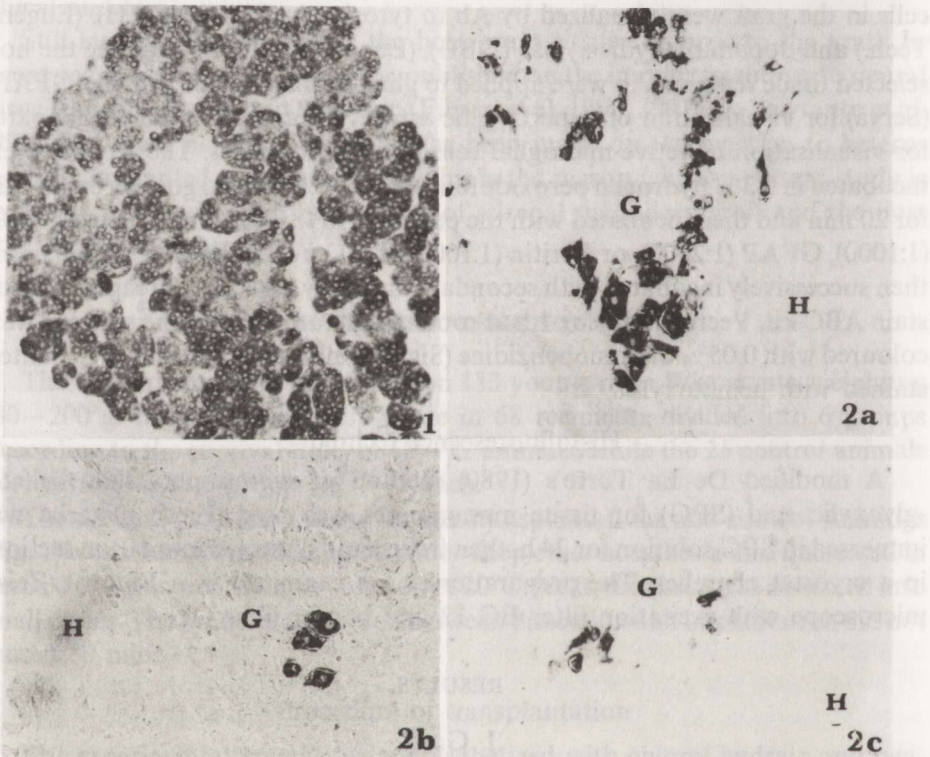


Fig. 1. Normal adrenal medulla – TH immunoreaction, $\times 160$.

Fig. 2a. Adrenal tissue graft 3 days after implantation with large number of preserved cells. Clusters of strongly immunoreactive cells as well as weakly immunoreactive cells are observed. G – graft, H – host, TH, $\times 160$

Fig. 2b. Small cluster of preserved cells in graft 7 days after implantation. TH, $\times 160$

Fig. 2c. Only few preserved cells with different signs of destruction in graft 21 days after implantation. TH, $\times 160$

postoperative day extensive edema surrounded the damaged area and myelin destruction was found along the cannula track. No significant differences were noted between experimental and control preparations. A small quantity of collagen fibers was found in the scar formed primarily by astroglial cells. A greater amount of collagen was detected in the experimental animals. Starting from the 3rd day in both groups of animals new capillary vessels started forming with the same intensity along the cannula track.

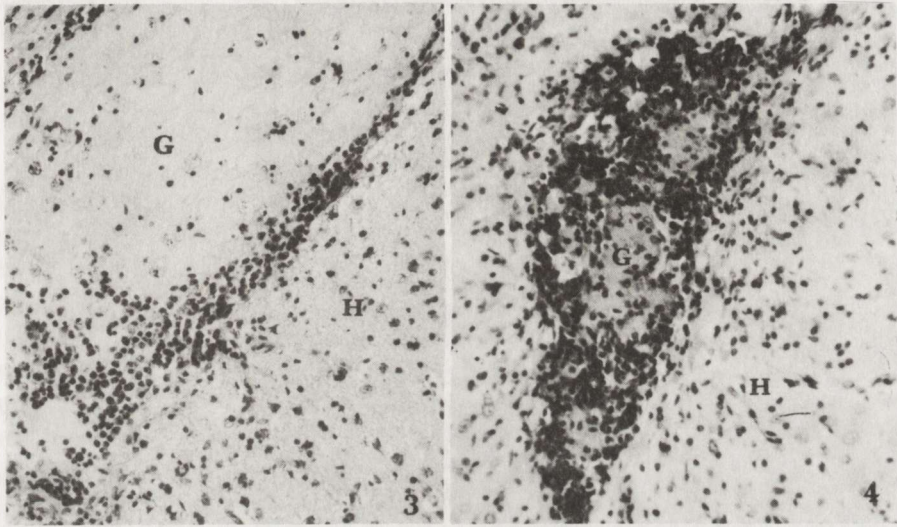


Fig. 3. Infiltration consisted mainly of phagocytic cells with a few lymphocytes around the graft 14 days after implantation. HE, $\times 160$

Fig. 4. Infiltration consisted mainly of a large number of lymphocytes within and around graft's remnants 21 days after implantation. HE, $\times 160$

From the 1st through the 7th day in both the experimental and control groups a small number of polynuclear leukocytes was observed along the cannula track, but soon disappeared from the infiltration. More of them were found, however, in the experimental group. On the 3rd postoperative day a growing number of macrophages were observed to predominate in the infiltration. The highest quantity was detected between days 7 and 14. They were slightly less numerous after 21 days. After 42 days only some large degenerating macrophages were found along the cannula track. No differences in intensity of macrophagic response were found in experimental and control groups.

In animals with the graft an infiltration of lymphocytes was observed starting from the 3rd day (Fig. 3). After 21 days the highest quantity of those cells was detected (Fig. 4) with single plasmacytes. After 42 days the number of lymphocytes was on the decrease. The infiltrations were most frequent in the vicinity of blood vessels. The lymphocyte response differed in intensity in particular

animals. In the brain tissue of control animals no lymphocyte response was observed.

From the 3rd day a growing number of GFAP-positive hypertrophic astrocytes was observed around the graft and along the cannula track (Fig. 5). Initially the cells were disseminated, but with time they formed a thick, concentrated ridge demarcating the area surrounding the graft remnants or the necrotic tissue. After 21-42 days an astroglial scar or small astroglia-lined cavity was detected (Fig. 6).

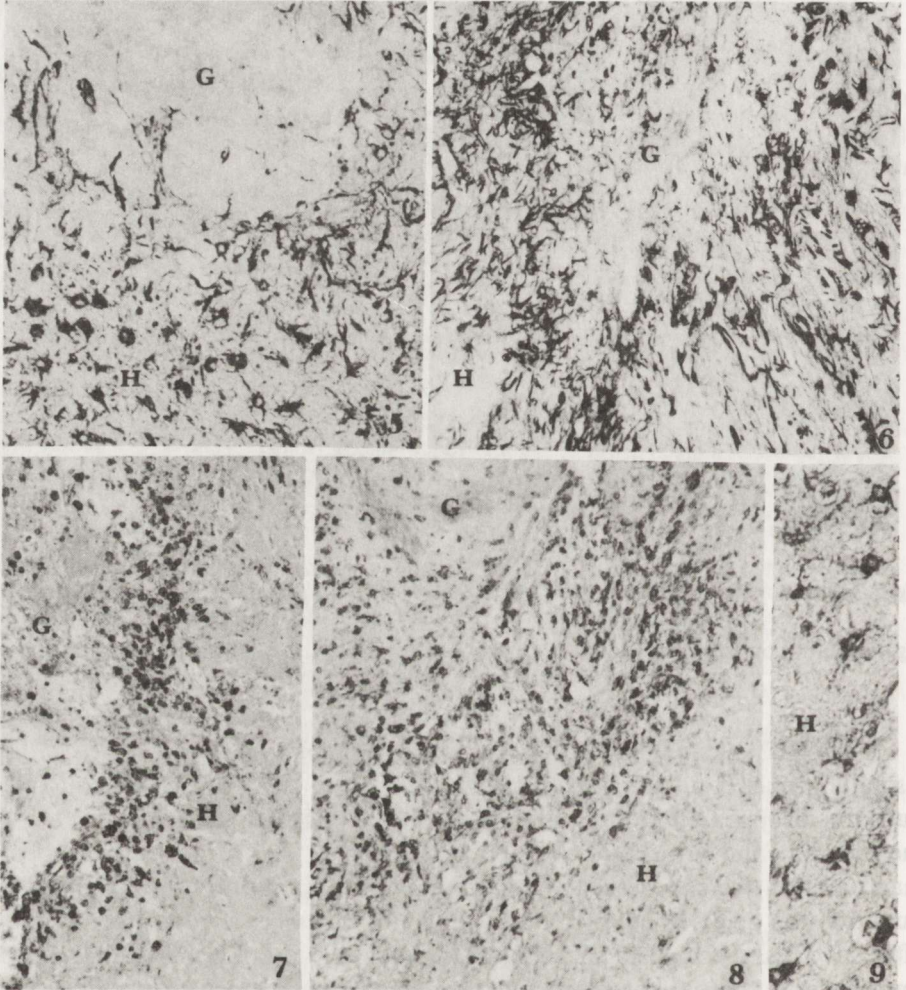


Fig. 5. Reactive astrocytes around the graft 7 days after implantation. GFAP, $\times 160$

Fig. 6. Astrocytic scar around graft remnants 21 days after implantation. GFAP, $\times 160$

Fig. 7. A large number of active microglial cells and macrophages around the graft 3 days after implantation. Ferritin, $\times 160$

Fig. 8. Active microglial cells and macrophages 14 days after implantation, Ferritin, $\times 160$

Fig. 9. Active microglial cells around the graft 21 days after implantation. Ferritin, $\times 320$

In both the experimental and control group the astroglial reaction was found to be similar.

From the 3rd day a growing number of active microglial cells and macrophages were observed in the tissue around the graft and along the cannula track (Fig. 7). The largest quantity of the cells was noted 14 days after implantation (Fig. 8). When compared with resting microglia the active microglial cells were characterized by larger cytoplasm and few thicker processes (Fig. 9). After 21–42 days the cells became even less numerous and additionally some rod cells were also noted. No essential differences were found between the experimental and control material.

DISCUSSION

Morphological analysis indicates that there are two types of host brain tissue responses to allografts of adrenal medulla. The first response is independent of the fact whether genuine grafting or sham transplantation has taken place. It is marked by the presence of phagocytic cells, reactive astrocytes, active microglia, connective tissue elements, and neovascularization. This response is effected by the damaged tissue, resorption and repairing processes. A similar reaction was observed by Finsen et al. (1990; 1991a, b) in the vicinity of intracerebral allo- and xenografts of neural tissue. Bankiewicz et al. (1991) and Plunkett et al. (1990) noted exactly the same reaction around an allograft of adrenal medulla and other non-neural tissue, also in response to what is called precavitation. All these observations seem to indicate that the reaction is nonspecific. However, it is only Finsen et al. (1990, 1991a, b) and Lawrance et al. (1990) who focus on the dynamics of the response. Their observations are similar to those made by the authors of the present study. Autopsy findings produce evidence of similar changes present around the necrotic graft remnants 4 up to 13 months after surgery (Hurtig et al. 1989; Jankovic et al. 1989; Peterson et al. 1989; Hirsch et al. 1990; Forno et al. 1991). The presence of more collagen fibers in the scar after grafting than in the control animals may be viewed as remnants of the graft connective tissue stroma. Similar fibrosis in the area of the necrotic graft was described by Hirsch et al. (1990).

The second type of response which is effected only by the grafts is the presence of lymphocytes, which tend to concentrate in the vicinity of blood vessels, from where they probably originate. Both the reaction timing (about the 3rd day) and its peak intensity after 21 days are the sign of typical immunological rejection. Other scientists who studied reactions to grafts implanted into the brain also observed similar dynamics of changes and with the help of specific immunocytochemical markers detected the prevalence of T-lymphocytes and only few B-lymphocytes (Finsen et al. 1990; 1991a, b; Lawrance et al. 1990). Immunocytochemical analysis of cellular immune response was done in only one patient after the autograft of adrenal tissue and a mixture of T and B-lymphocytes was found in the infiltration (Jankovic et al. 1989). This could be evidence of rejection of

the heterotopically implanted tissue. A similar view is also propounded by earlier reports, according to which autografts of non-neural tissue into the brain result in immunological rejection (Ridley, Cavanagh 1969).

Our observations seem to disprove the hypothesis of the immunological privilege of the brain which, it seems, has not stood the test of time. The existence of the blood-brain barrier (BBB) as well as the absence of typical lymphatic vessels in the brain, combined with the fact that grafts of a variety of tissues when transplanted into the brain at times showed longer survival than when implanted into extracerebral sites, had once generated this hypothesis (Barker, Billingham 1977). However, the very procedure of graft-implanting inflicts mechanical damage to the BBB and opens the brain to the penetration of different cells and substances from the blood. A long lasting inflammatory infiltration consisting of different cells, some of which produce cytokines, contributes to a higher permeability of the barrier. In the autopsy materials infiltration around the graft remnants was detected as late as 13 months after the implantation (Forno et al. 1991). Widner and Brundin (1989) proved, that a xenograft implanted into the brain effects a clear proliferation response in the deep cervical lymph nodes. Dymecki et al. (1990) found that the graft survival time tends to decrease as the degree of genetic donor-host disparity grows. It is also well known that immunosuppression increases the allograft's and xenograft's survival.

The changes in the brain due to graft implantation affect a considerably wide area and result in a scar or a small cavity. They are slightly larger in the experimental than the control animals. It may be concluded, therefore, that while a selection of implantation methods is made, the least invasive techniques should be chosen. It is also essential to find an adequate access to the site of grafting, to pick the right instruments which will minimize tissue damage. Stereotactic injections of cell suspension with the help of a fine needle are an alternative method to the implantation of a solid piece of tissue. Fine (1990) has even suggested that cells implanted as suspension may be more susceptible to absorb trophic factors directly from interstitial fluid without the mediation of vessels. It has already been reported that the implantation of adrenal cells suspension into the rat striatum yields positive effects (Nishino et al. 1988).

The solid piece of tissue implantation technique used in the present experiment showed poor survival of chromaffin cells implanted into the striatum, similarly to what was reported by Freed et al. (1990) and Fine (1990). The validity of our findings is further enhanced by the use of a broad variety of techniques to assess the survival of chromaffin cells. Initial reports on long term survival of adrenal grafts relied on a less specific method of histofluorescence. In our materials the donor-host histoincompatibility seems to be one of the factors which result in necrotic changes of the graft at a later time. The majority of cells die a few days after implantation. At this point the immunological rejection has not yet taken place in the host, who happens to be exposed to histocompatible antigens present in the donor's cells for the first time in his life.

Adrenal medullary tissue is particularly sensitive to hypoxia. Implanted into the striatum, it is surrounded by hemorrhages and damaged host tissue from the very beginning. At the time which is crucial for the cell viability the adrenal medullary tissue is deprived of trophic factors and oxygen — according to the reports (Nakano et al. 1990), the host-graft revascularisation starts on the 3rd day.

CONCLUSIONS

1. Adrenal medullary cells implanted as a solid piece of tissue into the parenchyma of the striatum show poor survival. The majority degenerate in the first days after implantation what is probably due to hypoxia and shortage of trophic factors. Even if the graft shows better survival it may, nevertheless, become subject to immunological rejection.

2. Implantation of the allogenic adrenal graft into the rat striatum gives rise to two kinds of the host tissue responses:

— resorption of the grafts remnants and damaged tissue by phagocytes, proliferation of reactive astrocytes and activated microglial cells, followed by formation of an astroglial scar or a cavity lined with astroglia;

— presence of lymphocytes in the inflammatory infiltration around the graft. The prevalence of these cells and the dynamics of the response seem to argue in favor of immunological rejection.

PRZESZCZEP RDZENIA NADNERCZA DO PRAŻKOWIA SZCZURA

— OCENA PRZEŻYCIA ORAZ DYNAMIKI REAKCJI TKANKI MÓZGU GOSPODARZA

Streszczenie

Przeszczep allogennej tkanki rdzenia nadnerczy implantowano do prążkowiec 68 szczurów. Materiał oceniano histologicznie, histochemicznie, immunocytochemicznie i histofluorescencyjnie po 1, 3, 7, 14, 21 i 42 dniach. Obecność żywych komórek w przeszczepie stwierdzono tylko do 21 dnia od implantacji. Stwierdzono dwa typy reakcji tkanek mózgu gospodarza. Pierwszy, polegający na rozbiórce obumierającego przeszczepu u zwierząt doświadczalnych i uszkodzonej w wyniku procedury implantacyjnej tkanki w obu grupach z następującą demarkacją zmian przez proliferujące reaktywne astrocyty i komórki aktywnego mikrogleju. Drugi, obserwowany tylko u zwierząt doświadczalnych w postaci nacieku z limfocytów wokół i w obrębie przeszczepu, świadczący o odzucaniu immunologicznym.

REFERENCES

1. Bankiewicz KS, Plunkett RJ, Jakobovitz DM, Kopin LJ, Oldfield EH: Fetal nondopaminergic neural implants in parkinsonian primates. *J Neurosurg*, 1991, 74, 97–104.
2. Barker CF, Billingham RE: Immunologically privileged sites. *Adv Immunol*, 1977, 25, 1–54.
3. Brundin P, Nilsson OG, Gage FH, Bjorklund A: Cyclosporin A increases survival of cross-species intrastriatal grafts of embryonic dopamine-containing neurons. *Exp Brain Res*, 1985, 60, 204–208.
4. De la Torre JC: An improvement approach to histofluorescence using the SPG method for tissue monoamines. *J Neurosci Meth*, 1980, 3, 1–5.

5. Dymecki J, Póltorak M, Markiewicz D, Hauptman M, Dziedzic W, Kostowski W: Effects of intracerebral transplantation of the adrenal medulla in rats with experimental Parkinson's disease. *Neuropatol Pol*, 1986, 24, 1–42.
6. Dymecki J, Póltorak M, Freed WJ: The degree of genetic disparity between donor and the host correlates with survival of intraventricular substantia nigra graft. *Reg Immunol*, 1990, 3, 17–22.
7. Fine A: Transplantation of adrenal tissue into the central nervous system. *Brain Res Rev*, 1990, 15, 121–133.
8. Finsen BR, Pedersen EB, Sorensen T, Hokland M, Zimmer J: Immune reactions against intracerebral murine xenografts of fetal hippocampal tissue and cultured cortical astrocytes in the adult rat. *Prog Brain Res*, 1990, 82, 111–127.
9. Finsen BR, Sorensen T, Gonsales B, Castellano B, Zimmer J: Immunological reactions to neural grafts in the central nervous system. *Restor Neurol Neurosci*, 1991a, 2, 271–282.
10. Finsen BR, Sorensen T, Castellano B, Pedersen EB, Zimmer J: Leukocyte infiltration and glial reaction in xenografts of mouse brain tissue undergoing rejection in the adult rat brain. A light and electron microscopical immunocytochemical study. *J Neuroimmunol* 1991b, 32, 159–183.
11. Forno LS, Langston JW: Unfavorable outcome of adrenal medullary transplant for Parkinson's disease. *Acta Neuropathol (Berl)*, 1991, 81, 691–694.
12. Frank F, Sturiale C, Gaist G, Manetto V: Adrenal medullary autografts in human brain for Parkinson's disease. *Acta Neurochir (Wien)* 1988, 94, 162–163.
13. Freed WJ, Póltorak M, Becker JB: Intracerebral adrenal medulla graft – a review. *Exp Neurol*, 1990, 110, 139–166.
14. Hirsch EC, Duyckaerts C, Javoy-Agid F, Hauw JJ, Agid Y: Does adrenal graft enhance recovery of dopaminergic neurons in Parkinson's disease. *Ann Neurol*, 1990, 27, 676–682.
15. Hsu SM, Raine L, Fanger H: Use of avidin-biotin-peroxidase complex (ABC) in immunoperoxidase techniques. *J Histochem Cytochem*, 1981, 29, 577–580.
16. Hurtig H, Joyce J, Sladek JR, Trojanowski JQ: Postmortem analysis of adrenal-medulla-to-caudate autograft in a patient with Parkinson's disease. *Ann Neurol* 1989, 25, 607–614.
17. Jankovic J, Grossman R, Godman C, Pirozzolo F, Schneider L, Zhu Z, Scardino P, Garber AJ, Jhingran SG, Martin S: Clinical biochemical and neuropathological findings following transplantation of adrenal medulla to the caudate nucleus for treatment of Parkinson's disease. *Neurology*, 1989, 39, 1227–1234.
18. Jiao SS, Ding YJ, Zhang WC, Cao JK, Zhang GF, Zhang ZM, Ding MC, Zhang Z, Meng JM: Adrenal medullary autograft in patients with Parkinson's disease. *N Engl J Med*, 1989, 321, 324–325.
19. Jędrzejewska A, Dymecki J: Intraatrial grafts of adrenal medulla in hemiparkinsonian rats – ultrastructural study. *Acta Neurobiol Exp* 1990, 50, 391–396.
20. Lawrance JM, Morris RR, Wilson DJ, Raisman G: Mechanisms of allograft rejection in the rat brain. *Neurosci*, 1990, 37, 431–462.
21. Madrazo I, Drucker-Colin R, Diaz V, Martinez-Marta J, Torres C, Becerril JJ: Open microsurgical autograft of adrenal medulla to the right caudate nucleus in Parkinson's disease: A report of two cases. *N Engl J Med*, 1987a, 316, 831–834.
22. Madrazo I, Leon V, Torres C, Del Carmen AM, Varela G, Alvarez F, Fraga A, Drucker-Colin R, Ostrosky F, Skurovich M, Franco R: Transplantation of fetal substantia nigra and adrenal medulla to the caudate in two patients with Parkinson's disease. *N Engl J Med*, 1987b, 318, 51.
23. Nakano Y, Takei K, Kohsaka S: Xenogenic neural transplantation: Role of vasculature and MHC antigens in immunological rejection. *Stereotact Funct Neurosurg*, 1990, 54, 358–363.
24. Nishino H, Shibata R, Nishijo H, Ono T, Watanabe H, Kawamata S, Tohyama M: Grafted rat neonatal adrenal medullary cells: structural and functional studies. *Prog Brain Res*, 1988, 78, 521–525.
25. Pearce AGE: *Histochemistry theoretical and applied*. Churchill Livingstone, Edinburgh and London, 1972, v2, 1382–1383.
26. Peterson ID, Price ML, Dmall CS: Autopsy findings in a patient who had an adrenal-to-brain transplant for Parkinson's disease. *Neurology* 1989, 39, 235–238.

27. Plunkett RJ, Bankiewicz KS, Cummins AC: Long-term evaluation of hemiparkinsonian monkey after adrenal autografting or cavitation alone. *J Neurosurg*, 1990, 73, 918–926.
28. Ridley A, Cavanagh JB: The cellular reaction to heterologous, homologous and autologous skin implanted into brain. *J Pathol*, 1969, 99, 193–203.
29. Sagen J, Pappas GD: Alleviation of chronic pain by adrenal medullary transplants. *Restor Neurol Neurosci*, 1992, 4, 229.
30. Widner H, Brundin P: Immunological aspects of grafting in the mammalian central nervous system. A review and speculative synthesis. *Brain Res Rev*, 1988, 13, 287–324.
31. Ząbek M, Mazurowski W, Dymecki J, Stelmachów J, Zawada E: A long-term follow-up of fetal dopaminergic neurons transplantation into the brain of three parkinsonian patients. *Restor Neurol Neurosci*, 1993, in press.

Author's address: Department of Neuropathology, Institute of Psychiatry and Neurology, Al. Sobieskiego 1/9, 02-957 Warsaw, Poland

EWA MATYJA, ELŻBIETA KIDA

VERAPAMIL REDUCES QUINOLINIC ACID-INDUCED NEURONAL DAMAGE IN RAT HIPPOCAMPUS *IN VITRO*

Department of Neuropathology, Medical Research Centre, Polish Academy of Sciences,
Warsaw, Poland

The effect of the organic calcium channel blocker, verapamil, on quinolinic acid (QUIN) neurotoxicity in rat hippocampal cultures was studied. Verapamil and QUIN, both in 100 μm concentration, were added simultaneously to the culture medium. Ultrastructural analysis showed that verapamil was able to reduce typical QUIN-induced tissue damages. Especially, 3 and 7 days after exposure to the two agents, majority of both neurons and postsynaptic dendrites revealed normally appearing morphological features. The results support the suggestion of the important role of calcium entry in the development of QUIN neurotoxicity.

Key words: verapamil, QUIN neurotoxicity, hippocampus *in vitro*.

The latest experimental studies point to the involvement of excessive calcium influx from the extracellular space in the neurotoxicity of acidic amino acids (Coyle et al. 1981; Berdichevsky et al. 1983; Griffiths et al. 1983; Retz, Coyle 1984; Mayer, Westbrook 1987, Tsuzuki et al. 1989). On the basis of this suggestion, it seems reasonable to determine, whether the calcium entry blockers can suppress the excitotoxic effects of different acidic amino acids. Since quinolinic acid (QUIN), the most potent of these compounds, is considered to be the main possible factor in the etiology of several degenerative CNS disorders (Schwarcz et al. 1984), prevention of its neurotoxicity became of especially important therapeutic value.

Our previous studies have indicated, that nimodipine eliminates some of the toxic effects of QUIN in hippocampal culture (Matyja, Kida 1991). Another calcium channel blocker, verapamil, proved capable of suppressing epileptiform activity in various experimental studies (Walden et al. 1985; Pockberger et al. 1986; Kretzschmar, Hoffmann 1986; Shelton et al. 1987).

The aim of the present study was to investigate the effectiveness of verapamil in protecting QUIN-induced morphological damages in the hippocampal formation *in vitro*.

MATERIAL AND METHODS

The experiments were performed on 21 day *in vitro* (DIV) organotypic cultures of rat hippocampus, well differentiated and sensitive to QUIN action (Kida, Matyja 1988). The cultures prepared from 2–3-day-old Wistar rats were kept in Maximow assemblies at 36.5°C and fed twice weekly. The nutrient medium consisted of 20% fetal bovine serum and 80% Minimal Essential Medium (MEM) supplemented with glucose to a final concentration of 600 mg%, without any antibiotics. On the 21st day *in vitro* selected cultures were divided into several groups. The first group was maintained in medium containing 100 µm of QUIN (Sigma). The second one was exposed to a medium supplemented with both QUIN and verapamil each at 100 µm concentration. Sister cultures were grown in medium supplemented with 100 µm of verapamil alone or under standard conditions in nutrient medium. The cultures were fixed for electron microscopy 24 hours, 3 and 7 days post exposure to the agents. They were fixed in 1.5% cold glutaraldehyde for 1 h, washed in cacodylate buffer, pH 7.2–7.6, postfixed in 2% osmium tetroxide, dehydrated in graded alcohols and embedded in Epon 812. Ultrathin sections were counterstained with lead citrate and uranyl acetate and examined in a JEM 1500 XB electron microscope.

RESULTS

The cultures of hippocampal formation exposed to the medium containing verapamil displayed normally appearing neurons, surrounded by densely packed neuropil rich in synaptic contacts, identical to the control cultures grown in standard conditions. The cultures exposed to the medium supplemented with 100 µm of QUIN alone showed ultrastructural changes typical for this neurotoxin, consisting of both neuronal and postsynaptic lesions (Fig. 1).

The group of cultures treated simultaneously with QUIN and verapamil, showed distinctly less pronounced tissue abnormalities in comparison to the QUIN applied cultures. After 24 hours of exposure only few nerve cells exhibited more or less advanced vacuolization of the cytoplasm, but even in the severely affected neurons the nucleus did not reveal clumping of nuclear chromatin, characteristic for the QUIN-induced pattern of tissue damage (Fig. 2). The majority of large pyramidal neurons displayed a well preserved nucleus and cytoplasmic organelles (Fig. 3). The neuropil was composed of densely packed glial and neuronal processes, most of which were intact (Fig. 4). Nevertheless, a few dendritic profiles showed different stages of morphological abnormalities. Some of them were electron-lucent and contained damaged mitochondria, (Fig. 5) or were filled with numerous vesicles and vacuoles of various size (Fig. 6).

In the later stages of observation, 3 and 7 days after application of QUIN together with verapamil, almost all neurons displayed normally appearing ultrastructural features (Fig. 7). The postsynaptic dendrites exhibiting little pronoun-

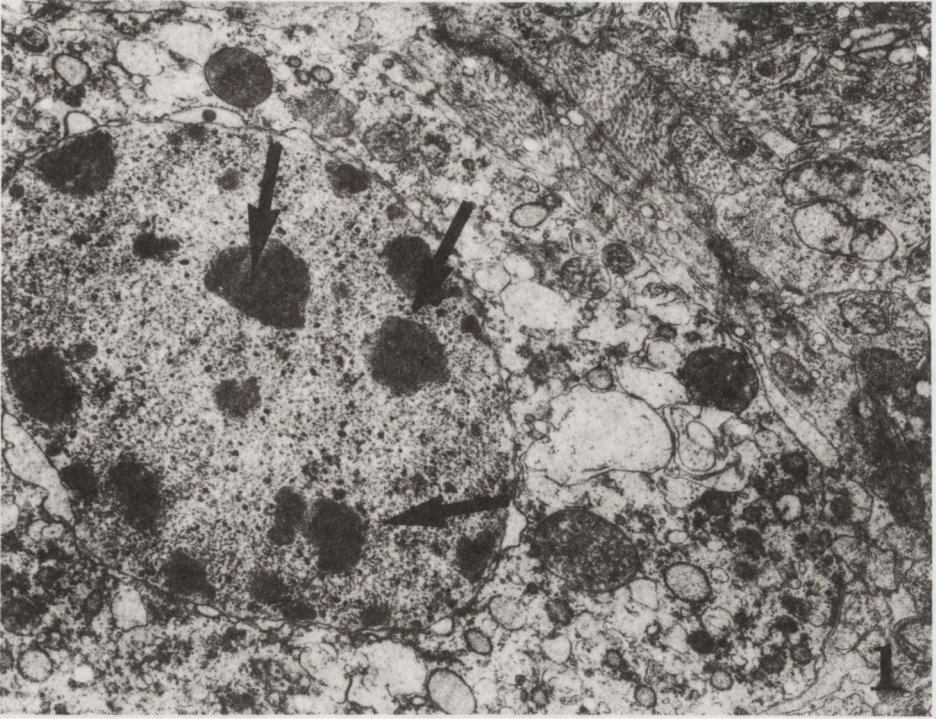


Fig. 1. Hippocampal culture, 24 h post QUIN exposure. Severely damaged neuron exhibiting clumping of nuclear chromatin (arrows) and damaged organelles. $\times 15\,000$

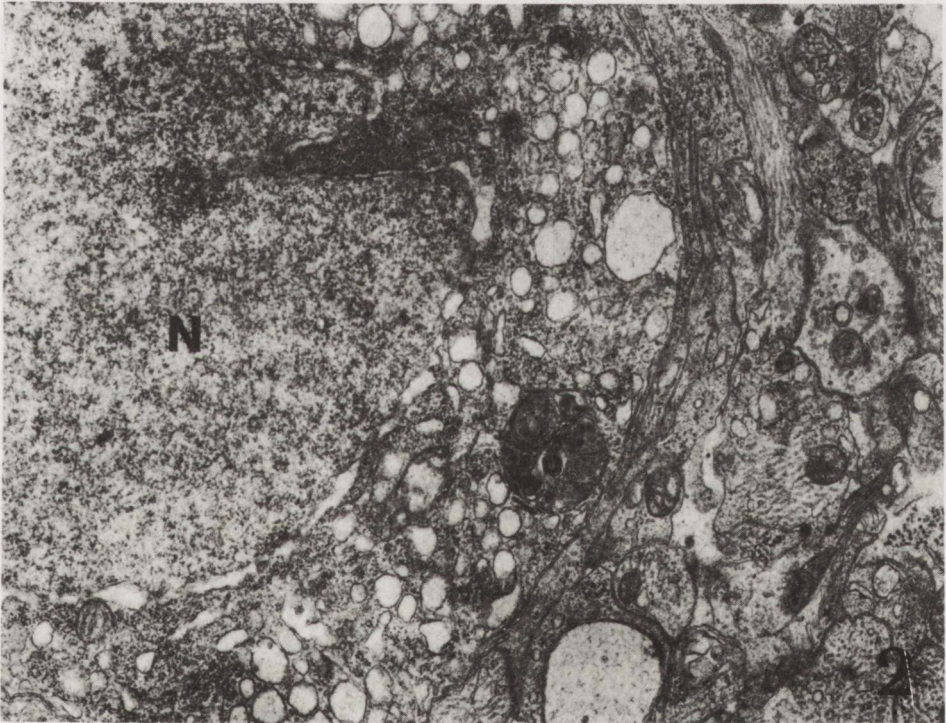


Fig. 2. Hippocampal culture, 24 h after QUIN + verapamil application. Neuron showing vacuolized cytoplasm. Well-preserved nucleus (N). $\times 15\,000$

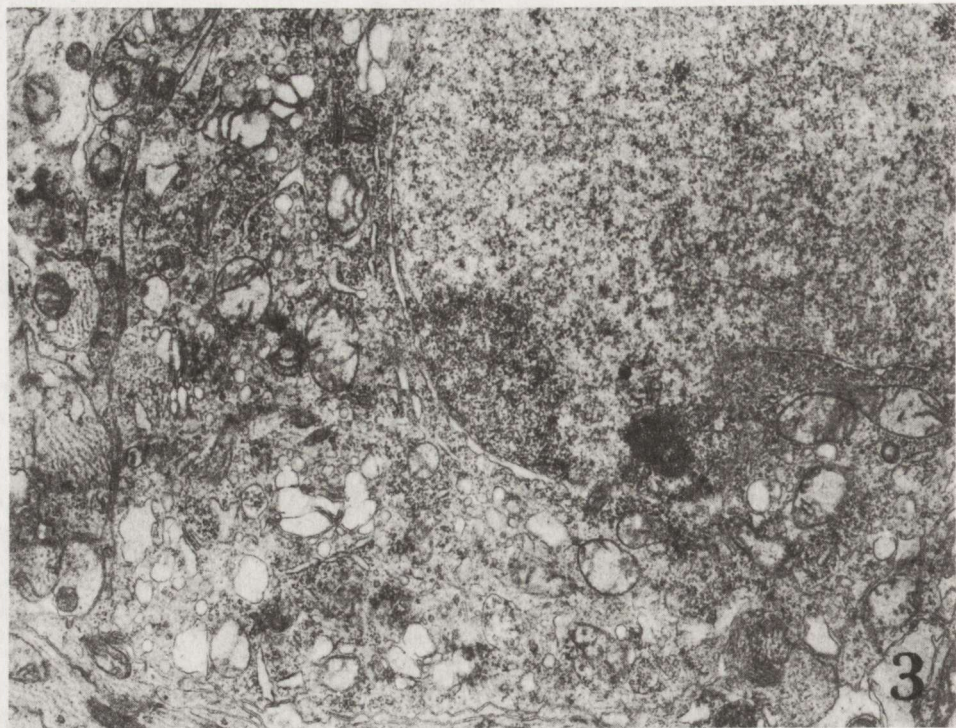


Fig. 3. The same culture. Quite well-preserved neuron. $\times 18\,750$

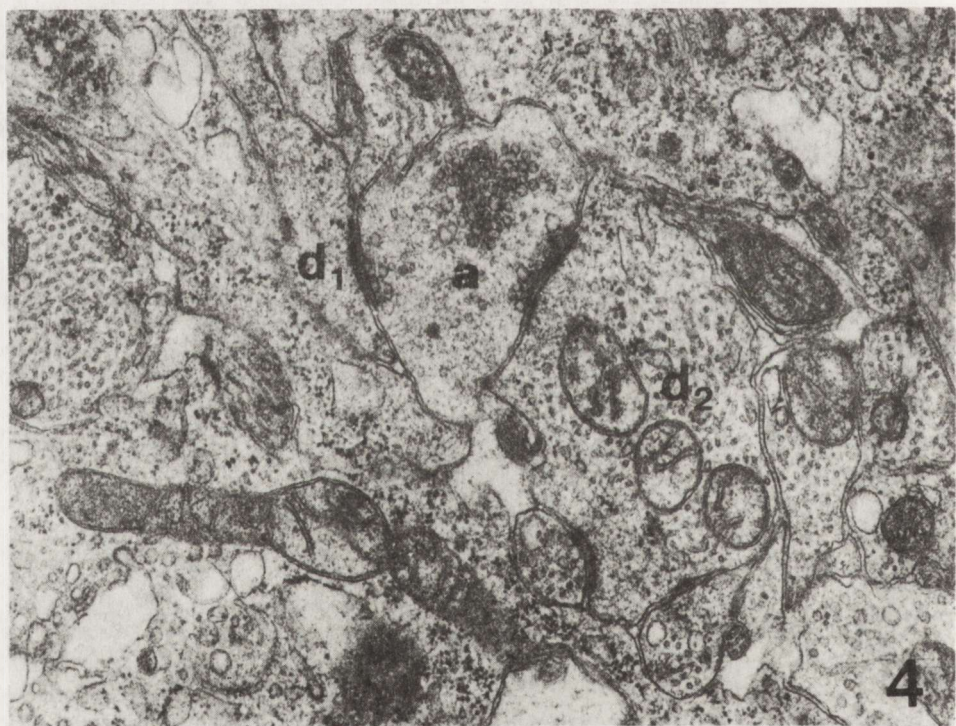


Fig. 4. The same culture. Normally appearing postsynaptic dendrites (d_1 , d_2). Intact axonal bouton (a). $\times 30\,000$



Fig. 5. The same culture. Swollen, electron-lucent dendrite (d) containing damaged mitochondria (MT), vacuoles and multivesicular bodies. Intact axonal bouton (a). $\times 25\ 000$

Fig. 6. The same culture. Dendritic process (d) filled with numerous vacuoles. $\times 30\ 000$

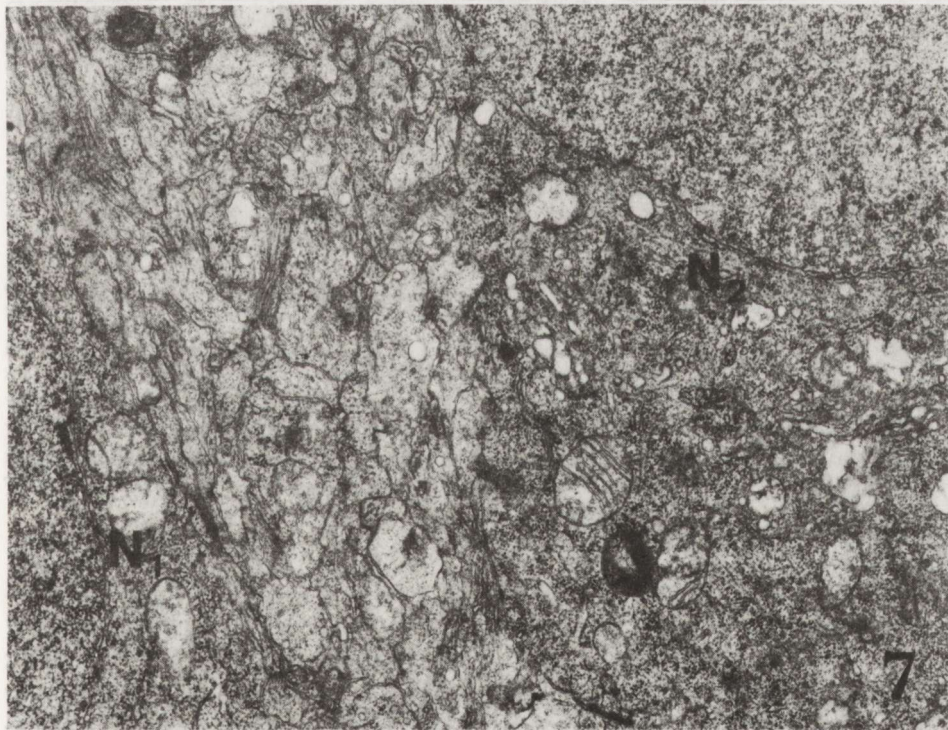


Fig. 7. 7 days post QUIN + verapamil exposure. Well-preserved neurons (N_1 , N_2). $\times 12\ 000$

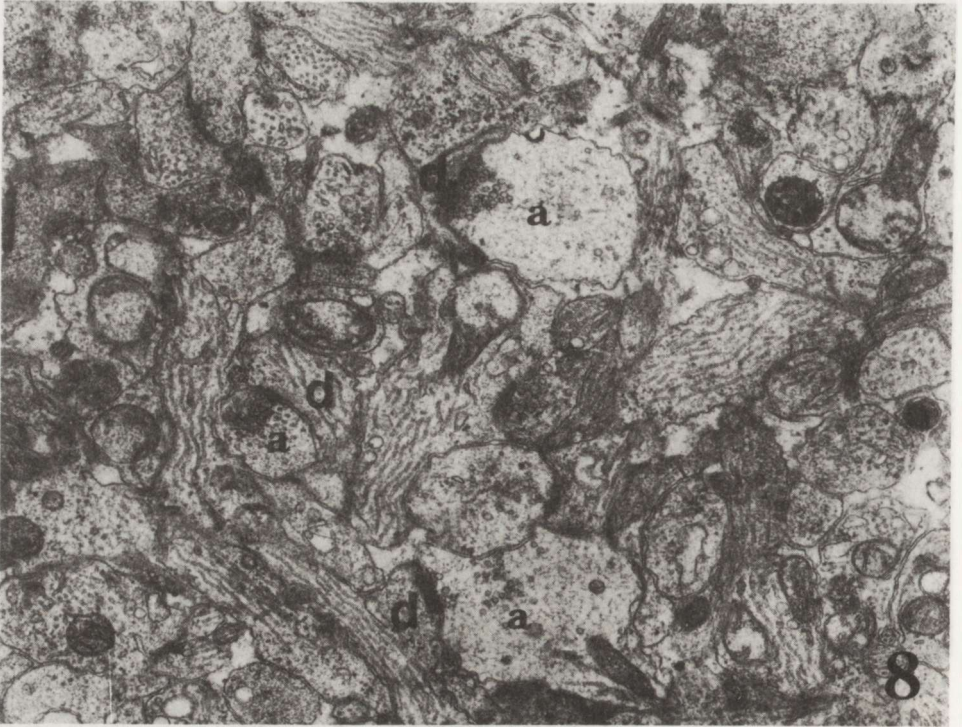


Fig. 8. The same culture. Neuropil containing unchanged axonal terminals (a) and postsynaptic dendrites (d). $\times 25\,000$

ced ultrastructural abnormalities, were very rarely seen. These changes consisted mostly of the presence of vacuoles and/or multivesicular bodies, whereas swelling and enlargement of dendrites did not occur. The majority of both, axonal endings and postsynaptic elements, forming numerous synapses visible in the neuropil remained unchanged (Fig. 8).

The glial cells revealed first swelling of their cytoplasm followed by an increase of gliofilaments.

DISCUSSION

The results of the present study indicate protective effect of the organic calcium entry blocker, verapamil, against QUIN neurotoxicity. The morphological evidence of such an effect was especially pronounced in the later stages of observation.

The exact mechanism of neuronal damage after QUIN is not yet fully understood, as it has been suggested that several factors including sustained depolarization, chloride or potassium influx and excessive calcium entry, may contribute to cell injury in different pathological states (Coyle et al. 1981; Berdichevsky et al. 1983; Mayer, Westbrook 1987). The action of QUIN *via* activation of NMDA subtype receptors has been evidenced in numerous ex-

perimental models (Perkins, Stone 1983; Stone, Connick 1985). The suggestion of association of calcium entry and voltage-sensitive calcium channels in the neurotoxic mechanism of excitatory acidic amino acids has been recently widely proved (Coyle et al. 1983; Choi 1987; Murphy et al. 1988a, b). The brain damage associated with anoxia and epilepsy may be partially due to excessive activation of NMDA receptors (Rothman, Olney 1987). The epileptiform activity could be suppressed by the organic calcium entry blocker-verapamil (Walden et al. 1985; Shelton et al. 1987), however, this effect seemed to be rather nonspecific, owing to inhibition of both postsynaptic and calcium and sodium conductances (Aicardi, Schwartzkroin 1990). Verapamil can partially block postsynaptic calcium channels in CA₁ cells and this block is sufficient to reduce some Ca-dependent potentials and hyperpolarization of pyramidal cells *in vitro* (Jones, Heinemann 1988).

The present morphological study demonstrated that verapamil, which is expected to block calcium channels, can reduce QUIN-induced structural abnormalities. The protective effect of verapamil seems to be more expressed than nimodipine in the same concentration (Matyja, Kida 1991), which was not efficient in eliminating all cytotoxic effects of QUIN. Nevertheless, both results suggest that calcium influx is not the only mechanism responsible for QUIN neurotoxicity. As verapamil appears to be a rather nonspecific tool, owing to inhibition of calcium conductance and postsynaptic sodium conductance, the latter may be involved in its protective effect against the excitatory action of QUIN. The important role of calcium entry in the consequences of QUIN-induced neuronal damage seems, however, to be supported by the present results.

VERAPAMIL ZMNIEJSZA USZKODZENIA NEURONALNE WYWOŁANE PRZEZ KWAS CHINOLINOWY W HODOWLI ORGANOTYPOWEJ HIPOKAMPA SZCZURA

Streszczenie

Celem badań była ocena wpływu werapamilu — blokera kanałów wapniowych na toksyczne działanie kwasu chinolinowego. Badania przeprowadzono na hodowlach organotypowych hipokampa szczura. Materiał oceniono w mikroskopie elektronowym. Werapamil i kwas chinolinowy podawano w stężeniu 100 µm do płynu odżywczego. Wykazano, że werapamil podany jednocześnie z kwasem chinolinowym powoduje zmniejszenie uszkodzeń struktury hipokampa; po 3 i 7 dniach większość neuronów i dendrytów postsynaptycznych była prawidłowo zachowana.

Wyniki potwierdzają sugerowaną rolę napływu jonów wapnia do komórki w mechanizmie neurotoksyczności aminokwasów pobudzających.

REFERENCES

1. Aicardi G, Schwartzkroin PA: Suppression of epileptiform burst discharges in CA₃ neurons of rat hippocampal slices by the organic calcium channel blocker, verapamil. *Exp Brain Res*, 1990, 81, 288—296.
2. Berdichevsky E, Riveros N, Sanches-Armass S, Orrego F: Kainate, N-methylaspartate and other excitatory amino acids increase calcium influx into rat brain cortex cells *in vitro*. *Neurosci Lett*, 1983, 36, 75—80.

3. Choi DW: Ionic dependence of glutamate neurotoxicity. *J Neurosci*, 1987, 7, 369–379.
4. Coyle JT, Bird SJ, Evans RH, Gulley RL, Nadler JV, Nicklas WJ, Olney JW: Excitatory amino acid neurotoxins: selectivity, specificity and mechanism of action. *Neurosci Res Prog Bull*, 1981, 19, 331–427.
5. Griffiths T, Evans MC, Meldrum BS: Temporal lobe epilepsy, excitotoxins and the mechanism of selective neuronal loss. In: *Excitotoxins*, Eds: K Fuxe, P Roberts, R Schwarcz. MacMillan, London, 1983, pp 331–342.
6. Jones RSG, Heinemann U: Verapamil blocks the after hyperpolarization but not the spike frequency accommodation of rat CA₁ pyramidal cells in vitro. *Brain Res*, 1988, 462, 367–371.
7. Kida E, Matyja E: Ultrastructural alterations induced by quinolinic acid in organotypic cultures of rat hippocampus. *Clin Neuropathol*, 1988, 176, 7, abstract.
8. Kretzschmar R, Hoffmann HP: Experimental results relating to CNS activity of verapamil-like calcium antagonists: are they of clinical relevance? In: *Epilepsy and calcium*, Eds: EJ Speckmann, H Schulze, J Walden, Urban and Schwartzberg, Munich, 1986, pp 379–386.
9. Matyja E, Kida E: Protective effect of nimodipine against quinolinic acid-induced damages of rat hippocampus in vitro. *Neuropathol Pol*, 1991, 29, 69–77.
10. Mayer ML, Westbrook GL: Cellular mechanisms underlying excitotoxicity. *Trends Neurosci*, 1987, 10, 59–61.
11. Murphy TH, Malouf AT, Sastre A, Schnaar RL, Coyle JT: Calcium-dependent glutamate cytotoxicity in a neuronal cell line. *Brain Res*, 1988a, 444, 325–332.
12. Murphy TH, Schnaar RL, Coyle JT, Sastre A: Glutamate cytotoxicity in a neuronal cell line is blocked by membrane depolarization. *Brain Res*, 1988b, 460, 155–160.
13. Perkins MN, Stone TW: Quinolinic acid: regional variations in neuronal sensitivity. *Brain Res*, 1987, 19, 172–176.
14. Pooner H, Ransberger P, Petsche H: Calcium antagonists and their effects on generation of interictal spikes: a field potential analysis in the neocortex of the rabbit. In: *Epilepsy and calcium*, Eds: EJ Speckmann, H Schulze, J Walden, Urban and Schwartzberg, Munich, 1986, pp 357–378.
15. Rętz KC, Coyle JT: The differential effects of excitatory amino acid on uptake of CaCl₂ by slices from mouse striatum. *Neuropharmacol*, 1984, 23, 89–94.
16. Rothman SM, Olney JW: Excitotoxicity and the NMDA receptor. *Trends Neurosci*, 1987, 10, 299–302.
17. Schwarcz R, Foster AC, French ED, Wetsell Jr WO, Kohler C: Excitotoxic models for neurodegenerative disorders. *Life Sci*, 1984, 35, 19–32.
18. Shelton RG, Greeb JA, Freed WJ: Induction of seizures in mice by intracerebroventricular administration of the calcium channel agonist BAY k 8644. *Brain Res*, 1987, 402, 399–402.
19. Stone TW, Connick JH: Quinolinic acid and other kynurenes in the central nervous system. *Neuroscience*, 1985, 15, 597–617.
20. Tsuzuki K, Iino M, Ozawa S: Change in calcium permeability caused by quinolinic acid in cultured rat hippocampal neurons. *Neurosci Lett*, 1989, 105, 269–274.
21. Walden J, Speckmann EJ, Witte OW: Suppression of focal discharges by intraventricular perfusion of a calcium antagonist. *Electroencephalogr Clin Neurophysiol*, 1985, 61, 299–309.

Authors' address: Department of Neuropathology, Medical Research Centre, Polish Academy of Sciences, 3 Dworkowa Str, 00-784 Warsaw, Poland

JANINA RAFAŁOWSKA^{1, 2}, DOROTA DZIEWULSKA¹, ZYGMUNT JAMROZIK¹

RARE COEXISTENCE OF CONGENITAL MALFORMATIONS IN ADULT

¹ Department of Neurology, School of Medicine, Warsaw; ² Neuromuscular Unit, Medical Research Centre, Polish Academy of Sciences, Warsaw

Coexistence of several developmental abnormalities in adults is very rare and often asymptomatic. In many instances appearance of clinical symptomatology is evoked by some additional factors, not related directly with the basic pathological process. In a 21-year-old oligophrenic man a progressive paresis of inferior limbs appeared in the course of the upper respiratory tract infection. During 5 days of hospitalization transient peripheral paresis of the right facial nerve, tetraplegia, sphincter and respiratory disturbances occurred. Guillain-Barré syndrome and subarachnoid hemorrhage were diagnosed. On autopsy hemorrhagic focus in the medulla and in the cervical and upper thoracic parts of the spinal cord was found. Microscopic examination revealed hypocellularity of the 2nd and 4th layers of the temporal cortex, presence of the central canal within the brain stem, and hemorrhagic focus in the medulla. Two malformations in spinal cord were revealed: intraspinal angioma extending from the C2 to the Th6 segments and diastematomyelia within Th11 and lumbar segments. Diastematomyelia, cortical hypocellularity and angioma composed of fetal, lacunar artery- and vein-like vessels, are related with different periods of the ontogenic development. Coexistence of these malformations indicates prolonged action of the pathogenic factor(s), both in the embryonic and fetal life.

Key words: *developmental abnormalities, angioma, diastematomyelia.*

Developmental abnormalities of the central nervous system (CNS) are an important cause of still-births and high mortality of neonates and infants. The frequency of these anomalies is different in various countries and oscillates between 5.7 (India) to 11.0 (Ireland) per 10,000 births. Investigations carried out within the prospective Collaborative Perinatal Project by 12 institutions of the United States from 1959 to 1964 registered 55,000 of CNS malformations. Autopsy rate for fetal and neonatal deaths was 92% (Myrianthopoulos 1987). Such a high mortality is usually connected with early and very severe developmental failures of one system (e.g. neuraxis) or with association of malformations in various systems and organs. However, the degree of developmental disturbances varies, and clinical symptoms depend on the degree of damage to the nervous system. Small developmental anomalies can be asymptomatic for a long time. Therefore, developmental abnormalities in adults are rarely diagnosed, until additional factors (trauma, infection, aging changes) lead to appearance of symptomato-

logy not characteristic for malformations. The case presented below exemplifies such a diagnostic error.

CASE REPORT

A 21-year-old man had been treated in the Neurological Department since 18.08.1990 to 25.08.1990. Upper respiratory tract infection, muscle pain and elevated temperature appeared 3 days before admission to the hospital. Two days later increasing weakness of legs was noted. Patient was mentally retarded (47 points in Wechsler's scale). General somatic status was normal. Blood pressure 115/70 mm Hg. Neurological investigation revealed the following abnormalities: central paresis of the right facial nerve, weakness of lower and upper extremities with muscular hypotonia, absence of knee jerks (other tendon reflexes were symmetrical). Flaccid paraplegia, respiratory insufficiency and exacerbation of paresis of the hands were noted the next day after admission. The patient was intubated. During the several following hours he developed flaccid tetraplegia, paresis of the right facial nerve, urinary incontinence and respiratory insufficiency requiring artificial ventilation. Transient clinical improvement of the facial nerve as well as limb paresis preceded circulatory arrest and death. Laboratory tests: CSF was hemorrhagic, after centrifugation dark-yellow, protein 1740 mg%, cell content 36, sediment: erythrocytes, 1 erythrophage, neutral leukocytes and monocytes. EMG normal. EEG: generalized, moderate degree pathological changes, in the left hemisphere predominance. Blood morphology, glucose, urea, creatinine, osmolality, transaminases, thymol test, electrolytes, urinalysis were normal. Clinical diagnosis: Guillain-Barré syndrome, subarachnoid hemorrhage, oligophrenia. At autopsy left side pneumonia and pulmonary edema were found (Dr. R. Wrzaszczyk).

NEUROPATHOLOGICAL EXAMINATION

Postmortem study of formalin-fixed brain and spinal cord revealed: a hemorrhagic focus within the medulla, cervical and upper thoracic spinal cord hemorrhage, subarachnoid hemorrhage and brain edema.

For histopathologic examination numerous paraffin-embedded slices taken from brain and spinal cord were stained with hematoxylin and eosin and according to van Gieson and Klüver-Barrera methods. A part of sections was additionally impregnated by Bielschowsky and Gomori methods. For immunocytochemical evaluation of the blood-brain barrier disturbances and astrocytic reactivity within the spinal cord the PAP technique of Sternberger et al. (1970) was used.

Microscopical examination of the brain revealed subarachnoid hemorrhage and small number of nerve cells in II and IV layers of the temporal (Fig. 1) and entorhinal cortex. In some places of the lateral ventricles wall ependymal cells were lacking and the adjacent subependymal area was rarefied. At the border of midbrain and pons an elongated central canal not contacting with the aqueduct

was visible (Fig. 2). Within the lower part of medulla, rostrally from the pyramid decussation, hemorrhagic focus was found. It involved nucleus nerve XII, dorsal motor nucleus of X nerve, tractus solitarius with its nucleus and cuneate nucleus. In the surrounding necrotic tissue small clusters of polymorphonuclears, some reactive astrocytes, rod cells and perivascular transudates were observed (Fig. 3). Within the bulbar raphe a wide and obliterated central canal was found (Fig. 4). Its walls in some places were formed by small canaliculi surrounded by ependymal cells. The cerebellar vermis and paramedial part of cerebellar hemispheres showed granular cell layer necrosis and considerable loss of Purkinje cells. Marked edema in cerebral and cerebellar hemispheres, and in brain stem was noted. Numerous vessels were fibrotic or hyalinized. Sporadically, thickened and fibrotic veins and lacunar vessels were observed within the pia mater.

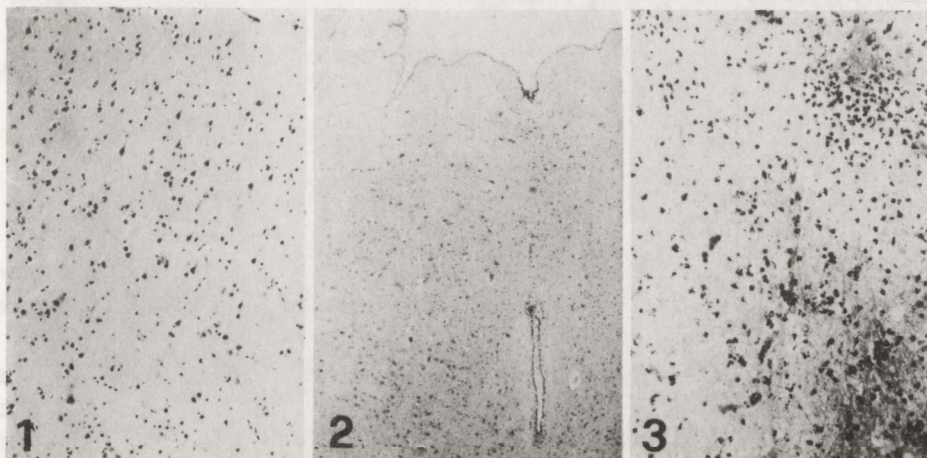


Fig. 1. Medial temporal gyrus. Hypocoellularity of the 2nd and 4th cortical layers. HE. $\times 112$

Fig. 2. Central canal at the border of midbrain and pons. HE. $\times 45$

Fig. 3. Medulla. Necrotic lesion with clusters of polymorphonuclear leukocytes and transudates. HE. $\times 224$

In the spinal cord two kinds of changes were observed: developmental abnormalities manifested by vascular and central canal malformations, and secondary lesions. From the C2 to the Th6 segments of the spinal cord arteriovenous malformation was present. The tumor was formed by vessels of different caliber (Fig. 5). Part of them were rather large arteriole- and venule-like vessels. The structure of their walls was abnormal, with blurred lamination, their walls were often hyalinized and lumina obliterated (Fig. 6). The walls of numerous smaller vessels were very thin, devoid both of muscles and elastic fibers. Greatly distended and lacunar vessels were also visible (Fig. 7). Very numerous vessels showed capillary-like structure.

Within the majority of C2-Th6 segments all kinds of vessels were observed. Within C8 segment capillary vessels predominated and silver impregnation was similar to picture seen in the capillary hemangioblastomas (Fig. 8). There was no

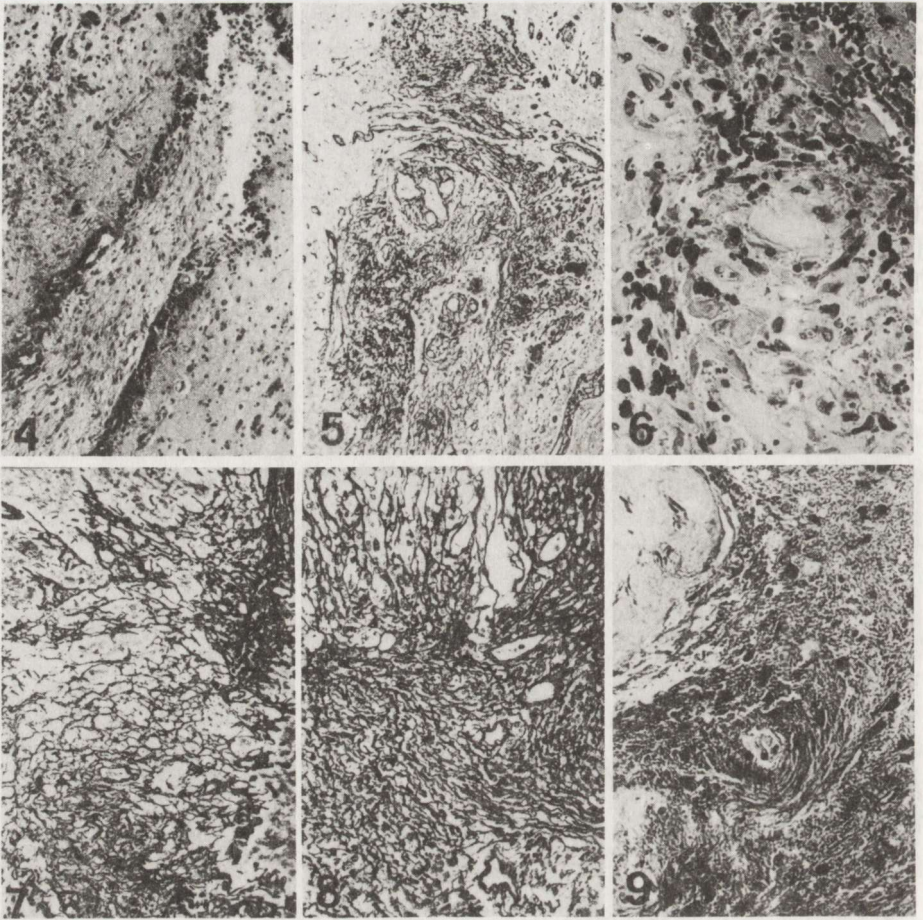


Fig. 4. Medulla. Obliterated central canal. HE. $\times 112$

Fig. 5. Th2 spinal segment. Vessels of various calibers within the tumor. Gomori. $\times 224$

Fig. 6. C5 spinal segment. Arteriole- and venule-like hyalinized vessels in the tumor. Particles of iron pigment. Echymosis. HE. $\times 448$

Fig. 7. C2 spinal level. Various caliber vessels with thin walls. Numerous lacunar vessels. Gomori. $\times 224$

Fig. 8. Th2 spinal level. Part of the tumor resembling a capillary hemangioblastoma. Gomori. $\times 224$

Fig. 9. C2 spinal segment. Reactive astrocytes and GFAP-positive granules in the tumor stroma. GFAP immunoreaction. $\times 448$

cellular stroma between blood vessels. Macrophages usually laden with iron-pigment and hematin pigment were seen within a scanty ground substance (Fig. 6). The surrounding of the tumor was composed of thin, regular, GFAP-positive glial fibers and not numerous reactive astrocytes (Fig. 9). At the Th6 segment, an oval conglomerate of hyalinized arteriole-like vessels within isomorphic glial scar was found (Fig. 10). A large caliber vessel with fibrotic wall along middle posterior fissure was noted at the C5 level. It connected the dorsal surface

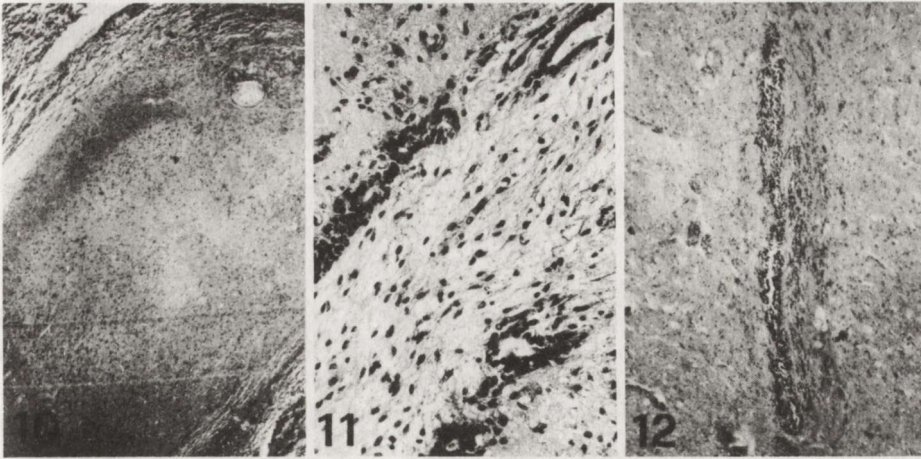


Fig. 10. Th6 spinal segment. Isomorphic glial scar in terminal part of the tumor. GFAP immunoreaction. $\times 45$

Fig. 11. Medulla. Obliterated central canal. Small canaliculi in walls of ventral canal. HE. $\times 224$

Fig. 12. Th11 spinal segment. Elongation of the central canal in dorsal direction. HE. $\times 45$

with the central part of the spinal cord, probably supplying intramedullary angioma.

A prominent irregular central canal was noted within medulla located cranially from the pyramids decussation. A great part of its wall comprised small, round or oval canaliculi surrounded by ependymal cells (Figs 4, 11). Transverse section of the C2 segment look syringomyelic-like because its central part was destroyed by a hemorrhagic lesion. The central canal at that level was not visible. At the remaining cervical cord levels the central canal was oval and greater than usual. Among numerous pathological vessels within central and posterior part of the Th2 level central canal was not detected. At the Th6 level the central canal was irregular, its posterior part had a Y-like shape. At the level of the Th1 segment the central canal was elongated in dorsal direction and occupied about 1/3 of the spinal cord diameter, as if dividing the cord into two halves (Fig. 12). The gray matter of anterior and posterior horns of every „half” was clearly visible. At the L1 level the central canal was also elongated in antero-posterior direction, but wider than at the previous level. In its anterior part numerous narrow finger-like canals were found. Within the canal irregularly arranged clusters of ependymal cells were observed (Fig. 13). At the L3 level the central canal was similar to that within the Th11 segment (Fig. 14). At S2 level a few canals of irregular and various shapes were observed (Fig. 15). Within all the examined spinal cord levels edematous changes (Figs 16, 17) and hemorrhagic lesions of various size were observed. Immunocytochemical reactions for IgG and alpha-1-antitrypsin indicated an increased blood vessels permeability, particularly at the levels of vascular malformation.

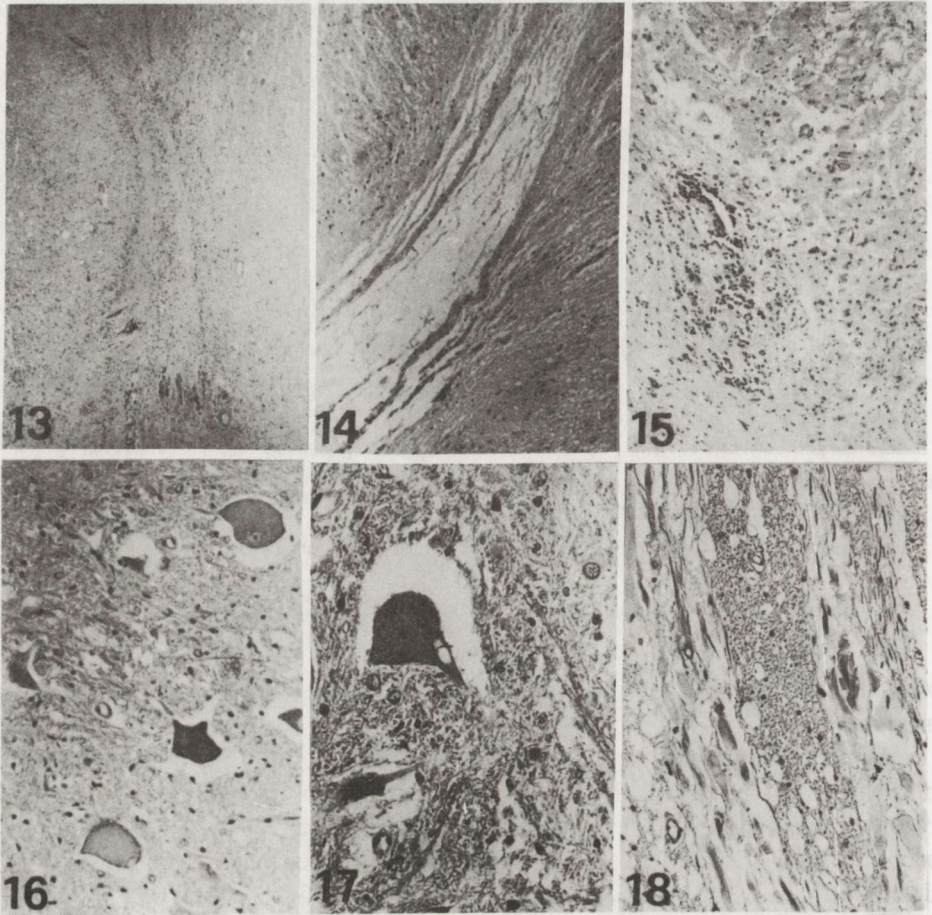


Fig. 13. L1 spinal level. Antero-posterior elongation of the central canal. HE. $\times 45$

Fig. 14. L3 spinal level. Part of the elongated central canal. HE. $\times 112$

Fig. 15. S2 spinal segment. A few irregular central canals. HE. $\times 112$

Fig. 16. S2 spinal segment. Edema in the anterior horn. HE. $\times 224$

Fig. 17. S2 spinal level. Vacuolar degeneration of the motor neuron. HE. $\times 224$

Fig. 18. S2 spinal level. Swelling of motor neuron axons. HE. $\times 112$

DISCUSSION

Neuropathological examination of the presented case revealed coexistence of two pathological processes involving brain stem and spinal cord. They took the form of intraspinal angioma and malformation of the central canal. Accumulation of blood vessels of different caliber characterized by various maturity of their walls, very small amount of foamy cells, and the presence of astrocytes and glial fibers within the stroma of angiomatous conglomerates enable to diagnose a vascular developmental abnormality. The other type of developmental abnormality was represented by the malformation of the central canal. The existence

of the central canal localized at the border of midbrain and pons, within the medulla and extending into the spinal cord, great enlargement and widening of which resulted in division of the spinal cord into two halves at the Th11 level, and lumbar segment points to the anomaly of raphe formation in the neural tube. This type of alteration is probably connected with disturbances in the neural plate fusion (Benda 1959), which begins on the 22nd day with closure of its rostral and caudal neuropores on 24th and 26th day of embryonic life, respectively (O'Rahilly, Muller 1987).

Factors evoking errors of the neural tube fusion often influence also the development of tissue deriving from other embryonic layers. Then, the degree of impairment is determined both by a period in which the pathogenic factor is active, and by interaction between the neural tube and the elements deriving from mesoderm (Kallen 1987). Malformations arising in this very early period, classified to dysraphic states, include, not rarely, both the nervous system as well as meninges and bone system. Within the spinal cord, dysraphism manifested by spina bifida in a light form, may be limited to the lack of fusion of the vertebral arches (*spina bifida occulta*). It probably appears later than more severe forms of spina bifida such as meningocele, myelomeningocele, diastematomyelia, diplomyelia and hydromyelia. Rarely spina bifida is associated with hyper- or hypoplasia of the spinal cord part (Friede 1975), anencephaly (Padget 1970), and with malformations containing also tissues deriving from the entodermal layer (Bentley, Smith 1960; Friede 1975; Yasuda et al. 1990). Diastematomyelia is most frequently localized at the lumbar region of the spinal cord. Lower thoracic and cervical spinal segments are less frequently involved (Sheptak, Susen 1967; Friede 1975; Simpson, Rose 1987). Basicranial localization of the pathological process is unusually rare (Pfeifer 1971).

Clinical manifestation of the anomaly appears usually in neonates (Glasier et al. 1990; Konner et al. 1990) or in children in the first decade of life (Sheptak, Susen 1967; Ritchie, Flanagan 1969; Elias-Jones et al. 1990). However, in a number of cases first clinical symptoms of the proces became apparent in the adult life (Benda 1967; James, Lassmann 1970; English, Maltby 1967; Whitney et al. 1990). The wide range of age in which clinical symptomatology of this early developmental disorder is manifested seem to depend on the degree of spinal duplication. Duplication with separation of the two halves by a bone spur represents an extreme degree of cord dysraphia. Duplication of the central canal or its dorsal elongation observed in our case represent also diastematomyelic changes (Friede 1975). Thus, our case presents two developmental abnormalities: intraspinal angioma within cervical and upper thoracic parts of the spinal cord, and incomplete diastematomyelia in its inferior thoracic and lumbar parts. The pathomechanism of these malformations seem to be different.

Fetal vascularization appears parallelly with nervous system development. In the stage of neural tube closing primitive vascular plexus, covering the surface of the developing nervous system, is formed. Then, capillary vessels appear approximately on the 28th embryonal day, penetrating to the brain and spinal cord.

After a few days (on 32nd embryonal day) some arteries can be distinguished (Streeter 1915, 1918). Like other tissues, blood vessels develop in abundance and according to the rostral-caudal gradient of fetal development; their quantity is gradually reduced.

Involution of the vascular overgrowth observed in chicken embryos, like other developing tissues, takes place through apoptosis of endothelial cells, migration of endothelial cells away from the vascularized regions and by mesenchymal transformation (Latker et al. 1986). Angioma, containing vessels of various caliber ranging from fetal and lacunar to thick, probably arterial and venous ones, seems to indicate either disturbances of physiologic cell death in ontogenesis or disturbances of relationship between vascular overgrowth and regression. The stage of primitive fetal vessels formation corresponds to a period of neural plate appearance. The presence of artery-like and vein-like vessels suggests two possible periods in which pathogenic factor had been operating upon the developing embryo. Firstly, the pathological factor was acting at the stage of neural tube closing; primitive vessels abundant within the proximal part of the neural tube matured within the developing spinal cord. Secondly, the pathogenic factor was operating for a longer time, disturbing the regression of larger caliber vessels. The presence of more than one artery, which supplies usually intramedullary cervical angioma (Djindjian 1978) rather supports the second hypothesis. Hypocellularity of the granular layers observed in the temporal cortex may support prolonged action of the pathogenic factor, whatever its nature. The second great wave of cell migration during cerebral cortex formation occurs from the 11th to the 15th week of the fetal life. Therefore, the possibility exists that disturbances in the central nervous system development occurred both in the embryonal and the fetal periods.

Fetal vessels persisting in the meninges are frequently observed in dysraphism (Friede 1975). In our case fetal vessels persisting both in meninges and within the spinal cord were disclosed. Intraspinial angioma has rarely been reported in cases with spina bifida. Clinically, intra- or retromedullary angiomas are manifested by subarachnoid hemorrhage or hematomyelia (Wyburn-Mason 1943; Russel, Rubinstein 1963), which frequently occur within the cervical and upper-thoracic spinal segments, and mostly in children and young adults (Djindjian 1978). The question arises what was the cause of massive hemorrhage in our case. Numerous hemosiderin-laden macrophages between vessel conglomerates may indicate occurrence of small hemorrhage in the past. However, within the cervical spinal segments perivascular lymphocytic cuffings were found. It is not clear whether they were due to reaction caused by slowly progressing damage of spinal cord in the presence of angioma, or were exponents of viral infection which led to permeability disturbances of pathological vessels within the spinal cord.

RZADKI PRZYPADEK WSPÓLISTNIENIA WAD ROZWOJOWYCH
U DOROSŁEGO MĘŻCZYZNY

Streszczenie

W wieku dorosłym współlistnienie kilku nieprawidłowości rozwojowych jest bardzo rzadkie i często bezobjawowe. Zadziałanie dodatkowego czynnika uszkadzającego może spowodować rozwój objawów klinicznych.

U 21-letniego oligofrenika po przebytej infekcji górnych dróg oddechowych wystąpił narażający niedowład kończyn dolnych. W trakcie 5-dniowej hospitalizacji obserwowano obwodowe porażenie n. VII, porażenie kończyn górnych i dolnych, zaburzenia zwieraczy i oddechowe. Zgon poprzedziło nagłe zatrzymanie czynności serca. Rozpoznano zespół Guillain-Barré oraz krwotok podpajęczynówkowy. Na sekcji stwierdzono ognisko krwotoczne w opuszce oraz w odcinku szyjnym i piersiowym górnym rdzenia kręgowego. Badanie mikroskopowe wykazało redukcję neuronów w 2 i 4 warstwie kory skroniowej, obecność kanału centralnego w obrębie pnia mózgu oraz ognisko krwotoczne w opuszce. W rdzeniu kręgowym stwierdzono obecność dwóch nieprawidłowości rozwojowych: śródrzeniowy naczyniak w odcinku C2 – Th6 i diastematomielię w obszarze Th11 – odcinek lędźwiowy. Ponieważ każda z trzech stwierdzonych nieprawidłowości powstaje w innym okresie rozwoju ontogenetycznego, ich współlistnienie wskazuje na przedłużone działanie czynnika/ków patogennego, obejmujące zarówno okres rozwoju embrionalnego, jak i płodowego.

REFERENCES

1. Barson AJ: Spina bifida: the significance of the level and extent of the defect to morphogenesis. *Dev Med Child Neurol*, 1970, 12, 129–144.
2. Benda CE: Dysraphic states. *J Neuropathol Exp Neurol*, 1959, 18, 56–74.
3. Bentley JFR, Smith JR: Developmental posterior enteric remnants and spinal malformations. *Arch Dis Child*, 1960, 35, 76–86.
4. Djindjian R: Angiomas of the spinal cord. In: *Handbook of Clinical Neurology*. Eds: PJ Vinken, GW Bruyn. North-Holland Publ, Amsterdam, 1978, vol 32, pp 465–510.
5. Elias-Jones AC, Jaspan T, Mellor DH, Worthington BS: Magnetic resonance imaging in neurological disorders. *Arch Dis Child*, 1990, 65, 922–929.
6. English WJ, Maltby GL: Diastematomyelia in adults. *J Neurosurg*, 1967, 27, 260–264.
7. Friede RL: *Developmental Neuropathology*, Springer, Wien-New York, 1975, pp 241–277.
8. Glasier CM, Chaddock WM, Leithiser RE Jr, Williamson SL, Seibert JJ: Screening spinal ultrasound in newborns with neural tube defects. *J Ultrasound Med*, 1990, 9, 339–343.
9. James CC, Lassman LP: Diastematomyelia and the tight filum terminale. *J Neurol Sci*, 1970, 10, 193–196.
10. Kallen B: Errors in the differentiation of the central nervous system. In: *Handbook of Clinical Neurology*. Ed: NC Myrianthopoulos. Elsevier, Amsterdam, 1987, vol 6(50), pp 19–47.
11. Konner C, Gasser J, Mayr U, Kreczy A: Diagnosis of diastematomyelia using ultrasound. *Klin Pediatr*, 1990, 202, 124–129.
12. Latker CH, Finberg RN, Beebe DC: Localized vascular regression during limb morphogenesis in the chicken embryo; II Morphological changes in the vasculature. *Anat Rec*, 1986, 214, 410–417.
13. Myrianthopoulos NC: Epidemiology of central nervous system malformations. In *Handbook of Clinical Neurology*. Ed NC Myrianthopoulos, Elsevier, Amsterdam, 1987, vol 6(50), pp 49–69.
14. O'Rahilly R, Muller F: The developmental anatomy and histology of the human central nervous system. In *Handbook of Clinical Neurology*. Ed NC Myrianthopoulos, Elsevier, Amsterdam, 1987, vol 6(50), pp 1–17.
15. Padget DH: Neuroschisis and human embryonic maldevelopment: new evidence on anencephaly, spina bifida and diverse mammalian defects. *J Neuropathol Exp Neurol*, 1970, 29, 192, 216.
16. Pfeifer JD: Basicranial diastematomyelia: a case report. *Clin Neuropathol*, 1991, 10, 232–236.

17. Ritchie GW, Flanagan MN: Diastematomyelia. *Can Med Assoc J*, 1969, 100, 428.
18. Russel DS, Rubinstein LJ: Tumors and hamartomas of the blood vessels. In *Pathology of Tumors of the Nervous System*, E Arnold, London, 1963, pp 73–92.
19. Sheptak PE, Susen AF: Diastematomyelia. *Am J Dis Child*, 1967, 19, 761–767.
20. Simpson RK, Rose JE: Cervical diastematomyelia: report of a case and review of a rare congenital anomaly. *Arch Neurol*, 1987, 44, 331–335.
21. Sternberger LA, Hardy PM Jr, Cuculis FF, Meyer MG: The unlabelled antibody enzyme method of immunochemistry preparation and properties of soluble antigen-antibody complex (horseradish peroxidase-antiperoxidase) and its use in identification of spirochetes. *J Histochem Cytochem*, 1970, 18, 315–333.
22. Streeter G: The development of the venous sinuses of the dura mater in the human embryo. *J Anat*, 1915, 18, 145–178.
23. Streeter G: The developmental alterations of the vascular system of the brain of the human embryo. *Contr Embryol*, 1918, 8, 5–38.
24. Whitney RW, Brenner R, Gulati R: Occult diastematomyelia in adults. Report of two cases. *Clin Radiol*, 1990, 41, 415–417.
25. Wyburn-Mason R: *The vascular abnormalities and tumors of the spinal cord and its membranes*. H Kimpton, London, 1943.
26. Yasuda Y, Konishi H, Kihara T, Tanimura T: Discontinuity of primary and secondary neural tube in spina bifida induced by retinoic acid in mice. *Teratology*, 1990, 41, 257–274.

Authors' address: Department of Neurology, School of Medicine, 1A Banacha Str., 02-097 Warszawa, Poland

HANNA DRAC^{1, 2}, JAROSŁAW PNIEWSKI¹, JANINA RAFAŁOWSKA^{1, 2}

MORPHOLOGICAL CHANGES IN THE PERIPHERAL NERVOUS SYSTEM IN THE CASE OF CONGENITAL MALFORMATIONS OF THE SPINAL CORD

¹ Department of Neurology, School of Medicine, Warsaw; ² Neuromuscular Unit, Medical Research Centre, Polish Academy of Sciences, Warsaw

A 21-year-old oligophrenic man developed after upper respiratory tract infection, quadriplegia with spincter and respiratory disturbances. Lumbar puncture revealed subarachnoid bleeding and elevated cerebrospinal protein level. Guillain-Barré syndrome and subarachnoid hemorrhage were diagnosed. At autopsy intraspinal angioma (C₂-D₆) and diastematomyelia (D₁₁, lumbar segments) were found. Beside, intraspinal hemorrhage was present. Morphological examination of posterior and anterior spinal roots as well as peripheral nerves was done. Spheroids, axonal degeneration and prominent loss of myelinated fibers were observed in the proximal parts of the spinal roots. Axonal degeneration of myelinated fibers and regenerated fibers were noted in the distal parts of spinal roots and in peripheral nerves. Abnormal, fetal-like vessels were present in the spinal roots. Two mechanisms of acute and chronic changes (transneuronal and Wallerian degeneration) are discussed.

Key words: *spinal cord malformations, peripheral nervous system, axonal degeneration-regeneration.*

Morphological changes in the peripheral nervous system due to congenital malformations in the nervous system are extremely rare. Similarly, Wallerian degeneration, except of traumatic damage to the nerve, is encountered exceptionally.

We present a case of malformations in the spinal cord with pathological changes in the peripheral nervous system. In this case Wallerian degeneration of the nerve fibers appeared before the patient's death.

CASE REPORT

R.P., 21-year-old oligophrenic workman was admitted to the Department of Neurology because of increasing paresis of lower limbs preceded by muscle pain and upper respiratory tract infection. Neurological examination on admission revealed: central paresis of the right facial nerve, flaccid paresis of all extremities, knee jerks absent. On the second day progression of the weakness of upper extremities and lower paraplegia as well as respiratory disturbances leading to intubation developed. Next, right facial nerve palsy and quadriplegia with

sphincter disturbances were observed. Artificial respiration was applied. After transient improvement the patient died on the 6th day of hospitalization because of cardiac arrest.

Laboratory investigations: CSF hemorrhagic, cytosis 36, protein level 1740 mg%, sediment: erythrocytes, erythrophages, granulocytes, monocytes. Electro-physiology: motor and sensory conduction velocity in the peripheral nerves on

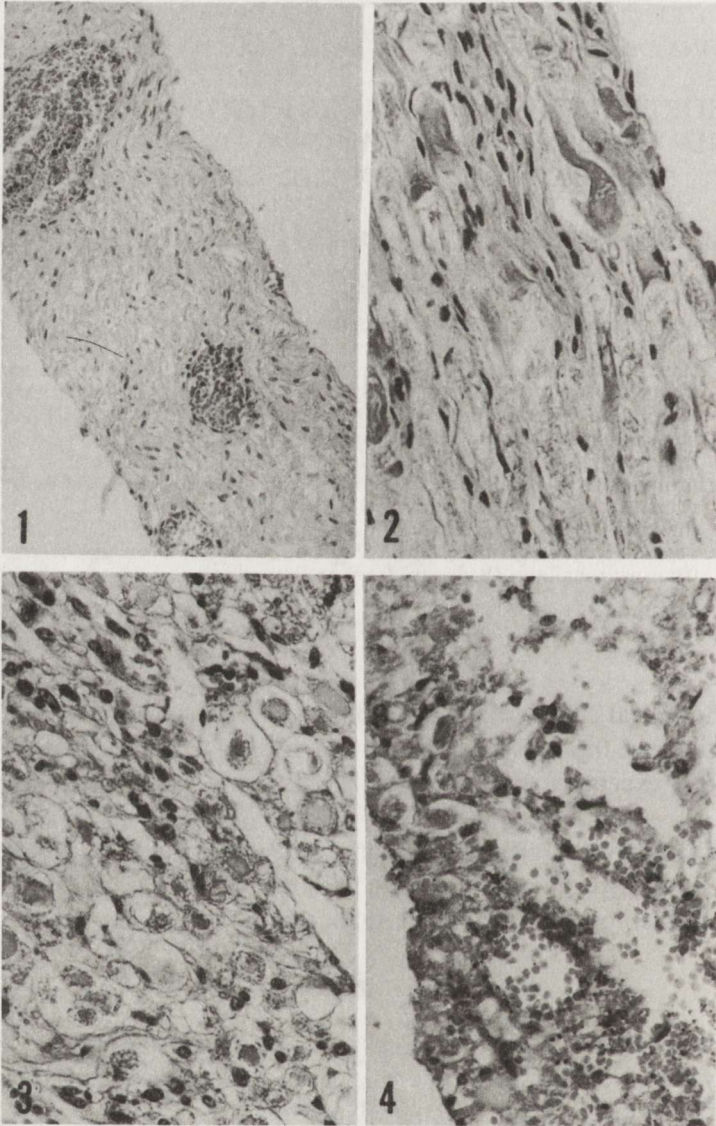


Fig. 1. Anterior root C₈ (proximal part). Thin-walled fetal-like venous vessels. HE × 110

Fig. 2. Anterior root C₈ (proximal part). Swollen axons. HE. × 220

Fig. 3. Posterior root S₁ (proximal part). Spheroids. Degeneration of axons. HE. × 220

Fig. 4. Posterior root S₂ (proximal part). Loss of fibers. Spheroids. Petechiae. HE. × 220

upper and lower extremities within normal range. ECG — ventricular tachycardia, myocardial ischemia. Routine biochemical examination — normal.

Guillain-Barré syndrome, subarachnoid hemorrhage, oligophrenia were diagnosed.

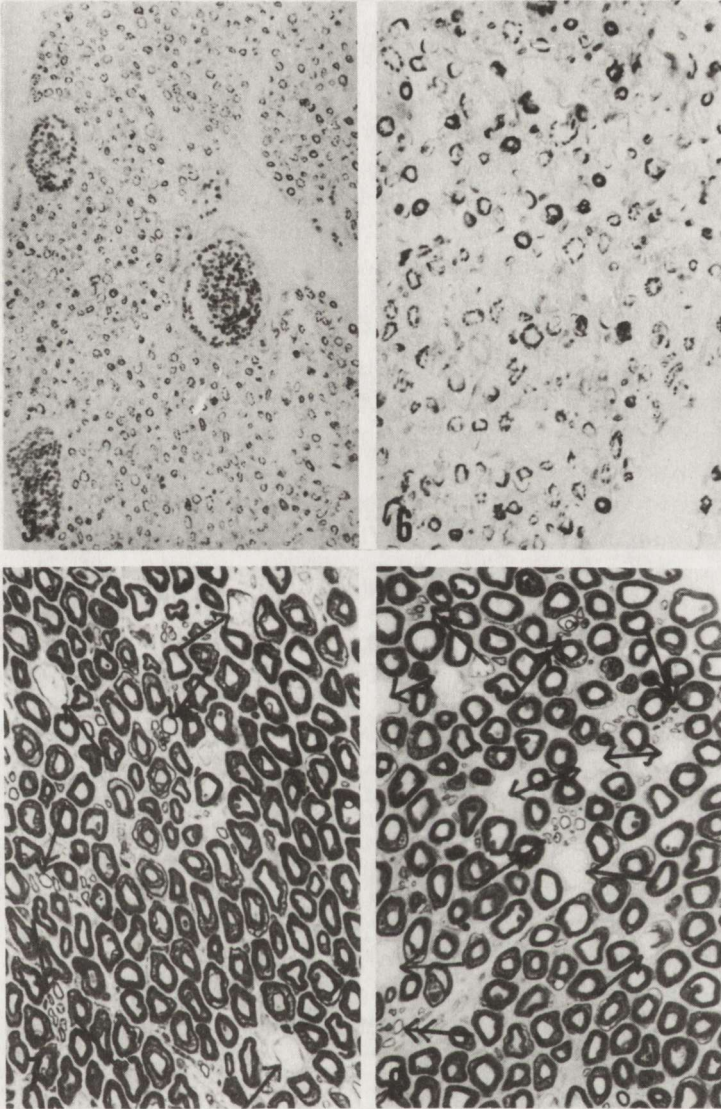


Fig. 5. Anterior root S_1 (proximal part). Abnormal vessels filled with blood. Klüver-Barrera. $\times 110$

Fig. 6. Anterior root S_1 (proximal part). Loss of myelinated fibers. Klüver-Barrera. $\times 220$

Fig. 7. Posterior root S_1 (distal part). Axonal degeneration (arrows). Regenerated fibers (double arrows). Epon section. $\times 220$

Fig. 8. Anterior root S_1 (distal part). Axonal degeneration (arrows). Regenerated fibers (double arrows). Epon section. $\times 220$

At autopsy of brain and spinal cord a hemorrhagic focus within the medulla oblongata, brain edema and subarachnoid hemorrhage were found.

Histological examination of the spinal cord revealed: 1. Needle-like intraspinal haemangioma C₂-Th₆ localized in the central and dorsal parts of the spinal cords, probably influencing configuration of the dorsal horns and the posterior cords; 2. Congenital malformation of spinal cord in the form of diastematomyelia at lower thoracic and lumbar levels. Malformation manifested by the presence of an elongated canal which protruded into the posterior spinal cord and dorsal horns at segments L₁, L₂ and L₃. A few irregular and different-shaped central canals were seen in S₁ and S₂ segments; 3. In segments C₈-Th₆ and at the lumbosacral level the hemorrhage had destroyed the dorsal horn and the adjoining lateral and posterior cord. Outstanding edema manifesting by interstitial rarefaction, acute edema of the neurons, especially of the motoneurons and their axons, was present at all examined levels of the spinal cord (For details see: Rafałowska et al. 1992).

Morphological changes in the dorsal roots and in the peripheral nerves.

In the proximal parts of the dorsal and the anterior roots at cervical and thoracic levels of the spinal cord numerous thin-walled venous vessels filled up with blood were present (Fig. 1). Swelling of numerous axons of the anterior roots could be discerned (Fig. 2). At the lumbosacral level interstitial rarefaction or lacunas surrounded by swollen axons (L₁, S₂) or petechiae (S₂) and fetal-like and lacunar vessels (S₂) were visible in the proximal parts of the dorsal and anterior roots (Figs 3 and 4). In some fascicles of the spinal roots loss of fibers was revealed by the Klüver-Barrera method (Fig 5 and 6). In the distal part of the dorsal root and the anterior root S₁, on the thick Epon sections numerous myelinated fibers

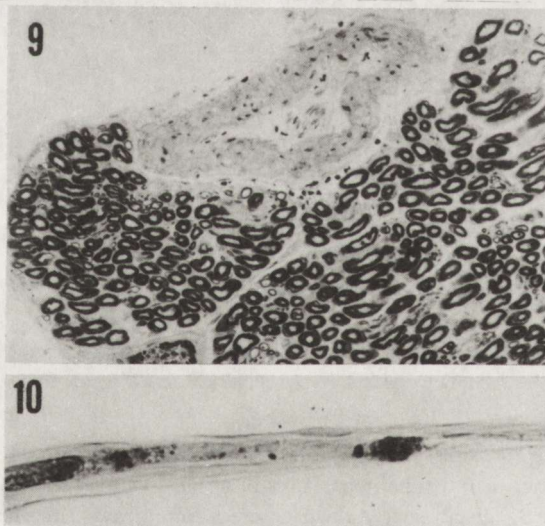


Fig. 9. Posterior root S₁ (distal part). Abnormal vessel. Epon section. $\times 110$

Fig. 10. Teased fiber from posterior root S₁ (distal part). Axonal degeneration $\times 110$

undergoing axonal degeneration and, occasional small groups of thin fibers (regenerated fibers) were visible (Figs 7 and 8). The intensity of pathological changes was similar in the posterior and the anterior roots. An abnormal large vessel was seen within the dorsal root S_1 (Fig. 9). Among the fibers teased out from dorsal root S_1 one fiber showed breakdown into ovoids (Fig. 10).

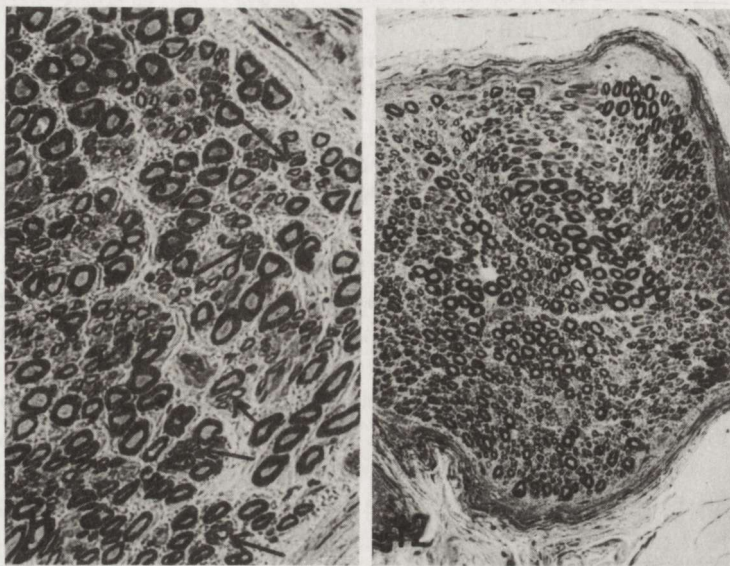


Fig. 11. Ulnar nerve. Regenerated fibers (arrows). Epon section. $\times 220$

Fig. 12. Sural nerve. Discrete loss of fibers. Numerous thin (regenerated?) fibers. Epon section. $\times 110$

The ulnar, radial and sural nerves were examined. In the ulnar nerve on thick Epon sections thin regenerated fibers were present (Fig. 11). The sural nerve showed a slight degree loss of myelinated fibers and the presence of numerous thin fibers (Fig. 12). The radial nerve was normal. There were no pathological changes in the fibers isolated from the examined nerves.

DISCUSSION

The morphological changes observed in our case in the spinal roots can be classified as acute (spheroids, breakdown of fibers, loss of fibers) and chronic ones (axonal degeneration and regeneration of fibers). Acute changes concern the proximal parts of the anterior and posterior roots. Chronic changes were encountered in the distal parts of the spinal roots. Moreover, thin-walled, fetal-like vessels were much more numerous in the proximal parts of the spinal roots. Acute changes in the proximal parts of the spinal roots are secondary to acute changes in the spinal cord (hemorrhage, petechiae). Spinal edema caused swelling of the motoneurons and their axons within the spinal cord and axonal degeneration leading to loss of fibers observed in the proximal parts of the anterior roots. Acute

changes in the spinal cord resulted in loss of fibers in the proximal (postganglionic) part of the posterior roots by the mechanism of Wallerian and retrograde degeneration.

Two mechanisms could be considered to explain chronic changes in the distal parts of the anterior and the posterior roots (preganglionic part) as well as in peripheral nerves. The first mechanism is the presence of chronic changes in the spinal cord, viz. recurrent erythrorrhagias from abnormal vessels evidenced by macrophages laden with iron pigment and hematin pigment. Unlike the anterior roots, axonal degeneration followed by regeneration of fibers in the posterior roots would be the result of transneuronal degeneration. Another mechanism resulting in chronic changes might be connected with the presence of abnormal fetal-like vessels in the spinal roots. Recurrent small hemorrhages from thin-walled vessels of little value and hemodynamic disturbances could play a role in the degeneration and regeneration in the distal parts of the anterior and posterior roots. Numerous thin regenerated fibers contribute to relatively good density in the proximal parts of the spinal roots and in the ulnar nerve.

Two questions seem to be worth underlining in the presented case. Axonal degeneration in the proximal parts of the dorsal roots is the equivalent of experimental Wallerian degeneration due to transection of the nerve (Waller 1850; Weddell, Glees 1941; Miledi, Slater 1970). In our case this entity had occurred and developed during the patient's life. Wallerian degeneration begins near the point of nerve interruption and progressively spreads distally (Joseph 1973; Lubińska 1975). The proximodistal advance of degeneration consists of a progressive involvement of consecutive internodes along the fiber. The speed of the subsequent advance depends on the fiber size being 250 mm/day for thin fibers and 46 mm/day for thick fibers of the rat phrenic nerve (Lubińska 1977). It is probable that the speed of distal axonal degeneration and ongoing proximodistal degeneration resulting from damage to the nerve cell is similar. This might explain the disproportion of degenerative changes in the proximal and the distal parts of the spinal roots and in the peripheral nerves, pointing to different mechanisms of degeneration in the two parts of the spinal roots.

As mentioned above, an abnormal central canal protruded in some segments into the dorsal cord and the posterior horn. Within these structures run fibers belonging to the first sensory neurons and lie cells sending connections to the second sensory neuron, interneurons and motoneurons (Rexed 1964; Sprague, Hongchein 1964). The patient was a workman; on neurological examination there was no sensory disturbances which would imply lack of substantial motor and sensory deficit during patient's life course, pointing at plasticity of the spinal cord — its adjustment to functioning in anatomically diverse conditions.

ZMIANY MORFOLOGICZNE W OBWODOWYM UKŁADZIE NERWOWYM
W PRZYPADKU WRODZONYCH MALFORMACJI RDZENIA KRĘGOWEGO

Streszczenie

U 21-letniego oligofrenika po przebyciu infekcji górnych dróg oddechowych wystąpił niedowład kończyn oraz zaburzenia zwieraczy i oddechowe. W płynie mózgowo-rdzeniowym stwierdzono obecność krwi i podwyższony poziom białka. Rozpoznano zespół Guillain-Barré oraz krwotok podpajęczynówkowy. Na sekcji stwierdzono obecność śródrdzeniowego naczyńniaka w odcinku C₂-Th₆ i diastematomielię (Th₁₁ — odcinek lędźwiowy). Badanie morfologiczne przednich i tylnych korzeni rdzeniowych oraz nerwów obwodowych wykazało: sferoidy, zwyrodnienie aksonów oraz znaczny ubytek włókien mielinowych w proksymalnych częściach korzeni rdzeniowych; w odcinkach dystalnych korzeni rdzeniowych i w nerwach obwodowych — zwyrodnienie aksonów i włókien mielinowych oraz regenerację włókien. W korzeniach rdzeniowych obserwowano ponadto nieprawidłowe naczynia, podobne do naczyń płodowych. Przedyskutowano mechanizm rozwoju ostrej i przewlekłej zmian (zwyrodnienie transneuronalne i Wallera).

REFERENCES

1. Joseph BS: Somatofugal events in Wallerian degeneration: a conceptual overview. *Brain Res*, 1973, 59, 1—18.
2. Lubinska L: On axoplasmic flow. *Int Rev Neurobiol*, 1975, 17, 241—249.
3. Lubinska L: Early course of Wallerian degeneration in myelinated fibers of the rat phrenic nerve. *Brain Res*, 1977, 130, 47—63.
4. Miledi R, Slater CR: On the degeneration of rat neuromuscular junctions after nerve section. *J Physiol (London)*, 1970, 207, 507—528.
5. Rafałowska J, Dzięwulska D, Jamrozik Z: Rare coexistence of congenital malformations of the spinal cord in an adult. *Neuropatol Pol*, 1992, subjected.
6. Rexed B: Some aspects of the cytoarchitectonics and synaptology of the spinal cord. In: *Organisation of the spinal cord*. Eds: JC Eccles, JP Schade. Elsevier, Amsterdam, 1964, pp 58—92.
7. Sprague JM, Hongchein H: The terminal fields of dorsal root fibers in the lumbosacral spinal cord of the cat, and the dendritic organisation of the motor nuclei. In: *Organisation of the spinal cord*. Eds: JC Eccles, JP Schade. Elsevier, Amsterdam, 1964, pp 120—154.
8. Waller AV: 1850, acc. to Lubinska L, 1977.
9. Weddel G, Glees P: The early stages in the degeneration of cutaneous nerve fibers. *J Anat (London)*, 1941, 76, 65—93.

Author's address: Department of Neurology, School of Medicine, 1A Banacha Str., 02-097 Warszawa, Poland

ELŻBIETA KIDA¹, MARIA BARCIKOWSKA¹, EWA JOACHIMOWICZ²,
TERESA MICHALSKA², ALINA SIEKIERZYŃSKA³, ANNA WALASIK⁴,
KRZYSZTOF ROSZKOWSKI³, EWA FIGURA³

PARANEOPLASTIC SUBACUTE SENSORY NEURONOPATHY. CLINICAL-PATHOLOGICAL STUDY

¹ Department of Neuropathology, Medical Research Centre, Polish Academy of Sciences, Warsaw;
² IInd Department of Neurology, School of Medicine, Czerniakowski Hospital, Warsaw; ³ Institute of
Tuberculosis and Chest Diseases, Warsaw; ⁴ Department of Neurology, Bródnowski Hospital,
Warsaw, Poland

We report 2 cases of subacute sensory neuropathy (SSN) in small cell cancer of the lung. In both cases motor disturbances were caused by motor neuropathy and neuropathy as well. In both cases we observed altered immunoreactivity of the nervous tissue, suggesting the participation of humoral immunity in the tissue damage.

Key words: *oat cell lung cancer, paraneoplastic syndrome, subacute sensory neuropathy, immunocytochemistry.*

The highest incidence of nonmetastatic neurological complications in patients with malignancy (paraneoplastic syndromes) is encountered with lung cancer (Croft, Wilkinson 1965; Henson, Urich 1982). One of them, ganglioradiculitis associated with lung cancer was first described by Denny-Brown (1948) as a distinct clinicopathological entity. It is a rare paraneoplastic syndrome, found in less than 1% of cases, typically in small cell lung cancer. Clinically, in pure form it corresponds to subacute sensory neuronopathy (SSN) characterized by painful dysesthesias and loss of sensation of all modalities. However, SSN may be accompanied by neurological alterations indicating the involvement of other parts of the neuraxis, falling thereafter into the category of paraneoplastic encephalomyelitis (PEM) (Graus et al. 1985, 1987; Anderson et al. 1988). The pathogenesis of SSN remains unclear, but after the detection of circulating antineuronal antibodies (CANA) numerous recent studies strongly support the role of the autoimmune process (Babikian et al. 1984, 1985; Graus et al. 1987, 1990ab; Anderson et al. 1988; Kornguth 1989). Some reports, however, confirming the high specificity of CANA for small cell lung cancer, found no definite correlation between their presence and the appearance of the paraneoplastic syndrome (Popp et al. 1988; Grisold et al. 1988ab, 1989).

In our material comprising cases of death of small cell lung cancer during the last five years we observed two cases of SSN. Both these cases showed lower motor neuron alterations, confirmed by electrophysiological studies. The results of postmortem immunocytochemical investigations provide further data suggesting the involvement of humoral immunity in the pathogenesis of SSN.

CASE REPORTS

Case 1

S.R., a 59-year-old man was admitted to the Department of Neurology on 15 July 1988 because of weakness of hands and legs, awkward gait, trunkal pains and severe painful dysesthesias of limbs which started one month earlier after a viral respiratory infection. At the time of admission neurological examination showed slight muscle atrophy of the shoulder and pelvic girdle, mild weakness of the flexors and extensors of hands and the pelvic girdle. Tendon reflexes were weak in the upper extremities (abolished from radius and ulna) with areflexia in the lower limbs. There was asymmetrical loss of touch and pain sensation (below Th10 level on the right involving the right thigh), hyperpathia of glove and sock type and slight sensory ataxia. Painful dysesthesias aggravating at night represented the patient's main complaint and produced persistent insomnia. On the basis of the clinical picture and proteinocytologic dissociation in the CSF (2 mononuclears, protein concentration of 145 mg% with increased to 12.6 mg% gammaglobulins) the Guillain-Barré syndrome was suspected. However, the results of electrophysiological examination were not typical for this syndrome: nerve conduction velocity was only slightly prolonged in the motor and sensory fibers of the median nerve, in the peroneal and sural nerve, and normal in the axillary and femoral nerves. Moreover, the amplitudes of responses were markedly decreased in all nerves studied suggesting rather axonal than myelin damage. EMG of distal and proximal muscles was normal. The patient was treated with Prednison (100 mg *pro die* gradually reduced) and with Endoxan (100 mg *pro die* in 10-day cycles) with subsequent improvement of motor disabilities, but persisting sensory disturbances. In January 1989 therapy was stopped because of bleeding from the alimentary tract and one month later chest X-ray disclosed a tumor mass in the right lung proved by biopsy to be a small cell cancer. The patient was transferred to the Institute of Pulmonology and received 6 courses of chemotherapy (Endoxan 1000 mg/m², Vepesid 600 mg and Epiadriamycin 70 mg/m²). After an initial regression of the tumor by X-ray the disease gradually progressed, with persisting sensory disturbances.

The following remarkable abnormalities were found after laboratory studies: elevated to 191 μ l alkaline phosphatase and increased to 86 U circulating immunological complexes (norm 20–80 U). The patient died in November 1989 because of a recent myocardial infarct, 16 months after the onset of neurological symptoms.

General autopsy revealed dissemination of the carcinoma (involvement of the right lung, hilar and mediastinal lymph nodes, liver, thyroid, suprarenal glands and pericardium), pneumonia, recent and old myocardial infarctions, advanced atheromatosis.

Neuropathological examination

The brain and spinal cord were grossly normal, without metastatic lesions. For microscopical studies sections from all representative CNS structures as well as from the spinal cord with spinal roots and ganglia were taken. Paraffin embedded sections were stained with HE, Heidenhain, Klüver-Barrera, Holmes and Bielschowsky methods. For immunohistochemical studies a panel of antisera was used for: GFAP, MBP, IgG, IgM, inter- α -trypsin inhibitor, fibrinogen, α -1-anti-trypsin (all from Dakopatts), ferritin, C3 complement (all from Sigma), α -1-anti-chymotrypsin (from Accurate Chem. Comp), α_2 -macroglobulin and C5b-9 complement (both from Behringer), and 3-39, for ubiquitin (gift from dr. I. Grundke-Iqbal). Immunocytochemistry was performed on paraffin sections using the extravidin-biotin-peroxidase complex method (reagents from Amersham and Sigma respectively) and diaminobenzidine (from Sigma) as chromogen. The sections were counterstained with hematoxylin.

Microscopical examination disclosed no distinct pathology of the brain. The spinal cord showed severe degeneration of posterior columns (Fig. 1) with scanty perivascular infiltrates, numerous macrophages loaded with ferritin-positive material and dense astroglial fibre network. In the anterior horn mild, patchy neuronal loss with gliosis was found. Anterior roots only sporadically showed



Fig. 1. Degeneration of the posterior columns of the spinal cord at the lumbar level. Case 1. Heidenhain. Gross. magn.

slight damage. In the posterior horn degeneration of neurons with marked gliosis revealed by GFAP and ferritin immunohistochemistry was seen. Posterior roots revealed pronounced alterations (Fig. 2) with myelin and axon loss and focal

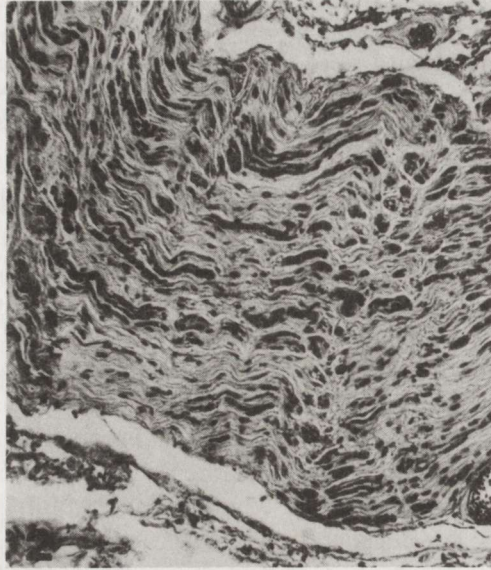


Fig. 2. Degeneration of the posterior root of the spinal cord. Case 1. Heidenhain. $\times 400$

axonal swellings, visualized also with anti-ubiquitin labeling. Posterior root ganglia exhibited neuronal loss with numerous nodules of Nageotte, however, with very scanty perivascular infiltrates, if any. Numerous ganglion cells showed IgG deposits in the cytoplasm, at dilutions up to 1:50 000, however, with only a few stained nuclei (Fig. 3). IgG immunoreactivity was also seen within the progressively changed astrocytes, Schwann cells and in the walls of blood vessels. Antiserum to the C3 fraction of the complement labeled many ganglion cells (Fig. 4). Complement fraction C5b-9 immunoreactivity was observed only in dorsal roots, labeling only heavily damaged and fragmented neurites (Figs 5 and 6). In 4 control cases (individuals without evidence of peripheral nervous system damage, who died because of brain vascular failure) only a few ganglion cells showed IgG and C3 immunoreactivity, but no labeling with the C5b-9 complement fraction. Mabs to IgM stained vessel walls, and besides them particular posterior roots only in the SSN case, and not in controls. Satellite ganglion cells showed weak expression of protease inhibitors as compared with 4 control cases, but the reaction was much stronger in satellite than in ganglion cells (Figs 7 and 8). However, there was no labeling either of the ganglion or satellite cells with antiserum to α_2 -macroglobulin whose expression was found also rarely in the controls, mainly in perivascular areas. There were no ubiquitin-positive intracytoplasmic inclusion bodies in neurons of the anterior horns.

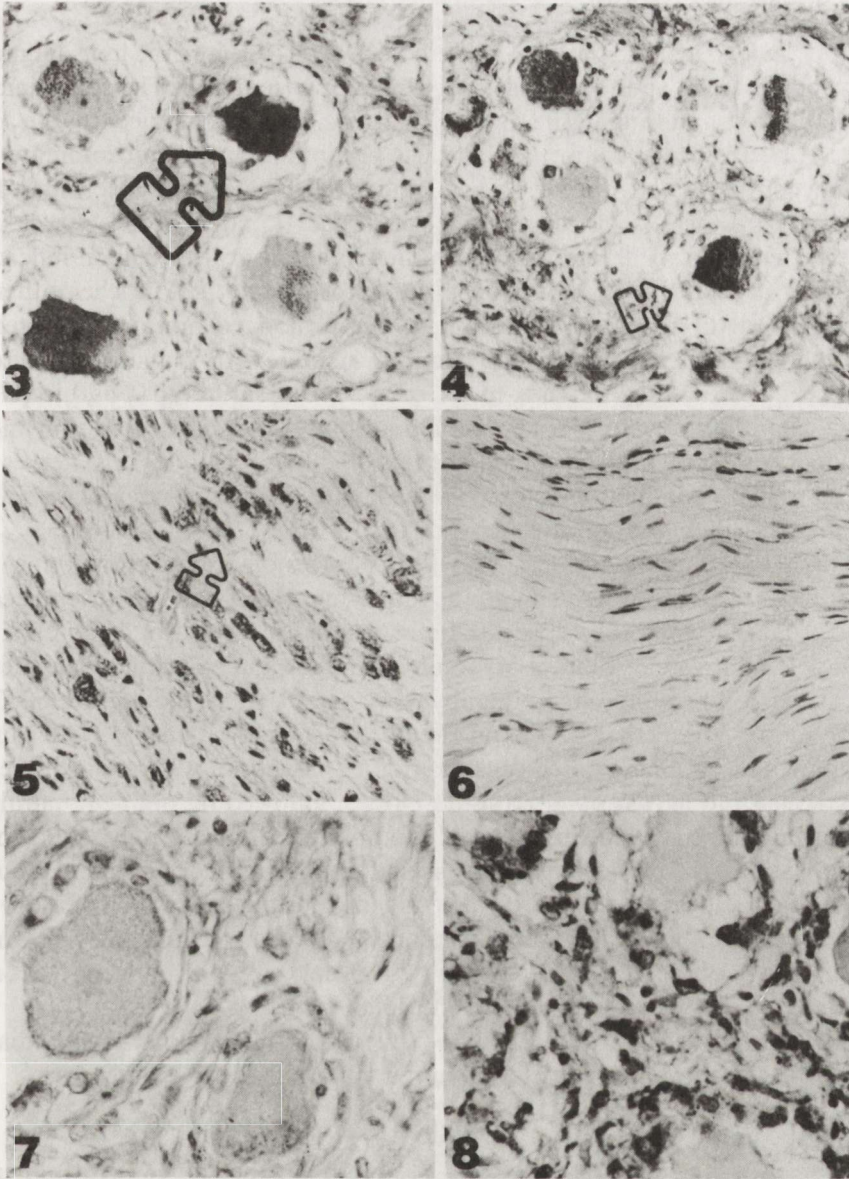


Fig. 3. Dorsal root ganglion. IgG deposits within ganglion cells (arrow). Case 1. Immunostaining with IgG. $\times 400$

Fig. 4. Dorsal root ganglion. C3 complement labeling of ganglion cells (arrow). Case 1. $\times 400$

Fig. 5. Dorsal root of the spinal cord. Immunostaining of degenerated neurites with C5b-9 complement fraction (arrow). Case 1. $\times 400$

Fig. 6. Dorsal root of the spinal cord. No labeling with C5b-9 complement fraction. Control case. $\times 400$

Fig. 7. Dorsal root ganglion. Weak α_1 -antichymotrypsin expression in satellite cells. Case 1. $\times 600$

Fig. 8. Dorsal root ganglion. Strong α_1 -antichymotrypsin expression in satellite cells. Control case. $\times 600$

Case 2.

B. G., a 55-year-old man with inoperable oat cell cancer of the lung diagnosed in December 1987 after examination of the biopsy material. The sole clinically detectable extrapulmonary site of the malignancy was confined to the bone marrow. Neurological abnormalities started 3 months earlier and dominated the clinical course of the disease. Neurological examination in December 1987 disclosed paresthesias of the hands and feet, radicular pain in both legs, weakness of feet extensors, sensory ataxia of lower left extremity, weak tendon reflexes of the upper extremities and areflexia in legs. EMG study before chemotherapy showed fibrillations in the abductor pollicis, prolonged motor unit potential duration in the same muscle and anterior tibialis with reduced interference pattern in all examined muscles; in the right first dorsal interosseus, biceps and vastus lateralis as well. Nerve conduction study showed decrease in motor conduction velocity in the median (43.1 m/s) and (peroneal 31.8 m/s) nerves and normal sensory conduction velocity in median and sural nerves but with a significant reduction in amplitude (to $3\mu\text{V}$).

The patient initially was treated with 2 courses of Adriamycin (60 mg) and Vepesid (600 mg) with regression of the tumor mass by X-ray. However, because of the progressive neurological disabilities, Vepesid was substituted by CTX and MTX with complete resolution of radiological signs, but still progressing neurological deficit. Therefore, chemotherapy was stopped, and radiotherapy (5000 r/t) on the tumor and mediastinum and Prednisone (60 mg *pro die*) started. Muscle weakness and wasting, altered sensation of all modalities with areflexia, severe dysesthesias and flaccid paraparesis developed, followed by sphincter paralysis. CSF examination at that time showed 5 mononuclears per 1 mm^3 and protein concentration of 80 mg%. The patient became cachectic, had febrile states, but no clinical data suggested relapse or dissemination of the cancer. Circulatory immunological complexes were: before therapy 82, during treatment 28-58, and at the final stage of the disease 89 U. The patient died suddenly in May 1988, nine months after the onset of the first symptoms of the disease.

General autopsy showed: Pneumocystis carinii pneumonia, myocardial ischemia and atheromatosis, without residual cancer in the organs.

Neuropathological examination

There was no gross pathology of the brain. In the spinal cord numerous petechiae were present. Tissue sections taken for histopathological study and the staining methods were the same as in case 1.

Microscopical examination of the brain showed no remarkable alterations. The spinal cord showed damage of posterior columns and horn. In the anterior horn moderate neuronal loss and degenerative changes with gliosis were present (Fig. 9). Numerous posterior roots, but only few anterior roots showed alterations, without any inflammatory reaction, however. In the posterior root ganglia neuronal loss with numerous nodules of Nageotte and abundant mononuclear perivascular infiltrates were seen (Fig. 10). There was similar to case

1 IgG expression in progressively changed astrocytes (Fig. 11) and the ganglion cells, but additionally extravazation of IgG in both spinal cord and roots. In the grey matter of the spinal cord diffuse IgG staining was observed. Numerous blood vessels showed IgM deposits, especially abundant in the capillary endothelium (Fig. 12), but without IgM deposits in the ganglion cells or spinal roots. Antiserum to C3, C5b-9 fraction of the complement, and to the protease inhibitors studied showed a similar pattern of immunostaining as in case 1. Besides, there were numerous delicate perivascular hemorrhages in the spinal cord.

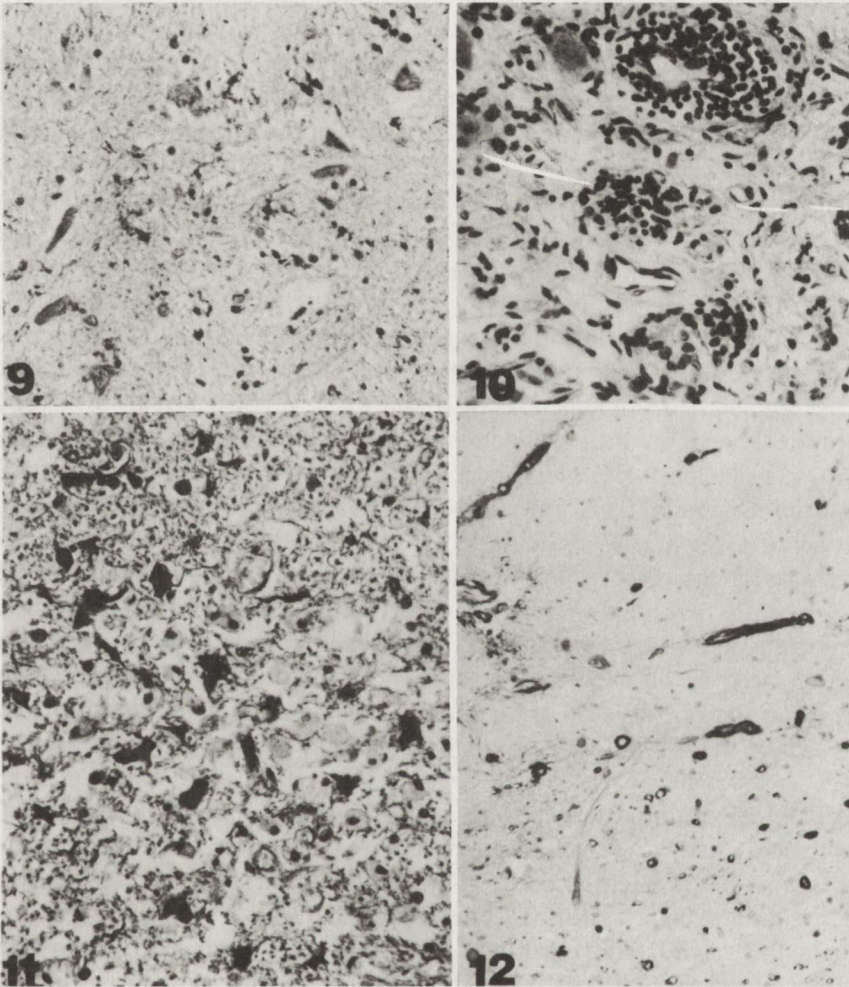


Fig. 9. Anterior root of the spinal cord. Degenerated neurons and numerous ferritin-positive microglial cells. Antiserum to ferritin. $\times 100$

Fig. 10. Dorsal root ganglion. Perivascular infiltrate (arrow) and nodules of Nageotte. Case 2. HE $\times 400$

Fig. 11. Numerous progressively changed astrocytes with IgG deposits and unlabeled macrophages in posterior column of the spinal cord. Case 2. IgG immunostaining. $\times 200$

Fig. 12. IgM expression within numerous blood vessel walls of the spinal cord. Case 2. $\times 100$

DISCUSSION

In both cases presented, neurological abnormalities preceded by many months the diagnosis of lung cancer, a phenomenon typically observed in SSN. Neither of the patients described had metastatic lesions within the CNS. However, one of the patients showed dissemination of the cancer in many internal organs, meanwhile the other patient was free of cancer at autopsy. It was previously observed that patients with small cell lung cancer and paraneoplastic syndrome have a more benign course and a lower degree of metastatic lesions in the CNS than other patients (Henson, Ulrich 1982; Graus et al. 1986). The presence of autoantibodies directed simultaneously against the common antigen expressed by both the cancer cells and the nervous system tissue might be responsible for this phenomenon and for the nervous system damage (Budde-Steffen et al. 1988; Graus et al. 1986, 1988, 1990ab; Babikian et al. 1984, 1985; Grisold et al. 1988ab). Polyclonal IgG, anti-Hu antibody, was detected in sera and CSF of PEM patients, reacting with neuronal nuclei and recognizing by Western blots 35–40 kD antigen in the tumor and nervous system tissue (Graus et al. 1984, 1986, 1990b). In the peripheral nervous system CANA-positive sera stained Schwann cell nuclei, but nerve teased-fiber and skeletal muscles remained unstained (Grisold et al. 1988ab). However, since the description of autoantibodies against neuronal nuclei in SSN and PEM, no evidence for their cardinal role in the development of paraneoplastic syndromes emerged. Neither chemotherapy nor plasmapheresis have been able to improve the clinical course of SSN, even if the plasma levels of autoantibodies were lowered by these therapeutical approaches (Grisold et al. 1988; Anderson et al. 1988; Graus et al. 1990a); arguing rather against the direct role of CANA in nervous tissue destruction. In both cases presently described we had no opportunity to study the CANA. However, postmortem, in both cases we observed altered immunoreactivity of the nervous tissue, suggesting the participation of humoral immunity in the tissue damage.

It is of interest that case 2, with more rapid clinical course and more severe neurological abnormalities showed complete remission of the cancer, although the therapy was limited because of progressive neurological deficit. Moreover, microscopical examination in this case showed a more active stage of the pathological process with marked inflammatory reaction within the dorsal root ganglia and altered integrity of the blood-brain barrier. Both cases in addition to SSN manifested lower motor neuron symptoms. In case 1 initially resembling the Guillain-Barré syndrome, the motor disabilities, which markedly improved after immunosuppressive therapy, were probably caused by motor neuropathy accompanying SSN. In case 2, the involvement of motor neurons of the anterior horn of the spinal cord was observed by EMG study. It was confirmed by neuropathological studies, however, neuronal loss in the anterior horn was mild, without infiltrates or neuronophagy. There were no ubiquitin inclusion bodies in the neuronal cytoplasm of the anterior horn, a finding observed in typical SLA cases (Leigh et al. 1988). According to immunohistochemical studies performed,

both cases showed a similar immunoreactivity pattern, except for IgM staining of dorsal root disclosed only in case 1. In both cases we observed IgG deposits and C3 complement fraction in numerous ganglion cells. The immunostaining of ganglion cells with IgG antiserum was mentioned previously in the cases of Graus et al (1990b) and Grisold et al. (1987). It should, however, be noted that marginal immunostaining of ganglion cells with IgG and C3 was observed in our material also in the control cases. The origin of serum protein in neural tissue is still a matter of debate. Data have been collected indicating the possible deposition of IgG in CNS neurons due to their retrograde axonal transport from the presynaptic membrane, mainly in areas lacking the blood-brain barrier (Fabian, Ritchie 1986; Fabian 198; Loberg, Torvik 1991). Nevertheless, it was suggested recently, that extravasated leakage and neuronal uptake of serum proteins is a postmortem phenomenon, conditioned by delay in autopsy or mishandling of brains, however, dependent in severity upon antemortem circumstances (Mori et al. 1991). In dorsal root ganglia postmortem uptake of serum proteins by damaged neurons might be additionally facilitated by absence of the blood-brain barrier. Therefore, the widespread presence of IgG in the cell cytoplasm may not have necessarily pathological consequences, however, at the same time we would like to underline that in the control cases examined we have found remarkably weaker immunostaining with IgG and the complement fractions studied. Thus, the participation of immunological complexes in the ganglion cells damage in oat cell cancer patients can not be at present eliminated and needs further studies. It is of interest, that the C5b-9 fraction of the complement was disclosed only in the SSN case, but not in controls. Therefore, it seems highly probable that the C5b-9 fraction of the complement might be involved in the tissue damage observed. It is postulated that this complement fraction, representing the membrane attack complex, may be implicated in various pathological conditions such as dermatomyositis (Engel, Beisecker 1982; Kissel et al. 1991). The presence of immunological complexes with weak protease inhibitors expression suggests the involvement of circulatory mechanism in tissue damage in SSN or/and altered proteolysis as a background mechanism. There are data indicating that immunoglobulins are able to inhibit protease inhibitors and produce uncontrolled proteolysis with tissue breakdown (Kornguth 1989). One of the protease inhibitors studied, alfa₂-macroglobulin, is of special interest, as due to its binding to a family of growth factors and cytokines probably is responsible for their clearance from the circulation (La Marre et al. 1991). Moreover, the antibody isolated from the sera of patients with the paraneoplastic syndrome binds to a protein showing a high sequence homology with the alfa₂-macroglobulin and the alfa-1-trypsin inhibitor (Kornguth 1989). The small number of cases examined does not allow for definitive conclusions, but a mechanism involving the participation of immunoglobulins and protease inhibitors is very tempting in SSN pathogenesis.

PODOSTRA CZUCIOWA NEURONOPATIA W RAKU OWSIANOKOMÓRKOWYM PŁUC.
IMMUNOHISTOCHEMICZNE BADANIE DWU PRZYPADKÓW

Streszczenie

Przedstawiono dwa przypadki podostrej czuciowej neuronopatii (PCN) związanej z obecnością raka owsianokomórkowego płuc. W obydwu przypadkach zaburzenia ruchowe były spowodowane przez neuronopatię ruchową i także neuropatię. Wyniki badań immunohistochemicznych potwierdziły sugestię zaangażowania odpowiedzi humoralnej i udziału inhibitorów proteazy w patogenezie PCN.

REFERENCES

1. Anderson NE, Rosenblum MK, Graus F, Wiley RG, Posner JB: Autoantibodies in paraneoplastic syndromes associated with small-cell lung cancer. *Neurology*, 1988, 38, 1391 – 1398.
2. Babikian V, Stefansson K, Liebermann F, Arnason BGW: Antibodies against antigens shared by oat-cell tumor and neural tissue in the serum of the patients with paraneoplastic disorder of peripheral nerve and spinal cord. *Neurology*, 1984, 34, suppl. 1.
3. Babikian VL, Stefansson K, Dieperink ME, Arnason BGW, Morton LS, Levy BE: Paraneoplastic myelopathy: Antibodies against protein in normal spinal cord and underlying neoplasm. *Lancet*, 1985, 2, 49 – 50.
4. Budde-Steffen C, Anderson NF, Rosenblum HK, Posner JB: Expression of an antigen in small cell lung carcinoma lines detected by antibodies from patients with paraneoplastic dorsal root gangliopathy. *Cancer Res*, 1988, 48, 430 – 434.
5. Croft PB, Wilkinson M: The incidence of carcinomatous neuromyopathy with special reference to lung and breast carcinoma. In: *The remote effects of cancer on the nervous system*. Eds. WR Brain, FH Norris, Grune, Stratton-New York, 1965, p 44.
6. Denny-Brown D: Primary sensory neuropathy with muscular changes associated with carcinoma. *J Neurol Neurosurg Psychiatry*, 1984, 11, 73 – 87.
7. Engel AG, Beisecker G: Complement activation in muscle fiber necrosis: demonstration of the membrane attack complex of complement in necrotic fibers. *Ann Neurol*, 1982, 12, 289 – 296.
8. Fabian RH: Uptake of plasma IgG by CNS motoneurons: Comparison of antineuronal and normal IgG. *Neurology*, 1988, 38, 1775 – 1780.
9. Fabian RH, Ritchie TC: Intraneuronal IgG in the central nervous system. *J Neurol Sci*, 1986, 73, 257 – 267.
10. Graus F, Cordon-Cardo C, Posner JB: Neuronal antinuclear antibody in sensory neuronopathy from lung cancer. *Neurology*, 1985, 35, 538 – 543.
11. Graus F, Elkon KB, Cordon-Cardo C, Posner JB: Sensory neuropathy and small cell lung cancer. Antineuronal antibody that also reacts with the tumor. *Am J Med*, 1986, 80, 45 – 52.
12. Graus F, Elkon KB, Lloberes P, Ribalta T, Torres A, Ussetti P, Valls J, Obach J, Agusti-Vidal A: Neuronal antinuclear antibody (anti-Hu) in paraneoplastic encephalomyelitis simulating acute polyneuritis. *Acta Neurol Scandinav*, 1987, 75, 249 – 252.
13. Graus F, Abos J, Roquer J, Mazzara R, Pereira A: Effects of plasmapheresis on serum and CSF autoantibody levels in CNS paraneoplastic syndromes. *Neurology*, 1990a, 40, 1621 – 1623.
14. Graus F, Ribalta T, Campo E, Monforte R, Urbano A, Rozman C: Immunohistochemical analysis of the immune reaction in the nervous system in paraneoplastic encephalomyelitis. *Neurology*, 1990b, 40, 219 – 222.
15. Grisold W, Drlicek M, Popp W, Jellinger K: Antineuronal antibodies in small cell lung carcinoma – a significance for paraneoplastic syndrome? *Acta Neuropathol (Berl)*, 1987, 75, 199 – 203.
16. Grisold W, Drlicek M, Popp W, Jellinger K: Paraneoplastic sensory neuronopathy, revisited. *Neurology*, 1988a, 38, 508.
17. Grisold W, Drlicek M, Liszka U, Jellinger K, Popp W: Reactivity of circulating antineuronal antibodies (CANAs) on peripheral nervous system structures. *Neurology*, 1988b, 77, 109 – 112.

18. Grisold W, Drlicek M, Liszka U, Popp W: Anti-Purkinje cell antibodies are specific for small-cell lung cancer but not for paraneoplastic neurological disorders. *J Neurol*, 1989, 236, 64.
19. Henson RA, Urich H: Peripheral neuropathy associated with malignant neoplasm. Eds: RA Henson, H Urich. In: *Cancer and the nervous system*. Blackwell Scientific Publications, Oxford, 1982.
20. Kissel JT, Halterman RK, Rammohan KW, Mendell JR: The relationship of complement-mediated microvasculopathy to the histologic features and clinical duration of disease in dermatomyositis. *Arch Neurol*, 1991, 48, 26–30.
21. Kornguth SE: Neuronal proteins and paraneoplastic syndromes. *N Engl J Med*, 1989, 321, 1607–1608.
22. La Marre J, Hayes MA, Wollenberg GK, Hussaini I, Hall SW, Gonias SL: An alpha₂-macroglobulin receptor-dependent mechanism for the plasma clearance of transforming growth factor b-1 in mice. *J Clin Invest*, 1991, 87, 39–44.
23. Leigh PN, Anderton BH, Dodson A, Gallo J.-M, Swash M, Power DM: Ubiquitin deposits in anterior horn cells in motor neuron disease. *Neurosci Lett*, 1988, 93, 197–203.
24. Loberg EM, Torvik A: Uptake of plasma proteins into damaged neurons. An experimental study on cryogenic lesions in rats. *Acta Neuropathol (Berl)*, 1991, 81, 479–485.
25. Mori S, Sternberger NH, Herman MM, Sternberger L: Leakage and neuronal uptake of serum protein in aged and Alzheimer brain. *Lab Invest*, 1991, 64, 345–351.
26. Popp W, Drlicek M, Grisold W, Zwick H: Circulating antineuronal antibodies in small cell lung cancer. *Lung*, 1988, 166, 243–251.

Correspondence adress: M. Barcikowska, Centrum Medycyny Doświadczalnej i Klinicznej, Dworkowa 3, 00-784 Warszawa, Poland

HALINA KROH, JERZY BIDZIŃSKI

GLIAL DIFFERENTIATION IN MEDULLOBLASTOMA. CASE REPORT

Department of Neuropathology, Medical Research Centre, Polish Academy of Sciences, Warsaw;
Department of Neurosurgery, School of Medicine, Warsaw

A 30-year-old man suffered for a year of a typical syndrome of cerebellar tumor. At suboccipital craniectomy a soft tumor infiltrating both hemispheres and vermis, filling up part of the IV ventricle was found. After subtotal removal of the neoplasm the postoperative course was poor and the patient died 5 weeks later. Biopsy material consisted of three types of tissue: 1. large nests of carrot-shaped, hyperchromatic cells, 2. fields of "halo" cells presenting myelin basic protein (MBP) immunoreactivity and 3. fields and scattered strongly GFAP-positive cells. The histological and immunocytochemical pattern of the neoplasm indicates differentiation of the tumor into oligodendroglomatous and astrocytomatous line being an uncommon example of dual glial differentiation capability in medulloblastoma.

Key words: *medulloblastoma, differentiation, GFAP, MBP.*

Cellular differentiation of cerebellar medulloblastomas along glial, neuroblastic or ependymal lines is rare. Among glial ones the most common is astrocytic differentiation, confirmed lately by immunohistochemical studies of glial fibrillary acidic protein (GFAP). Medulloblastomas presenting cellular features of more than one type of the neoplastic glial component are an extreme rarity. Tumors showing oligodendroglial differentiation alone or together with the astrocytic one have been observed only sporadically. We are privileged to report such a case of differentiating medulloblastoma in an adult.

CASE REPORT

A 30-year-old man, P.A., admitted to the Department of Neurosurgery, suffered for a year of progressing ataxia, ataxic gait with left lateralization, without headache or vomiting. Neurological investigation revealed nystagmus to the left, diplopia, papilloedema 3.0 D, left central n. VII hemiparesis, dysarthry, slurred speech. CT investigation showed a cerebellar, midline, contrast-enhanced homogeneous mass 40 × 36 × 45 mm exerting pressure on IV ventricle and a dilated ventricular system. Suboccipital craniectomy displayed a deep, soft tumor infiltrating the vermis and both hemispheres, filling the IV ventricle. The

tumor was removed subtotally, its part infiltrating the lateral wall of the IV ventricle was left *in situ*. Two days later revision of posterior fossa was performed with additional resection of the hemisphere due to edema and tonsillar invagination into the vertebral channel. The postoperative course was poor. Constant drainage of the ventricular system was installed for daily hypersecretion of cerebral spinal fluid up to 500 ml. The patient died 5 weeks after operation. Postmortem was not performed.

For tumor biopsy the following routine methods on paraffin sections were applied: HE, Gomori, PAS. Immunohistochemical methods were: for GFAP with polyclonal antibodies (Daco, Copenhagen) concentration 1:500, ABC method; for myelin basic protein (MBP) with polyclonal antibodies (Daco) concentration 1:1000, extravidin-biotin method; for transferrin (Tf) polyclonal antibody (Polfa, Warsaw), concentration 1:10 000, extravidin-biotin method.

Histology: most areas of neoplastic tissue consisted of large compact nests of carrot-shaped hyperchromatic cells among which many showed mitotic divisions (Fig. 1). Neither rosettes nor other formations could be detected. Necrotic foci were scarce. Cellular nests were well merged into the adjacent tissue though their demarcation was distinct.

Surrounding neoplastic tissue was of lesser density and consisted of small cells with dark nucleus with clear "halo" (Fig. 2) coexisting with scattered less defined

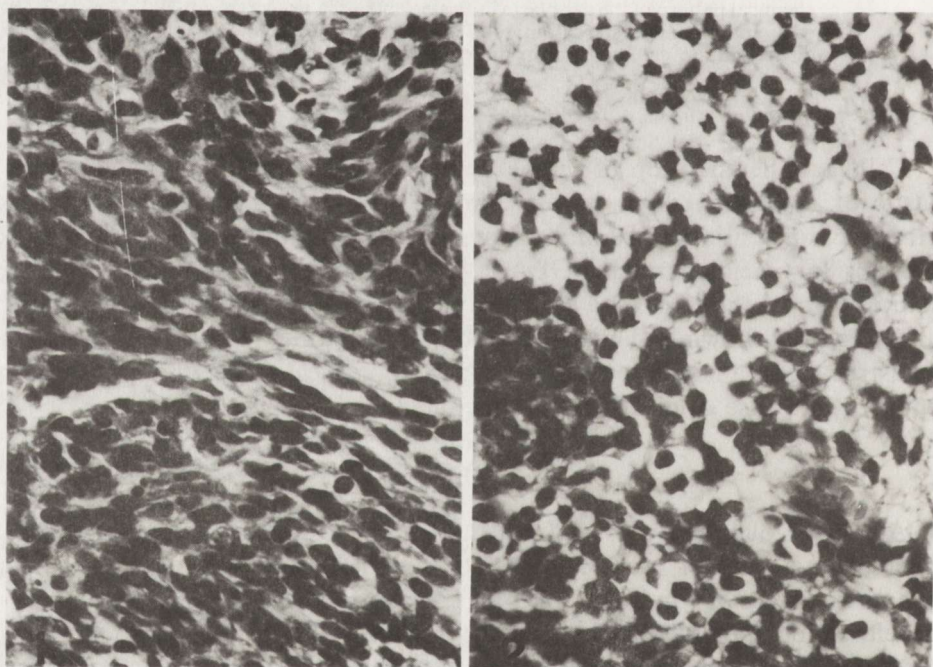


Fig. 1. Abundant mitotic figures in carrot-shaped cells of medulloblastoma. HE. $\times 400$

Fig. 2. Oligodendrogloma fields adjacent to medulloblastoma nest. HE. $\times 400$

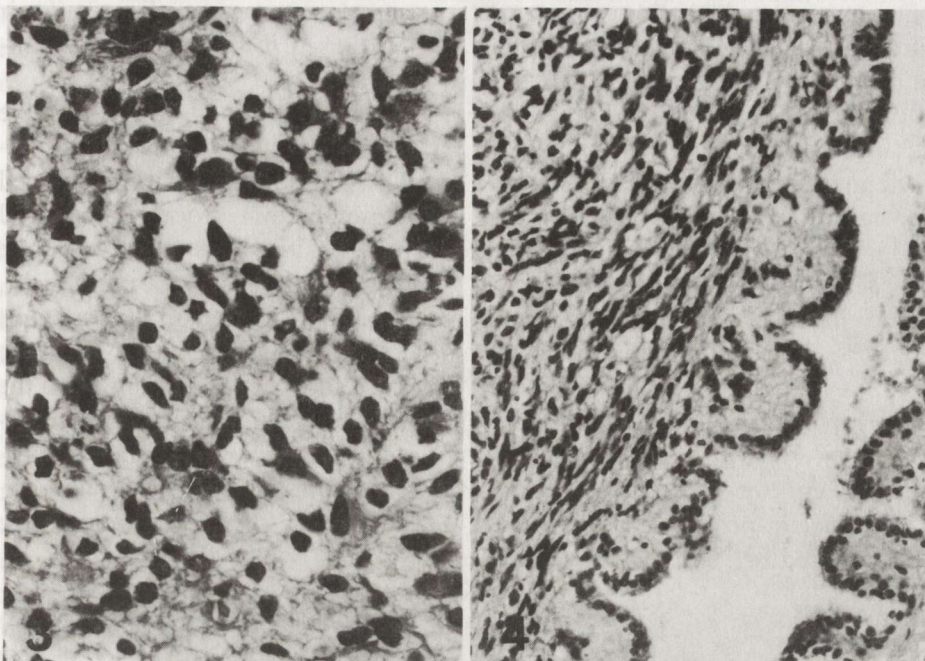


Fig. 3. Astrocytoma areas mixed with oligodendroglioma elements. HE. $\times 400$

Fig. 4. Astrocytoma infiltration of the wall of the IV ventricle. HE $\times 200$

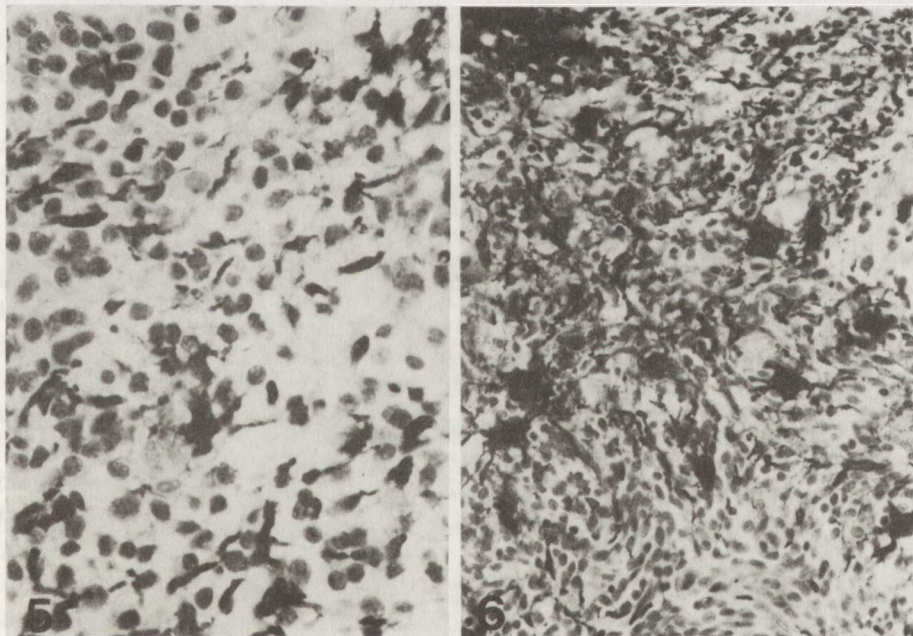


Fig. 5. GFAP-positive cells and processes among immunonegative population. $\times 400$

Fig. 6. GFAP-positive reactive astrocytes with distinct processes and smaller neoplastic cells lacking them. $\times 200$

cellular elements with elongated cytoplasm and polar processes (Fig. 3). Their astrocytic character was best cytologically recognised in subependymal infiltration of the IV ventricle (Fig. 4).

The fields of mixed astro-glial population exhibited strong GFAP-positive immunostaining, whereas in the nests of carrot-shaped cells only long, immunopositive processes were visible. The GFAP-immunopositivity concerned the majority of small cells with minute processes or thin processes scattered among neoplastic cells (Figs. 5, 6); larger GFAP-positive cells which could be regarded as reactive astrocytes were also found among the neoplastic population.

Myelin basic protein (MBP) immunostaining was visualized on the surface of cells in small accumulations and in some processes and only exceptionally in the cellular cytoplasm (Figs 7, 8). The reaction consisted of irregular granules on the cellular membrane and extracellularly. MBP immunostaining concerned relatively only a small part of cells which cytologically corresponded to oligodendroglioma cells. Nests of carrot-shaped cells did not present any MBP staining.

Transferrin-positive cells were endothelial, whereas the others were scarce and scattered in oligo-astroglial areas.

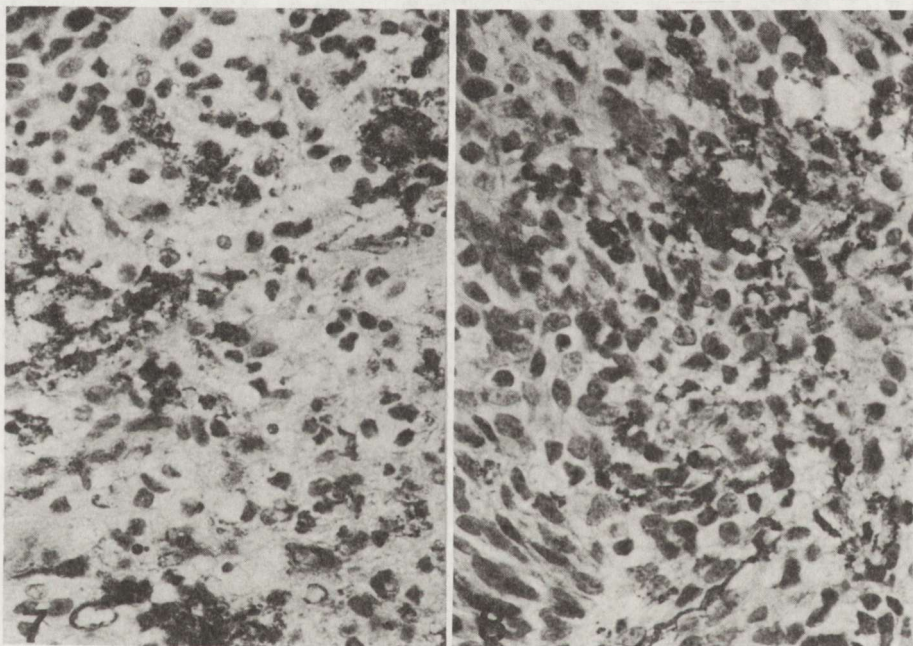


Fig. 7. Area of MBP-positive cells. Immunostaining of cytoplasm and short processes of some cells, visible also on cellular membranes. $\times 400$

Fig. 8. Area of MBP-immunostained cells and their processes. $\times 400$

The cells in the areas of mixed oligo-astroglial population did not exhibit any necrotic foci and only sporadic mitotic activity. In the whole tumor area the number of vessels was moderate and vascular walls thin. Reticulin fibers were

restricted to the vascular walls. Reticulin bands between cellular nests could not be detected. Diagnosis: medulloblastoma with astrocytomatous and oligodendroglomatous differentiation.

DISCUSSION

The origin of cerebellar medulloblastomas is unequivocal, but the studies by immunohistochemical methods have shed some light on their multipotential properties. These were postulated by some authors (Ringertz, Tola 1950; Willis 1957), but strongly denied on the ground of only morphological studies (Polak 1967). Even presently some authors using immunohistochemical evidence doubt in its reliability for identification of glial differentiation in medulloblastomas (Schindler, Gulotta 1983). The reported case seems to be an example of the capability of undifferentiated neuroepithelioma to higher differentiation to astrocytic and oligodendroglial neoplastic tissue. Marked astrocytomatous differentiation in medulloblastomas in the form of scattered cells and focal areas has been already reported with detailed description of various cellular forms in singular cases and in large statistics (Delpech et al. 1978; Barnard, Pambakian 1980; Velasco et al. 1980; Mannoji et al. 1981; Palmer et al. 1981; Kumanishi et al. 1985; Belza et al. 1991). Our observation concerns GFAP-positive cells of type 1 and 2 according to the classification of Mannoji et al. (1981). Contrary to the opinion of many authors, the described tumor does not belong to the desmoplastic type, in which astrocytic differentiation is regarded to take place in "light", reticulin-free islands (Deck et al. 1978; Mannoji et al. 1981; Pasquier et al. 1983; Herpers, Budka 1985). Multipotential capability has been observed in patients with medulloblastomas differentiating simultaneously along two lines, astrocytic and neuronal, apparent in immunohistochemical investigations (Roessmann et al. 1983; Hayashi et al. 1987; Hubbard et al. 1989).

Differentiation of medulloblastomas along the oligodendroglial line as in our case, is very rare but already reported by Rubinstein and Northfield (1964) during classification of cerebellar medulloblastomas, who observed in 6/22 cases of classical medulloblastomas "microscopic fields indistinguishable from those of oligodendroglioma; they were in the absence of any evidence of tissue degeneration marked by a characteristic perinuclear vacuolation of spherical tumor cells, supported and partitioned by a tenuous and regular vascular stroma" and "in all six cases, the microscopic appearances in most areas were otherwise indistinguishable from those of other medulloblastomas". The same authors among 8 "transitional" medulloblastomas with mixed desmoplastic and classical features found one tumor with areas "highly suggestive of an oligodendroglial element". These cytological observations are supported by an earlier suggestion (Bodian, Lawson 1953) on medulloblastomas indifferent enough to give rise to glia of both astrocytic and the oligodendroglial series.

More recent studies on large series of medulloblastomas present evidence of a small number of cases (3/201) of glial and sole oligodendroglial differentiation

(Chatty, Earle 1971; Ammar et al. 1991) but possibly, for the lack of a suitable marker of oligodendroglial cells, the differentiating potential of so-called medulloblasts has not been fully recognized. MBP immunohistochemical labeling of oligodendroglia cells in differentiating medulloblastoma presented by us is the first documented evidence of capability of multipotential glial differentiation of this tumor. MBP immunostaining in human gliomas (Figols et al. 1985) indicated highest labeling in oligodendrogliomas, to a lesser degree expressed in astrocytomas of various grades. In our experience, the GFAP reaction, with total absence in medulloblastoma nests, greatly exceeds the MBP reaction; if MBP would concern only the part of astrocytic population, the extent of MBP localization would be much wider. On the other hand, only a small part of participating oligodendroglia, comparing with that histologically recognized, seems to be immunolabeled. We are prone to explain this phenomenon by various stages of cellular differentiation and various MBP cellular content as observed in other studies on development. This discrepancy between the number of GFAP-positive cells and small number of MBP-positive oligodendrocytes with reverse relation in routine histology may express GFAP-positive labeling of the transitional oligodendroglia cell type (Herpers, Budka 1984); in dual differentiated medulloblastoma this data supports the original idea of multipotentiality of primary cell.

The phenomenon of GFAP-labeled immature oligodendroglia originates in „transitional” cellular forms between astroglia and oligodendroglia arising from radial glia in developing human fetal cerebrum, cerebellum and spinal cord. This immunonegative radial glia becomes at first by the 9-10th week cytologically and immunologically GFAP-positive astroglia, then at the 15-16th week changes into cytologically identifiable in EM oligodendroglia, preserving GFAP-immunoproperties and demonstrating MBP-immunostaining in cellular processes and myelin sheaths. Such oligodendroglia loses its GFAP immunoreactivity on the 17-18th week (Choi, Kim 1983, 1984).

Transferrin immunostaining of a few scattered cells does not correspond to MBP reaction in oligodendroglial fields of the tumor, though it is considered to be specific for 3 types of rat oligodendroglia, appearing from the 5th day of age in the spinal cord and on 30th day reaching in whole CNS the adult pattern reflecting differentiation of oligodendrocytes and myelinogenesis (Connor, Fine 1986, 1987). In human optic nerves and chiasma the staining of intrafascicular oligodendrocytes was also noted (Connor et al. 1986). The lack of transferrin staining of neoplastic oligodendroglia reflects most probably low differentiation of oligoglia not capable to produce and sustain myelin sheaths. On the other hand, we obtained positive staining by this plasma protein of the majority of vascular endothelia in the tumor area, as observed previously in rat brain capillaries (Jefferies et al. 1984). Immunologically documented participation of dual neoplastic glial cells in our case among medulloblastoma tissue practically excludes the earlier interpretation of Rubinstein et al. (1974) of concomitant cerebellar medulloblastoma and astrocytoma as possible example

of diffuse astrocytoma dedifferentiating into medulloblastoma, what in our case would suggest dedifferentiation of various glial components into medulloblastoma.

GLEJOWE RÓŻNICOWANIE W RDZENIAKU MÓZDŻKU

Streszczenie

30-letni mężczyzna przez rok cierpiał z powodu typowych objawów guza mózdzku. Podczas kraniektomii podpotylicznej usunięto częściowo miękki guz naciekający robak, obie półkule i część wnikającą do komory IV. Przebieg pooperacyjny był zły i pacjent zmarł 5 tygodni później. Autopsji nie wykonano. Materiał biopsyjny zawierał trzy rodzaje tkanki: 1. duże gniazda nadbarwliwych komórek o kształcie marchewkowatym, z licznymi figurami podziału, 2. pola komórek z jasną cytoplazmą „halo” wykazujących immunoreaktywność MBP i 3. pola i rozsiane komórki, wybitnie GFAP-dodatnie. Struktura histologiczna i immunoreaktywność nowotworu wskazuje na różnicowanie się guza w kierunku skąpodrzewiaka i gwiaździaka, stanowiąc rzadki przykład zdolności dwukierunkowego różnicowania się rdzenia mózdzku.

REFERENCES

1. Ammar AAI, Majid H, Anim JT, Kutty MK, Ibrahim AW: Differentiating medulloblastoma in adults. *Neurol Res*, 1991, 13, 125–127.
2. Barnard RO, Pambakian H: Astrocytic differentiation in medulloblastoma. *J Neurol Neurosurg Psych*, 1980, 43, 1041–1044.
3. Belza M, Donaldson S, Steinberg G, Cox R, Cogen Ph: Medulloblastoma: freedom from relapse longer than 8 years – a therapeutic cure? *J Neurosurg*, 1991, 75, 575–582.
4. Bodian M, Lawson D: The intracranial neoplastic disease of childhood. A description of their natural history based on a clinicopathological study of 129 cases. *Brit J Surg*, 1953, 40, 368–392.
5. Chatty EM, Earle KM: Medulloblastoma. A report of 201 cases with emphasis on the relationship of histologic variants to survival. *Cancer*, 1971, 28, 977–983.
6. Choi B, Kim R: Immature oligodendroglial cells in developing human fetal spinal cord contain immunoreactive glial fibrillary acidic protein (GFAP). Abstract, *J Neuropathol Exp Neurol*, 1983, 42, 325.
7. Choi B, Kim R: Expression of glial fibrillary acidic protein in immature oligodendroglia. *Science*, 1984, 223, 407–409.
8. Connor J, Saini N, Fine R: Transferrin antiserum is a specific marker for oligodendrocytes in the rat and human optic nerve. *Anat Rec*, 1986, 214, 25.
9. Connor J, Fine R: The distribution of transferrin immunoreactivity in the rat central nervous system. *Brain Res*, 1986, 368, 319–328.
10. Connor J, Fine R: Development of transferrin-positive oligodendrocytes in the rat central nervous system. *J Neurosci Res*, 1987, 17, 51–59.
11. Deck JHN, Eng LF, Bigbee J, Woodcock SM: The role of glial fibrillary acidic protein in the diagnosis of central nervous system tumors. *Acta Neuropathol (Berl)*, 1978, 42, 183–190.
12. Delpech B, Delpech A, Vidard MN, Girard N, Tayot J, Clement JC, Creissard P: Glial fibrillary acidic protein in tumours of the nervous system. *Brit J Cancer*, 1978, 37, 33–40.
13. Figols J, Iglasias-Rozas JR, Kazner E: Myelin basic protein (MBP) in human gliomas: a study of twenty five cases. *Clin Neuropathol*, 1985, 4, 116–120.
14. Hayashi K, Motoi M, Nose S, Horie Y, Akagi T, Ogawa K, Taguchi K, Mizobuchi K, Nishimoto A: An immunohistochemical study on the distribution of glial fibrillary acidic protein, S-100 protein, neuron-specific enolase and neurofilament in medulloblastomas. *Acta Pathol*, 1987, 37, 85–96.

15. Herpers MJHM, Budka H: Glial fibrillary acidic protein (GFAP) in oligodendroglial tumors: gliofibrillary oligodendroglioma and transitional oligoastrocytoma as subtypes of oligodendroglioma. *Acta Neuropathol (Berl)*, 1984, 64, 265–272.
16. Herpers MJHM, Budka H: Primitive neuroectodermal tumors including the medulloblastoma: glial differentiation signaled by immunoreactivity for GFAP is restricted to the pure desmoplastic medulloblastoma („arachnoidal sarcoma of the cerebellum”). *Clin Neuropathol*, 1985, 4, 12–18.
17. Hubbard JL, Scheithauer BW, Kispert DB, Carpenter SM, Wick MR, Laws ER: Adult cerebellar medulloblastomas: the pathological, radiographic and clinical disease spectrum. *J Neurosurg*, 1989, 70, 536–544.
18. Jefferies W, Brandon M, Hunt WA, Gatter K, Mason D: Transferrin receptor on endothelium of brain capillaries. *Nature*, 1984, 312, 162–163.
19. Kumanishi T, Washiyama K, Watabe K, Sekiguchi K: Glial fibrillary acidic protein in medulloblastomas. *Acta Neuropathol (Berl)*, 1985, 67, 1–5.
20. Mannoji H, Takeshita I, Fukui M, Ohta M, Kitamura K: Glial fibrillary acidic protein in medulloblastoma. *Acta Neuropathol (Berl)*, 1981, 55, 63–69.
21. Palmer J, Kasselberg K, Netsky M: Differentiation of medulloblastoma. Studies including immunohistochemical localization of glial fibrillary acidic protein. *J Neurosurg*, 1981, 55, 161–169.
22. Pasquier B, Lachard A, Pasquier D, Couderc P, Delpech B, Courel MN: Proteine gliofibrillaire acide (GFAP) et tumeurs nerveuses centrales. *Ann Pathol*, 1983, 3, 203–211.
23. Polak M. On the true nature of so-called medulloblastoma. *Acta Neuropathol (Berl)*, 1967, 8, 84–95.
24. Ringertz N, Tola JH: Medulloblastoma. *J Neuropathol Exp Neurol*, 1950, 9, 354–372.
25. Roessmann V, Velasco ME, Gambetti P, Autilio-Gambetti L: Neuronal and astrocytic differentiation in human neuroepithelial neoplasms. *J Neuropathol Exp Neurol*, 1983, 42, 113–121.
26. Rubinstein LJ, Northfield DWC: The medulloblastoma and the so-called „arachnoidal cerebellar sarcoma”. *Brain*, 1964, 87, 375–412.
27. Rubinstein LJ, Herman MM, Hanbery JW: The relationship between differentiating medulloblastoma and dedifferentiating diffuse cerebellar astrocytoma. Light, electron microscopic, tissue, and organ culture observations. *Cancer*, 1974, 33, 675–690.
28. Schindler E, Gulotta F: Glial fibrillary acidic protein in medulloblastomas and other embryonic CNS tumors in children. *Virchows Arch (Pathol Anat)*, 1983, 398, 263–275.
29. Velasco M, Dahl D, Roessmann V, Gambetti P: Immunohistochemical localization of glial fibrillary acidic protein in human glial neoplasm. *Cancer*, 1980, 45, 484–494.
30. Willis RA: Pathology of tumours. Butterworth Publ, London, 2nd Ed, 1953, pp 816–817.

Authors address: Department of Neuropathology, Medical Research Centre, Polish Academy of Sciences, 3 Dworkowa Str, 00-784 Warsaw, Poland

PRZEMYSŁAW NOWACKI, BARBARA ZDZIARSKA

INTRAVASCULAR COAGULATION IN THE CENTRAL NERVOUS SYSTEM IN PATIENTS WITH ACUTE MYELOBLASTIC LEUKEMIAS

Department of Neurology and Department of Hematology, School of Medicine, Szczecin, Poland

The frequency and distribution of intravascular coagulation (IVC) were studied in brains of 121 patients who had died due to acute myeloblastic leukemias type M1 or M2. The IVC within the brain was observed in 59% of cases, more frequently in patients treated with polychemotherapy, especially according to TAD or VAPA protocols. The microthrombi were found predominantly in capillaries and small venous vessels. IVC was more frequent in cerebral and cerebellar white matter and in the neighbourhood of lateral ventricles (hippocampus, thalamus). In patients who had developed brain hemorrhage in the course of primary neoplastic disease IVC was very frequent phenomenon, thus IVC is considered to be an important factor in the development of CNS hemorrhages in myeloblastic leukemias, irrespective of thrombocytopenia related to bone marrow involvement.

Key words: intravascular coagulation, myeloblastic leukemias, intracerebral hemorrhage.

Bleeding is a major problem in patients with acute leukemias and is primarily related to thrombocytopenia. Coagulation defects may also be present. Intravascular coagulation (IVC), antithrombin III and factor XIII deficiency as well as hyperfibrinolysis are most common among them (Rodeghiero et al. 1980; Rasche et al. 1982; Sanz et al. 1988; Woitinas 1991). Studies on IVC have shown that procoagulant activity is generated by leukemic blasts due to release of plasminogen activators, and have suggested that this may sometimes contribute to disorders in hemostasis (Bennett et al. 1989). IVC can also be related to vessel wall damage, chemotherapy and septic shock (Sakuragawa et al. 1976; Hardaway et al. 1979; Sampaolo et al. 1987; Huber, Cervós-Navarro 1992). In acute leukemias chronic IVC is usually observed. It is accompanied by laboratory abnormalities without evident clinical manifestation of thrombosis or hemorrhage (Sochacka-Kuzko et al. 1978; De Aquino Jaso et al. 1979; Kuratowska 1984), nevertheless IVC can intensify thrombocytopenia dependent on aplasia or bone marrow infiltration.

IVC seems to be underestimated in the etiopathology of the central nervous system (CNS) hemorrhages in leukemic patients. Only few papers on IVC in the CNS are found (McGauley et al. 1975; Kozłowski 1981; Shimamura et al. 1983;

Nowacki et al. 1985). Our study is an attempt to estimate: 1. the frequency and distribution of microthrombi in the CNS, 2. the influence of polychemotherapy on IVC development in the CNS and 3. the role of IVC in the etiopathology of CNS hemorrhages.

MATERIAL AND METHODS

The studies of hemostasis and neuropathological investigations have been done on 121 patients of both sexes, aged 17 to 75 years (mean age 42.6 years) deceased due to acute myelogenous leukemia, type M1 or M2. Before 1985, 53 patients were treated with chemotherapy according to COAP (1–4 cycles: cyclophosphamide 850 mg, oncovin 2 mg, cytosine arabinoside 850 mg, prednisone 500 mg) and 15 patients according to AR (5–10 cycles: cytosine arabinoside 1400 mg, daunorubicin 210 mg). Since 1986, 22 patients had been treated according to TAD (1–4 cycles: 6-thioguanine 2400 mg, cytosine arabinoside 2400 mg, daunorubicin 300 mg), 20 patients according to VAPA (1–4 cycles: vincristine 3 mg, adriamycin 150 mg, prednisone 600 mg, cytosine arabinoside 1200 mg). Eleven patients were not treated with chemotherapy.

Paraffin-embedded material was stained with hematoxylin and eosin, cresyl violet, Weigert, PAS and Astra blue. IVC was admitted to be distinct (3+) if microthrombi were observed in many vessels in the majority out of 9 investigated regions, moderate (2+) if microthrombi appeared in 10–20 vessels in each of 4–6 regions, minimal (1+) if microthrombi were seen in 5–10 vessels in each of 2–3 regions. In cases with a smaller number of microthrombi IVC was not diagnosed. The results were analysed by the Chi-square test.

RESULTS

Morphological characteristics of microthrombi

The microthrombi as fibrinoid deposits were usually observed in capillaries and small veins, 50 to 100 μm in diameter (Figs 1 and 2). Microthrombi were much less frequent in larger veins and in arterial vessels (Fig. 3). Within the wall of some vessels filled with microthrombi an increased amount of highly acidic mucopolysaccharides, well stained with Astra blue was observed (Fig. 4).

Frequency and distribution of microthrombi in the CNS

Microthrombi appeared in 71 cases (58.7%): in 31 of them (25.6%) the intensity of IVC was estimated as distinct (3+), in 21 (17.3%) as moderate (2+), and in 19 (15.7%) as minimal. The distribution of microthrombi in the brain was unequal. Next to areas with pronounced appearance of IVC, numerous regions with no microthrombi were seen. IVC was more frequent in cerebral and cerebellar white matter, hippocampus, and thalamus. In cases with marked brain leukostasis the intensity of IVC was minimal or microthrombi were not found at all.

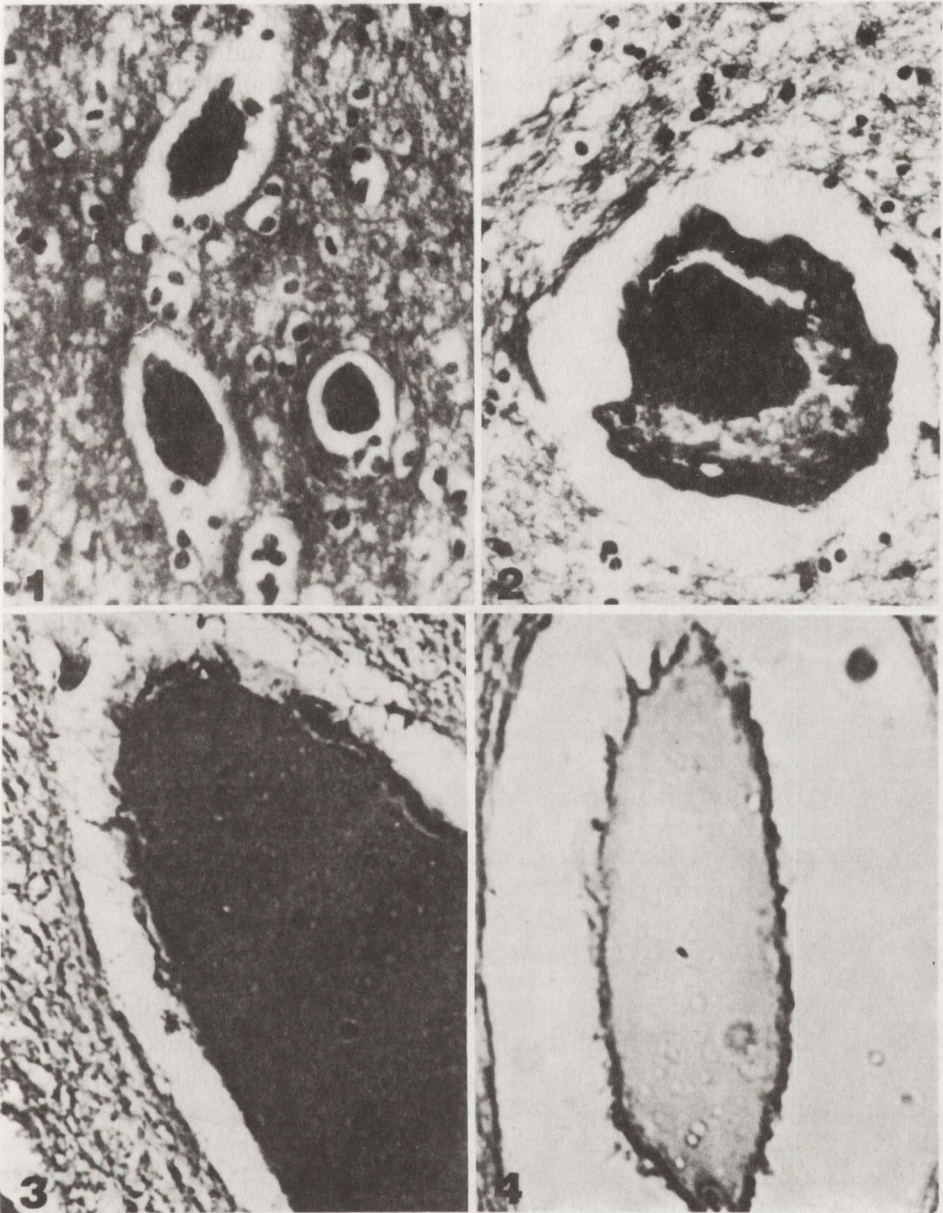


Fig. 1. and 2. Microthrombi within small and medium-size veins. Weigert. $\times 100$

Fig. 3. Microthrombus within a large thin-walled vein. PAS. $\times 240$

Fig. 4. Acid mucopolysaccharides are visible within wall of vein filled with microthrombus. Astra blue. $\times 240$

Chemotherapy and IVC in the CNS

IVC was common in patients who had died within 14 days after chemotherapy had been finished or interrupted (64.1% of cases — group I), less frequently in patients deceased after a period longer than 14 days (53.1%

— group II), and more seldom in patients untreated with chemotherapy (36.4% — group III) (Fig. 5). The difference between groups I and II was statistically nonsignificant. The differences between groups I and III and between groups II and III were statistically significant. IVC was more pronounced in patients treated according to TAD (81.3%) and VAPA (78.5%) protocols than according to AR or COAP schedules (54.5% and 53.8%, respectively); the difference was statistically significant.

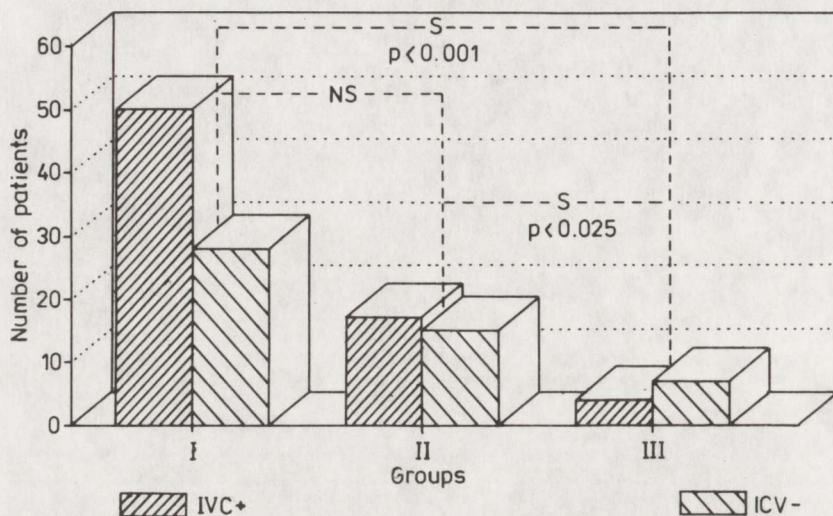


Fig. 5. Chemotherapy and intravascular coagulation (IVC) in the brain. S — statistically significant, NS — non-significant

IVC and CNS-hemorrhages

Neuropathological examinations were performed in 81 cases without or with minimal leukostasis. The remaining 40 cases with marked leukostasis were omitted to avoid the direct effect of blastic cells on the development of CNS hemorrhages. In patients with IVC hemorrhages were much more frequent (56.9%) than in those with no microthrombi (23.3%). (Fig. 6).

Disorders of hemostasis and appearance of IVC in the CNS

Among patients with distinct or moderate IVC in the CNS, the amount of fibrin degradation products was more than three times that in patients with no microthrombi or with their minimal number in the CNS. Platelet count both in patients with and without IVC was clearly low (Tab. 1). Thrombin and prothrombin time as well as fibrinogen level ranged within normal values, whereas partial thromboplastin time was slightly prolonged. The results confirm chronic appearance of IVC.

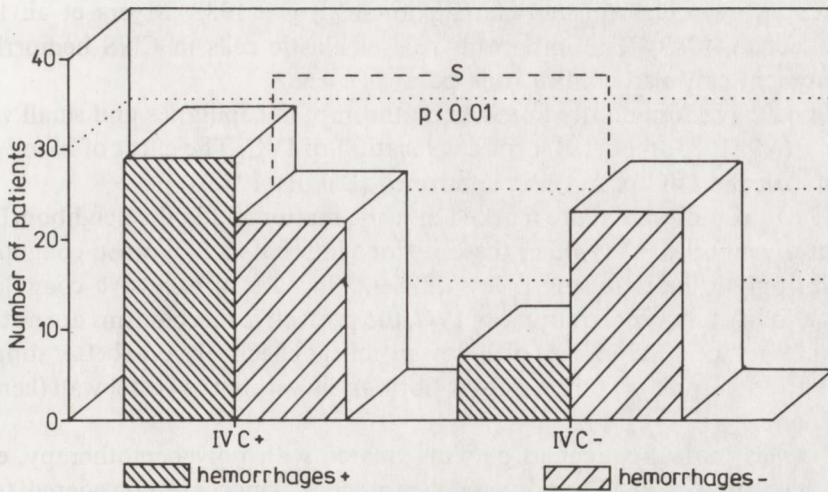


Fig. 6. Intravascular coagulation (IVC) and CNS hemorrhagic changes. S — statistically significant

Table 1. Disorders of hemostasis and IVC in the brain

IVC	FDP 0–10 μ g/ml*	PtC 150–300G/l	Fb 250–400mg%	TT 14–16s	PT 12–16s	PTT 42–64s
+++ or ++	10–120 (44.4)	4–313 (34)	210–453 (337)	10–17 (12.4)	11–21 (16.4)	34–88 (57.6)
+ or 0	5–63 (14.9)	6–230 (35)	110–610 (343)	12–16 (13.6)	15–23 (17.2)	32–87 (52.4)
	p < 0.05	ns	ns	ns	ns	ns

IVC — intravascular coagulation, FDP — fibrinogen degradation products, PtC — platelet count, Fb — fibrinogen, TT — thrombin time, PT — prothrombin time, PTT — partial thromboplastin time.

* norms. In parentheses are means.

DISCUSSION

Microthrombi were observed within the brain in 59% of cases. In 26% of patients IVC was distinct. The number of cases demonstrating IVC should be admitted as large compared with the results of other authors which revealed microthrombi mostly in the lungs, kidneys and liver (Parafiniuk et al. 1977; Collins et al. 1978). The number of microthrombi in the brain may be still larger. It is possible that many microthrombi can undergo postmortem autolysis (Wasutyński 1978). Such clear IVC probably results from the high concentration of procoagulants in the nervous tissue (Keimowitz, Annis 1973). IVC has assumed a chronic appearance. It is worth noting that IVC was minimal or did not appear at all in cases with doubtless leukostasis. It can follow, from what was mentioned above, that leukemic cells, besides their procoagulative properties, are able to

activate intravascular fibrinolysis (Lichtman, Rowe 1982; Myers et al. 1983; Bennett et al. 1989). The important role of blastic cells in CNS hemorrhage development can also confirm this point of view.

We have predominantly found microthrombi in capillaries and small veins. Weller et al. (1983) reported a similar location of IVC. The effect of blood flow velocity on the IVC origin was confirmed (Bakuła 1982).

Microthrombi were more marked in white matter and in the neighbourhood of lateral ventricles. May be in these regions interbalance between coagulative and fibrinolytic mechanisms is less efficient. In case of excessive coagulative activity, for instance in the course of IVC, the protective mechanisms are not able to counteract the development of microthrombi as effectively as in better supplied gray matter, in spite of compensatory fibrinolysis within the vessel wall (heparin activation).

IVC was more frequent in patients treated with polychemotherapy, especially according to TAD and VAPA protocols, which are considered to be more "aggressive" as compared with AR and COAP schedules. It is difficult to explain what is the reason for this. Cytostatics can either destroy the vessel wall by releasing procoagulative substances (Astrup, Buluk 1963) or eliminate the gentle fibrinolytic area located on its inner surface (Nowak 1980). A little more prominent IVC within 14 days after chemotherapy can also be generated by infections following chemotherapy. The effect of chemotherapy on the origin of IVC was also pointed out by others (Drapkin et al. 1978; Capellato et al. 1986).

IVC is considered to be an important factor in the development of CNS hemorrhages in myeloblastic leukemias. The majority of cases with IVC have exhibited brain hemorrhages. We believe that local fibrinolysis, even followed by local IVC within the brain, intensified by thrombocytopenia related to bone marrow infiltrations, may cause CNS hemorrhages. Hyperactive fibrinolysis in the etiopathology of IVC was also stressed by Bomski (1982).

We have not found necrotic changes in the brain involved by IVC, probably due to the fact that microthrombi appeared in the capillaries and small veins rather than in arterial vessels.

CONCLUSIONS

1. Intravascular coagulation in the CNS is a frequent phenomenon in patients with acute myeloblastic leukemias.
2. Polychemotherapy especially according to TAD and VAPA protocols may cause intravascular coagulation in the CNS.
3. Intravascular coagulation seems to be an important risk factor of CNS hemorrhages, irrespective of thrombocytopenia related to bone marrow involvement.

WYKRZEPIANIE WEWNĄTRZNA CZYNIOWE W OŚRODKOWYM UKŁADZIE NERWOWYM U CHORYCH NA OSTRE BIAŁACZKI MIELOBLASTYCZNE

Streszczenie

Autorzy podjęli próbę określenia częstości występowania wykrzepiania wewnątrznaczyniowego (WW) i jego rozmieszczenia w ośrodkowym układzie nerwowym (OUN) u chorych zmarłych z powodu ostrej białaczki mieloblastycznej typu M1 i M2. Ocenę układu krzepnięcia i badania neuropatologiczne przeprowadzono u 121 osób. Badania wykazały obecność mikrozakrzepów w 59% przypadków – w 26% WW było wyraźne. Pozwoliło to na stwierdzenie, że wykrzepianie jest zjawiskiem częstym w OUN u chorych na ostre białaczki mieloblastyczne. Wydaje się, że WW może być wywoływane przez chemioterapię. Spośród badanych schematów leczenia cytostatykami, bardziej sprzyjają występowaniu WW TAD i VAPA (odpowiednio: 81% i 79% leczonych). Wysunięto przypuszczenie, że WW w OUN jest jednym z czynników ryzyka krwotoków mózgowych w ostrych białaczkach mieloblastycznych. Powikłania krwotoczne wystąpiły w 57% przypadków z wykrzepianiem w OUN.

REFERENCES

1. Astrup T, Buluk K: Thromboplastic and fibrinolytic activities in vessels of animals. *Circulation Res*, 1963, 13, 253–260.
2. Bakula S: Zespół wykrzepiania śródnaczyniowego w ostrych zatruciach. *Pol Tyg Lek*, 1988, 37, 1251–1253.
3. Bennett S, Booth A, Croll A, Dawson A: The bleeding disorder in acute promyelocytic leukemia. Fibrinolysis due to u-PA rather than defibrination. *J Haematol*, 1989, 71, 511–517.
4. Bomski H: Test obserwacji skrzepu w rozpoznawaniu ostrego wykrzepiania wewnątrznaczyniowego z hiperfibrinolizą. *Pol Tyg Lek*, 1982, 37, 1411–1414.
5. Capellato M, Rosolen A, Zanesco L, Girolami A: Clotting complications of L-asparaginase therapy in children with ALL. *Blut*, 1986, 52, 377–378.
6. Collins A, Bloomfield C, Peterson B, McKenna B, Edson J: Acute promyelocytic leukemia. Management of the coagulopathy during Daunorubicin-Prednisone remission induction. *Arch Intern Med*, 1978, 138, 1677–1680.
7. De Aquino Jaso M, Portilla Aguilar J, Guiscafröe H, Olivera Hidalgo C: Disseminated intravascular coagulation in children under 1 year of age. *Bol Med Hosp Infant Mex*, 1979, 36, 35–43.
8. Drapkin R, Gee T, Dowling M, Arlin Z, McKenzie S, Kempin S, Clarkson R: Prophylactic heparin therapy in acute promyelocytic leukemia. *Cancer*, 1978, 41, 2484–2490.
9. Hardaway R, Dumke R, Gee T, Meyers T, Joyner J, Graf J, Lee D, Revels J: The danger of hemolysis in shock. *Ann Surg*, 1979, 189, 373–376.
10. Huber A, Cervós-Navarro J: Hemorrhheological changes in traumatized brain tissue. *Clin Neuro-pathol*, 1992, 11, 187.
11. Keimowitz RM, Annis BL: Disseminated intravascular coagulation associated with massive brain injury. *J Neurosurg*, 1973, 39, 178–180.
12. Kozłowski PB: Uszkodzenia okołokomorowej istoty białej mózgu noworodka a zespół wykrzepiania śródnaczyniowego. *Neuropatol Pol*, 1981, 19, 461–472.
13. Kuratowska Z: O produktach rozpadu fibrynogenu (FDP) i hemostazie. *Pol Tyg Lek*, 1984, 39, 349–351.
14. Lichtman M, Rowe J: Hyperleukocytic leukemias. Rheological, clinical and therapeutic considerations. *Blood*, 1982, 60, 279–283.
15. McGauley J, Miller C, Penner J: Diagnosis and treatment of diffuse intravascular coagulation following cerebral trauma. *J Neurosurg*, 1975, 43, 374–384.

16. Myers T, Cole S, Klatsky A, Hild D: Respiratory failure due to pulmonary leukostasis following chemotherapy of acute nonlymphocytic leukemia. *Cancer (Phil)*, 1983, 51, 1808–1813.
17. Nowacki P, Fryze C, Wichert K: Appearance of microthrombi in vessels of central nervous system in the course of disseminated intravascular coagulation syndrome in acute leukemias. *Folia Haematol (Leipzig)*, 1985, 112, 879–885.
18. Nowak E: Udział fibrynolizy w patogenezie śródnaczyniowego odkładania fibryny. Ossolineum, Wrocław, 1980, B series, Nr 204.
19. Parafiniuk W, Januszewski J, Miętkiewski J: Rozsiane wykrzepianie śródnaczyniowe (DIC). *Patol Pol*, 1977, 28, 191–199.
20. Rasche H, Haghout F, Gaus W, Dietrich M, Hoelzer D, Pflieger H, Seifried E, Heimpele H: Blutgerinnungsfactor XIII – Substitution bei akuter Leukämie. *Dtsch med Wschr*, 1982, 107, 1882–1886.
21. Rodeghiero F, Barbuti T, Battista R, Chisesi T, Rigoni G, Dini E: Molecular subunits and transamidase activity of factor XIII in disseminated intravascular coagulation in acute leukemia. *Thrombos Haemost*, 1980, 43 (suppl 1), 1–8.
22. Sakuragawa N, Takahashi K, Hoshijama M, Jimbo C, Matsuoka M: Pathologic cells as procoagulant substance of disseminated intravascular coagulation syndrome in acute promyelocytic leukemia. *Thromb Res*, 1976, 8, 263–273.
23. Sampaolo S, Cervós-Navarro J, Djouchadar D: Clinical and experimental evidence of microthrombosis in cerebral ischemia: In: *Cerebral ischemia and hemorrhology*. Eds: A Hartmann, W Kuschinsky. Springer, Berlin-Heidelberg, 1987.
24. Sanz A, Jarque I, Martin G, Lorenzo I, Martinez J, Rafecas J, Pastor E, Sayas M, Sanz G, Gomis F: Acute promyelocytic leukemia. *Cancer (Phil)*, 1988, 61, 7–13.
25. Shimamura K, Nakazawa M, Kojima M: Distribution pattern of microthrombi in disseminated intravascular coagulation. *Arch Pathol Lab Med*, 1983, 107, 543–549.
26. Sochacka-Kuzko B, Wichert K, Urasiński I: Ostre i przewlekłe wykrzepianie wewnątrznaczyniowe w białaczkach niedojrzałokomórkowych (ostrzych). *Pol Arch Med Wewn*, 1978, 60, 162–167.
27. Wasutyński A: Patomorfologia mikrozatorowości płucnej. *Pol Arch Med Wewn*, 1978, 60, 295–301.
28. Weller R, Swash M, McLellan D, Scholz C: *Clinical Neuropathology*. Springer, Berlin-Heidelberg, 1983.
29. Woitinas F: Hämostasestörungen bei acuten und chronischen Leukämien. *Dtsch med Wschr*, 1991, 116, 1154–1159.

Author's address: Department of Neurology, School of Medicine, 1 Unii Lubelskiej Str., 71-344 Szczecin, Poland

ANDRZEJ KAPUŚCIŃSKI

EFFECT OF CLINICAL DEATH ON INOSITOL 1, 4, 5-TRISPHOSPHATE IN THE RAT BRAIN

Department of Neuropathology, Medical Research Centre, Polish Academy of Sciences, Warsaw

Changes of inositol 1, 4, 5-trisphosphate content in the rat brain have been evaluated by means of the radioimmunologic method during 5-min clinical death and up to 2 hrs after resuscitation. Ischemia produced a decrease of IP_3 content in the brain on the average to 63% of the control values. IP_3 concentration in the brain increased on the average to 197% of the control values at the 15th min after resuscitation, and decreased to 127% at the 60 min. Two hours after resuscitation the IP_3 content in the brain again increased on the average to 187%. The new data on brain metabolism in the ischemic conditions and the role of IP_3 as the second messenger and mediator of neuro-modulation processes are discussed.

Key words: *inositol 1, 4, 5-trisphosphate, ischemia, brain.*

Cyclic nucleotide second messengers (cAMP and cGMP) have been extensively studied and are known to play a key role in the physiology and pathology of many disease states. In recent years our understanding of the mechanisms by which cells respond to extracellular signals has progressed considerably. It is known that hormones, peptide growth factors and neurotransmitters bind to specific receptors on the external cell surface. Occupation of these receptors initiates the signal transduction process which, in turn, leads to the release of second messenger molecules. The identification of second messengers is proving to be of fundamental importance in elucidating how cellular activity is governed. Besides cyclic nucleotides, a new generation of phospho-inositide-derived second messengers have been identified in recent years (Berridge 1984; Berridge, Irvine 1984; Nishizuka 1984).

Receptor stimulation triggers the phospholipase C catalyzed hydrolytic cleavage of membrane phosphatidylinositol 4, 5-bisphosphate (PIP_2) to yield two second messenger molecules, namely, inositol 1, 4, 5-trisphosphate (IP_3) and sn-1, 2-diacylglycerol (DAG). Since then the role of inositol phospholipid hydrolysis in second messenger activation, first proposed by Michell (1975), has received considerable attention. It is now well established that IP_3 acts as a second messenger of Ca^{2+} -mobilizing hormones in a variety of cell types (Berridge, Irvine 1984). DAG, the other product of PIP_2 hydrolysis, seems to be an essential

cofactor for the enzyme protein kinase C (Nishizuka 1984). This enzyme plays a crucial role in signal transduction for a variety of biologically active substances (Berridge 1991).

Recently, specific intracellular receptors for IP_3 have been identified and characterized in a variety of cells and tissues (Guillemette et al. 1987). The identification of these intracellular binding sites for IP_3 has considerably advanced our understanding of the stoichiometric relationship between agonist occupation of a cell-surface receptor, PIP_2 hydrolysis and Ca^{2+} release from intracellular stores by IP_3 . Since its discovery as a second messenger, IP_3 has been implicated in a wide variety of physiological and pathological events.

The aim of the present study was to evaluate the content of IP_3 in the rat brain during clinical death and in the early period after resuscitation.

MATERIAL AND METHODS

Under ether anesthesia 5-min clinical death was induced in 35 adult female rats, weighing 170–180 g, by intrathoracic compression of the cardiac vessels bundle at the base of the heart, with a hook-like device without major surgery (Korpachev et al. 1982). Cardio-pulmonary resuscitation was performed by external cardiac massage and artificial ventilation with air. The animals were sacrificed in groups of five at the end of ischemia and 5, 15, 30, 60 and 120 min after resuscitation. Five animals served as a control group in which under ether anesthesia a sham-operation was performed.

Preparation of brain samples and extraction procedures: brains were removed from the skull in less than 30 s, frozen in liquid nitrogen, and stored at $-70^\circ C$ until analyzed. Brain samples were cut-off, weighed (approximately 100 mg) and IP_3 was extracted with perchloric acid (Ikeda et al. 1986). Brain samples were homogenized in 0.5 ml ice-cold 5% perchloric acid and kept on ice for 20 min. Proteins were sedimented by centrifugation at 2000 g for 15 min at $4^\circ C$. Supernatants were titrated to pH 7.5 with 10 N KOH and kept ice-cold. Precipitated $KClO_4$ was sedimented and removed as above. At this stage, and in all successive procedures siliconized glassware or plasticware was used to minimize losses of phosphorylated inositol species. Due to the highly specific nature of IP_3 assay system, it was possible to measure IP_3 levels in neutralized acid extracts directly without extensive sample purification.

The D-myo-Inositol 1, 4, 5-trisphosphate (3H) assay system (Amersham) was used according to the recommended protocol. The assay involved a 15 min incubation period on ice followed by a centrifugation separation procedure and IP_3 measurement within the range 0.19–25 pmol per tube. All unknown samples were measured in duplicate including standards to construct the standard curve for calculations. Distilled and deionized water was used to dilute the tracer and standard. Radioactivity was measured for 4 min in 2 ml of Bray's scintillant in an LS 5000TA Beckman beta scintillation counter. The results were expressed as means \pm SD and were analysed by Student's t test.

RESULTS

The dynamics of changes of IP₃ concentration in the rat brain in the control group, at the end of 5-min clinical death, and up to two hours after resuscitation is presented in Table 1.

Table 1. Inositol 1, 4, 5-trisphosphate in the rat brain during clinical death and after resuscitation

Control	End of clinical death	Period after resuscitation				
		5 min	15 min	30 min	60 min	120 min
0.278 ± 0.010	0.175 ± 0.013*	0.380 ± 0.022*	0.549 ± 0.027*	0.413 ± 0.034*	0.354 ± 0.027*	0.519 ± 0.033*
100%	62.9%	136.7%	197.4%	148.6%	127%	186.7%

* Values represent means ± S.D. from 5 animals in µmol/g of wet tissue. Significant in reference to control; p < 0.01.

As can be seen in Table 1, in the control sham-operated group the mean level of IP₃ in the brain was 0.278 ± 0.010 µmol/g of wet tissue. At the end of the 5-min clinical death period this level significantly decreased, on the average to 0.175 ± 0.013 µmol/g. In the early period after resuscitation, concentration of IP₃ quickly increased significantly, reaching in 5 min on the average, 0.380 ± 0.022 µmol/g and in 15 min of recovery the maximum of 0.549 ± 0.027 µmol/g. In the later period after resuscitation the level of IP₃ significantly decreased, reaching in 30 min the mean value of 0.413 ± 0.034 µmol/g, and in 60 min the minimum of 0.354 ± 0.027 µmol/g in the recovery period. Two hours after resuscitation the concentration of IP₃ once again significantly increased, reaching the mean value of 0.519 ± 0.033 µmol/g.

DISCUSSION

The obtained results indicated substantial alterations in IP₃ content in the brain during clinical death and after resuscitation. The mean level of IP₃ in the brain in control rats was 0.278 µmol/g which fits the data quoted by other authors as 0.1-0.5 µmol/g (Wikieł 1989). At the end of the 5-min clinical death this level significantly decreased, on the average to 63.0% of the control value. The data quoted by authors analysing changes of phosphatidyl-inositol (PI), polyphosphoinositides (PIP + PIP₂) and IP₃ content in the brain under the influence of ischemia are widely divergent and depend on the experimental model applied and time of ischemia (Ikeda et al. 1986; Strosznajder et al. 1987; Sun, Huang 1987; Wikieł 1989). Analysing IP₃ changes, Strosznajder et al. (1987) and Wikieł (1989) observed in the brain homogenates and in synaptosomes an increase of radioactivity related to IP₃ by about 60% of the control value after 1-min bilateral ligation of the common carotid artery in the gerbil. When extending the time of ischemia up to 10 min, these authors observed a decrease of radioactivity related to IP₃ to about 40% of the control value for homogenates and synaptosomes, and to about 50% for cytosol. Our results are comparable to the observation of

Sun and Huang (1987) who noticed a decrease of IP_3 content in the rat brain after 5 min of complete ischemia. Short lasting ischemia (1 min) triggers phospholipase C hydrolytic degradation of PIP_2 resulting in an increase of IP_3 concentration. Prolongation of ischemia raises the activity of phosphoinositol phosphatases and gives in effect a decrease of IP_3 content (Wikieł 1989). Ten minutes of ischemia produces also a drastic decrease of high-energy compounds, preventing conversion of PI to PIP_2 (Domańska-Janik et al. 1985).

In the accessible literature we found no papers dealing with alterations of IP_3 content in the brain after an ischemic episode, especially after clinical death. Our results showed the biphasic character of changes after resuscitation. In the early period of recovery, concentration of IP_3 in the brain rose significantly and quickly, reaching the peak value of 197% of the control 15 min after resuscitation. Later the content of IP_3 in the brain decreased reaching the lowest postresuscitation level of 127% of the control in 60th minute. Two hours after resuscitation it again significantly increased, reaching on the average 187% of the control value.

The quick and relatively high reversible rise of IP_3 content in the brain in the early postresuscitation period, seems to represent the intensive stimulation of phospholipase C-catalyzed degradation of membrane PIP_2 . In this early postresuscitation period in the same experimental model the following pathophysiological and molecular alterations have been observed: an increase of cerebral blood flow (Kapuściński 1987), an increase of several eicosanoids concentrations (PGF_{2a} , PGD_2 and TXB_2) in the brain as the result of accumulation of arachidonic acid during ischemia (Kapuściński, Hilgier 1989), and a rise of cyclic GMP in the brain (Kapuściński, 1993). Re-establishment of cerebral blood flow restores tissue oxygen and permits intensive degradation of PIP_2 and conversion of arachidonic acid to prostaglandins and leukotrienes. The second phase of increase of IP_3 content in the brain two hours after resuscitation is difficult to explain, however, the relative decrease of cerebral blood flow during this period after resuscitation might be responsible for this phenomenon.

Papers dealing with ischemic changes of the membrane lipids of the central nervous system describe many alterations without extensive explanation of the observed results, because the mechanisms involved are very complex and multidirectional (Strosznajder et al. 1987; Gordon-Majrzak 1987; Wikieł 1989; Berridge 1991). Receptors which act by stimulating inositol lipid hydrolysis generate two intracellular signalling pathways (Berridge 1987). The water-soluble IP_3 , released to the cytosol, functions to mobilize intracellular calcium. IP_3 is metabolized *via* two pathways, either by dephosphorylation ($IP_3 - IP_2 - IP - I$) or on a phosphorylation/dephosphorylation pathway ($IP_3 - IP_4 - IP_3 - IP_2 - IP - I$). The significance of the latter pathway is that IP_4 might function as a messenger to control the entry of external calcium. In addition to these agonist-sensitive pathways there are agonist-insensitive pathways responsible for the formation of IP_5 and IP_6 which may function as neurotransmitters (Vallejo et al. 1987). The DAG which remains within the membrane activates

protein kinase, including inhibition of inositol lipid hydrolysis. Such feedback interactions between second messenger pathways may account for the oscillations in calcium recorded from many different cells.

IP₃ is thought to play a role in both the receptor-controlled and cytoplasmic oscillatory mechanisms which may co-exist in many cells. Such oscillatory activity might form the basis of a novel frequency-dependent intracellular signaling system for controlling a variety of cellular functions (Berridge 1991). A particularly important role is found in the nervous system, where inositol hydrolysis mediates the action of many neuromodulators.

WPLYW ŚMIERCI KLINICZNEJ NA INOZYTOŁO 1, 4, 5-TRÓJFOSFORAN W MÓZGU SZCZURA

Streszczenie

Za pomocą metody radioimmunologicznej oceniono zmiany zawartości inozytołu 1, 4, 5-trójfosforanu w mózgu szczura w trakcie 5-minutowej śmierci klinicznej i w okresie do 2 godzin po resuscytacji. Ischemia powodowała zmniejszenie zawartości IP₃ w mózgu średnio do 63% wartości kontrolnych. W okresie po resuscytacji wystąpił szybki wzrost stężenia IP₃ w mózgu, osiągając w 15 minutach średnio 197% wartości kontrolnych. Stężenie IP₃ zmniejszyło się, średnio do 127% wartości kontrolnych w 60 minutach po resuscytacji, i ponownie wzrosło, średnio do 187% po 2 godzinach. Przedyskutowano najnowsze dane dotyczące metabolizmu IP₃ w niedokrwieniu mózgu, jak również roli IP₃ jako wtórnego przekaźnika i mediatora neuromodulacji.

REFERENCES

1. Berridge MJ: Inositol trisphosphate and diacylglycerol as second messengers. *Biochem J*, 1984, 220, 345–360.
2. Berridge MJ: Inositol trisphosphate and diacylglycerol: two interacting second messengers. *Ann Rev Biochem*, 1987, 56, 159–193.
3. Berridge MJ: Inositol lipids and calcium signalling. Constituent Congress International Society for Pathophysiology. Moscow, May 28-June 1, 1991, abstr p 218.
4. Berridge MJ, Irvine RF: Inositol trisphosphate a novel second messenger in cellular signal transduction. *Nature*, 1984, 312, 315–321.
5. Domanska-Janik K, Łazarewicz J, Norembek K, Strosznajder J, Zalewska T: Metabolic disturbances of synaptosomes isolated from ischemic gerbil brain. *Neurochem Res*, 1985, 10, 573–589.
6. Gordon-Majszak W: Zmiany właściwości biochemicznych zakończeń synaptycznych mózgu pod wpływem wolnorodnikowego utleniania *in vivo* i *in vitro*. Doctor's thesis. Medical Research Centre, Polish Academy of Sciences, Warsaw, 1987.
7. Guillemette G, Balla T, Baukal AJ, Catt KJ: Inositol 1, 4, 5-trisphosphate binds to a specific receptor and releases microsomal calcium in the anterior pituitary gland. *Proc Natl Acad Sci USA*, 1987, 84, 8195–8199.
8. Ikeda M, Yoshida S, Busto R, Santiso M, Ginsberg MD: Polyphosphoinositides as a probable source of brain free fatty acids accumulated at the onset of ischemia. *J Neurochem*, 1986, 47, 123–132.
9. Kapuściński A: Mózgowy przepływ krwi w doświadczalnym modelu śmierci klinicznej u szczurów. *Neuropatol Pol*, 1987, 25, 287–298.
10. Kapuściński A: Cyclic GMP levels in the rat brain and plasma during clinical death and after resuscitation. *Neuropatol Pol*, 1993, 31, in press.

11. Kapuściński A, Hilgier W: Eicosanoids in rat brain and plasma after resuscitation from clinical death. *Neuropatol Pol*, 1989, 27, 519–525.
12. Korpachev GW, Lysenkov SP, Tiel LZ: Modelirovanije klinicheskoj smerti i postreanimacionnoj boleznj u krys. *Patol Fizjol Eksp Ter*, 1982, 3, 78–80.
13. Michell RH: Inositol phospholipids and cell surface receptor function. *Biochem Biophys Acta*, 1975, 415, 81–147.
14. Nishizuka Y: The role of protein kinase C in cell surface signal transduction. *Nature*, 1984, 308, 693–698.
15. Strosznajder J, Wikeł H, Sun GY: Effect of ischemia in polyphosphoinositides in gerbil brain subcellular fraction. *J Neurochem*, 1987, 48, 943–948.
16. Sun GY, Huang S: Labeling of phosphoinositides in rat brain membranes: an assessment of changes due to postdecapitative ischemic treatment. *Neurochem Int*, 1987, 10, 361–369.
17. Vallejo M, Jackson T, Lightman S, Hanley MR: Occurrence and extracellular actions of inositol pentakis and hexakis phosphate in mammalian brain. *Nature*, 1987, 330, 656–658.
18. Wikeł H: Mechanizm degradacji fosfolipidów inozytolowych w niedokrwieniu ośrodkowego układu nerwowego u chomika mongolskiego. Doctor's thesis. Medical Research Centre, Polish Academy of Sciences, Warsaw, 1989.

Author's address: Department of Neuropathology, Medical Research Centre, Polish Academy of Sciences, 3 Dworkowa Str., 00-784 Warszawa, Poland

MARIA DAŃBBSKA¹, IZABELA KUCHNA¹, MARIA WRÓBLEWSKA-KAŁUŻEWSKA²

CEREBRAL INFARCTS IN NEWBORNS AND INFANTS WITH CYANOTIC CARDIAC ANOMALIES

¹ Laboratory of Developmental Neuropathology, Medical Research Centre, Polish Academy of Sciences, Warsaw; ² Clinic of Pediatric Cardiology, School of Medicine, Warsaw

Neuropathological examination of six brains of newborns and infants who died in the course of congenital cyanotic cardiac anomalies showed focal brain lesions. The material included five cases from two weeks to two months of age, and one two-year-old infant. In two of them, the periventricular ischemic infarcts were found, in one multifocal encephalomalacia due to multiple vascular occlusions, and in three the necrotic foci corresponded to the supply of large cerebral arteries. The character and topography of severe brain lesions, particularly within the hemispheric white matter, were clearly influenced by the immaturity of the cerebral structures.

Key words: *cerebral infarcts, cyanotic cardiac anomalies.*

Ischemic focal brain lesions in childhood are very rare. Their incidence and possible causes were recently reviewed by Kapelle et al. (1989). Among them congenital heart diseases are considered as an important cause of cerebral infarcts (Fritsch et al. 1986). It has been observed, that infants with cyanotic heart anomalies are particularly at risk for development of cerebrovascular incidents (Cottrill 1973; Schmaltz et al. 1980; Keck et al. 1981).

The neuropathological examination of brains of the newborn and infants who died in the course of this type of cardiac diseases allowed to characterize and discuss the CNS damage in this group of cases.

MATERIAL AND METHODS

Our material includes five cases, aged from two weeks to two months, and one two-year-old infant. In all of them the cyanotic congenital cardiac anomaly was found (Table 1). None of our patients had a diagnosis of focal neurological deficit. Severe anoxic attacks were observed in cases 3, 5, 6 and respiratory insufficiency requiring the use of respirator occurred in cases 1 and 4. Two infants were without any surgical intervention, one had balloon atrial septostomy *modo* Ruskind and three were operated. In all cases hypoxia and acidosis were clinically evident. Postmortem examination confirmed the diagnosis of cardiac anomalies.

Table 1. Clinical and neuropathological data

Case/Age	Clinico-pathological data	Neuropathology
1 12/90 12 days	transposition of the great arteries (TGA). Atrioseptostomia m. Ruskinda	old and recent periventricular infarcts. Disseminated neuronal damage
2 11/90 16 days	truncus arteriosus communis type IV. Single ventricle	periventricular infarcts recent and with advanced organization. Hyperemia
3 37/91 2 months	tetralogy of Fallot with complete atrioventricular canal. Anastomosis Blalock-Taussig	recent and older foci of multifocal necrosis
4 51/90 6 weeks	tricuspid atresia. Anastomosis m. Waterston	softening in region of right middle cerebral artery supply
5 33/91 2 months	tetralogy of Fallot	softening in region of left middle cerebral artery supply
6 30/91 2 years	tetralogy of Fallot. Anastomosis Blalock-Taussig	encephalomalacia in left occipital lobe

Neuropathological examination was performed on routine sections from cerebral hemispheres, cerebellum and brain stem. Hematoxylin-cosin (HE) and cresyl violet staining were used and immunohistochemical reaction for detection of glial fibrillary acidic proteins (GFAP) was applied.

RESULTS

In all the examined cases smaller or larger foci of tissue necrosis were found.

In cases 1 and 2 several ischemic infarcts in the periventricular white matter at frontal, parietal and in case 2 even temporal level were observed. All of them presented focal coagulative necrosis at different stages of tissue damage and reparative processes. More recent necroses dominated in case 1 (Fig. 1), and well organized post-infarction scars, containing several vessels and proliferating glial cells were numerous in case 2 (Fig. 2). GFAP-positive cells were seen on the border of necrotic changes. In both cases the gray structures were mostly spared.

In the 3rd case the changes appeared as bilateral multifocal encephalomalacia. The focal lesions were recent and older, located mainly in the white matter but also in the cerebral and cerebellar cortex. Some of the older lesions resulted in the formation of mostly periventricular cavities. Between them the GFAP-positive reaction was seen (Fig. 3). Thrombotic changes were found in some meningeal arteries and veins. Generalized hyperemia in the above described cases 1-3 resulted in extravasations into some necrotic foci. A well delineated vascular malformation of teleclastic type in case 3 in the cerebellum was an additional finding.

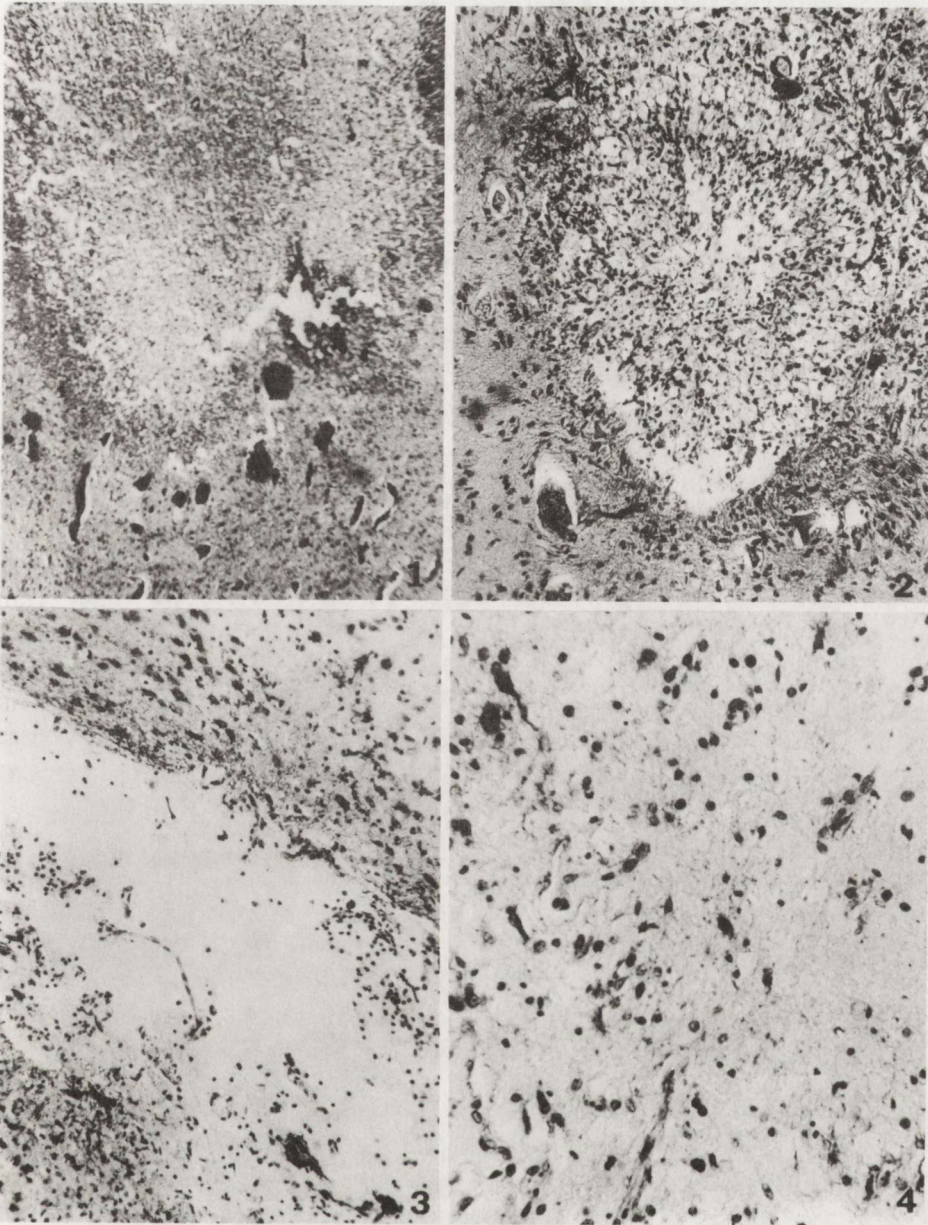


Fig. 1. Case 1. Focus of recent periventricular coagulative necrosis. HE. $\times 60$

Fig. 2. Case 2. Well organized post-infarction scar. HE. $\times 60$

Fig. 3. Case 3. Astroglial proliferation on the border of a cavity within the white matter. GFAP. $\times 100$

Fig. 4. Case 4. Subtotal cortical necrosis with vascular proliferation. Cresyl violet. $\times 200$

The other three cases (4, 5, 6) presented more extensive lesions in the form of encephalomalatia in the territory of the middle cerebral artery supply (cases 4, 5) or vascularized by branches of posterior cerebral artery (case 6). In all of them

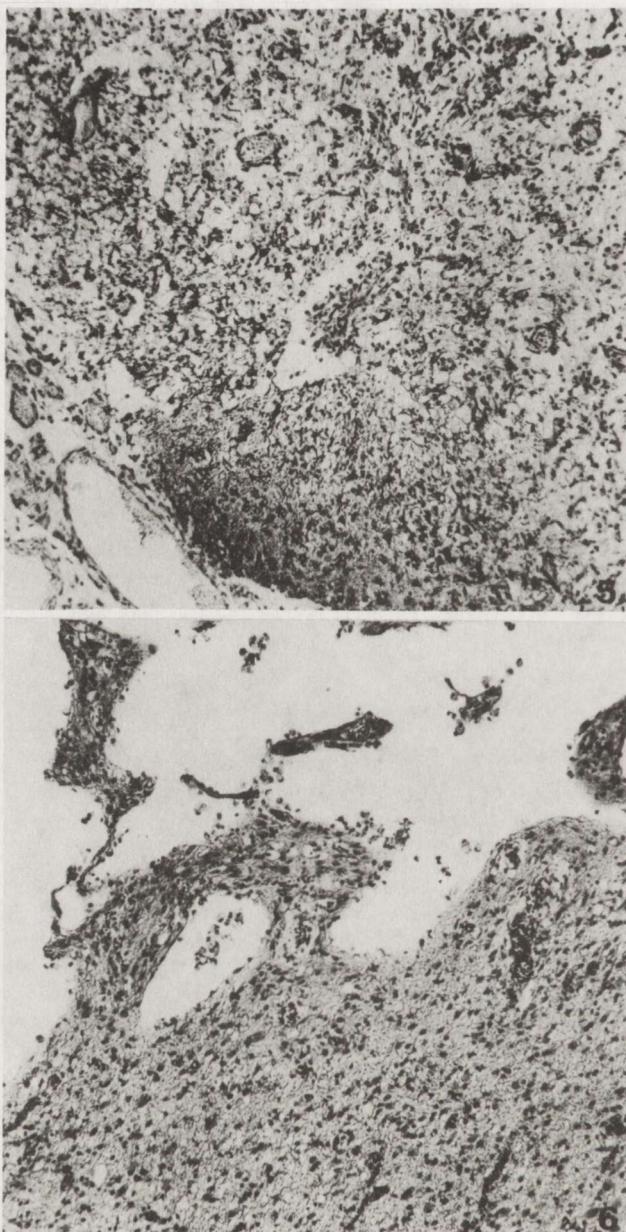


Fig. 5. Case 4. GFAP-positive cells penetrating the necrotic cortex. $\times 100$

Fig. 6. Case 6. The border of an old post-necrotic cavity. HE. $\times 100$

the white matter was severely destroyed leading to formation of large cavities. Only some vessels penetrated into disintegrated tissue where a moderate number of macrophages was disseminated. The cortex was irreversibly damaged (Fig. 4) in several segments, but an abundant network of vessels and a great number of

macrophages demarcated the cortical strip. In the large segment with only partial cortical damage the GFAP-positive cells were abundant (Fig. 5). They were particularly hypertrophied within the subpial glial membranes. The GFAP-positive astrocytes also penetrated into the necrotic areas forming a network on the border of large cavities.

In case 6, the oldest one in our cohort, the postnecrotic cavity in the occipital lobe was outlined by particularly hypertrophied astrocytes (Fig. 6).

DISCUSSION

The findings in our group of cases illustrate well the tendency to cerebral focal lesions during the first months of life in the course of congenital cyanotic heart anomalies (Schmaltz et al. 1980). One of our infants (case 1) had atrioseptostomia and three others surgical interventions. This confirms that cerebral complications occur in both surgical and non surgical cases (Cohen 1960; Terplan 1973).

The cerebral changes in all of them revealed some agedependent features. In cases 1 and 2 the lesions correspond to the picture of periventricular ischemic infarcts, known in perinatal brain pathology. Banker and Larroche (1962) found that severe perinatal anoxia requiring resuscitation is their principal clinical cause. Friede (1989) suggested that the periventricular tissue may be sensitive to impairment of perfusion. Recent and older foci of coagulative necrosis in our cases indicate that the periventricular infarcts could exhibit one of the possible types of brain lesions in the newborn with cyanotic cardiac anomaly.

The 3rd case with multifocal infarctions suggested multiple and repetitive vascular occlusions. Thrombotic changes in some cerebral vessels were often observed in similar cases. Berthrang and Sabiston (1951) found occlusive changes in veins more often. Terplan (1973) considered arterial changes as most frequent and Schmaltz et al. (1980) estimated thromboemboli as occurring equally often in both types of vessels. In our case we could only state that the changes were observed in arteries as well as in veins within the meninges.

In the other three cases (4, 5, 6), the topography of lesions suggested occlusion of larger vessels — twice of the middle cerebral artery and once of the branches of the posterior cerebral artery. The large necrotic foci showed some particular features connected with immaturity of the nervous tissue. Unmyelinated white matter containing only scarce and immature elements (fibers and glial cells) disappeared very rapidly leading to the formation of large cavities. The astroglial cells outlined the walls of such cavities. Total lack of perivascular symptomatic infiltrations due to immunologic immaturity of small infants is a very well known fact, thus it may be only briefly mentioned. Finally, we could shortly point out that the vascular malformation found in our 3rd case is observed relatively often as coexisting with cyanotic cardiac diseases (Cohen 1960).

In conclusion, we may say that immaturity of cerebral structures influences the character and topography of extensive brain lesions in the course of cyanotic cardiac anomalies.

ZAWAŁY MÓZGOWE U NOWORODKÓW I DZIECI Z SINICZYMI WADAMI SERCA

Streszczenie

Badanie neuropatologiczne mózgu sześciu noworodków i małych dzieci, które zmarły w przebiegu sinicznych wad serca, wykazało ogniskowe uszkodzenia. W grupie tej było 5 przypadków w wieku od 2 tygodni do 2 lat życia i jedno dziecko dwuletnie. W dwu przypadkach stwierdzono okołokomorowe zawały niedokrwienne, w jednym wieloogniskowe rozmiękanie wywołane zamknięciem licznych naczyń, w trzech zmiany martwicze odpowiadały zakresowi unaczynienia dużych tętnic mózgowych. Struktura i topografia ciężkich uszkodzeń mózgu, zwłaszcza w obrębie istoty białej, były zależne od niedojrzałości ośrodkowego układu nerwowego.

REFERENCES

1. Banker BQ, Larroche J: Periventricular leucomalacia in infancy. *Arch Neurol*, 1962, 7, 386–410.
2. Berthrang M, Sabiston D: Cerebral lesions in congenital heart disease. *Bull Hopkins Hosp*, 1951, 89, 384–401.
3. Cohen MM: The central nervous system in congenital heart disease. *Neurology*, 1960, 10, 452–456.
4. Cottrill CM, Kaplan S: Cerebral vascular accidents in cyanotic congenital heart disease. *Am J Dis Child*, 1973, 125, 484–487.
5. Friede RL: *Developmental Neuropathology*. Springer Berlin, Heidelberg-N.York-London-Toronto, 1989, 125, 484–487.
6. Fritsch G, Ladurner G, Schneider G: Zerebrovaskuläre Krankheiten im Kindesalter-Ätiologie, Klinik und Prognose. *Fortschr Neurol Psychiatr*, 1986, 54, 47–53.
7. Kappelle LJ, Willemsse J, Ramos LMP, van Gijn J: Ischaemic stroke in the basal ganglia and internal capsule in childhood. *Brain Dev*, 1989, 11, 283–292.
8. Keck EW, Kimm E, Gravinghoff L, Sieg K, Lagenstein I, Kuhne D: Neurologische Veränderungen und cerebrale Läsionen bei Kindern mit Transposition der grossen Arterien (TGA). *Monatsschr Kinderheilkd*, 1981, 129, 45–47.
9. Schmaltz AA, Siegler P, Nolte R, Apitz J: Neurologische Komplikationen bei Kindern mit zyanotischen Herzfehlern. *Monatsschr Kinderheilkd*, 1980, 128, 606–610.
10. Terplan K. L.: Patterns of brain damage in infants and children with congenital heart disease. *Am J Dis Child*, 1973, 125, 175–185.
11. Schmaltz AA, Siegler P, Nolte R, Apitz J: Neurologische Komplikationen bei Kindern mit zyanotischen Herzfehlern. *Monatsschr Kinderheilkd*, 1980, 128, 606–610.

Author's address: Laboratory of Developmental Neuropathology, Medical Research Centre, Polish Academy of Sciences, 3 Pasteura Str, 02-093 Warsaw, Poland

Zakład Narodowy im. Ossolińskich. Wydawnictwo. Wrocław 1994 r.
Objętość: ark. wyd. 7,40, ark. druk. 6,50, w. A₁- 9.
Druk i oprawa: Drukarnia Uniwersytetu Wrocławskiego

<http://rcin.org.pl>

WYDAWNICTWO OSSOLINEUM

Rynek 9, 50-106 Wrocław
Tel. 386-25 Telex 0712771 oss pl Fax 44-81-03

**Najkorzystniejsze ceny i najbogatsza oferta
w placówkach własnych Wydawnictwa Ossolineum:**

Księgarnie

80-855 GDAŃSK, ul. Łągiewniki 56, tel. 314-122 (książki); 315-133 (muzykalia)
44-100 GLIWICE, ul. Zwycięstwa 37, tel. 382-511
31-018 KRAKÓW, ul. Św. Marka 12, tel. 225-844 (wejście od ul. Sławkowskiej 17)
90-447 ŁÓDŹ, ul. Piotrkowska 181, tel. 361-943
61-745 POZNAŃ, ul. K. Marcinkowskiego 30, tel. 521-916
70-551 SZCZECIN, pl. Żołnierza Polskiego 1, tel. 88-565
00-634 WARSZAWA, ul. Jaworzyńska 4, tel. 254-366
50-106 WROCLAW, Rynek 6, tel. 336-66

Księgarnia wysyłkowa

50-106 WROCLAW, Rynek 6, tel. 336-66

Hurtownia

50-227 WROCLAW, ul. Kleczkowska 44, tel. 214-861

Sprzedaż hurtową prowadzą również księgarnie w Gdańsku, Gliwicach, Krakowie, Łodzi, Poznaniu, Szczecinie i Warszawie.

Zapraszamy do współpracy księgarzy, agencje kolporterskie i odbiorców indywidualnych. Hurtownicy i księgarze handlowe ilości książek mogą kupić bezpośrednio od Wydawnictwa. Odbiór książek następuje transportem własnym, a także transportem Wydawnictwa lub pocztą na koszt odbiorcy. Rozliczenie należności — gotówką, przelewem lub przekazem telegraficznym na nasze konto:

**Wielkopolski Bank Kredytowy S.A. w Poznaniu, Oddział we Wrocławiu
nr 359209-1078**

Pełny asortyment wydawnictw ossolińskich oferują też księgarnie
Ośrodka Rozpowszechniania Wydawnictw Naukowych PAN:

15-082 BIAŁYSTOK, ul. Świętojańska 13
40-077 KATOWICE, ul. Bankowa 14, pawilon D, I piętro
31-020 KRAKÓW, ul. Św. Marka 22
20-031 LUBLIN, pl. M. Curie-Skłodowskiej 5
61-725 POZNAŃ, ul. S. Mielżyńskiego 27/29
00-901 WARSZAWA, Pałac Kultury i Nauki

CONTENTS

P. P. Liberski, R. Yanagihara, G. A. H. Wells, D. C. Gajdusek: Bovine spongiform encephalopathy in cattle mimics ultrastructurally experimental scrapie and Creutzfeldt-Jakob disease in rodents	1
M. Wender, J. Szczech, S. Hoffmann: Analysis of heavy metals content in the brain with the use of electron paramagnetic resonance in a clinically unusual case of hepato-lenticular degeneration	17
H. Mierzewska-Rzeszot: Adrenal medulla grafts into the rat striatum — an evaluation of survival and dynamics of the host brain response	25
E. Matyja, E. Kida: Verapamil reduces quinolinic acid-induced neuronal damage in rat hippocampus <i>in vitro</i>	37
J. Rafałowska, D. Dziewulska, Z. Jamrozik: Rare coexistence of congenital malformations in adult	45
H. Drac, J. Pniewski, J. Rafałowska: Morphological changes in the peripheral nervous system in the case of congenital malformations of the spinal cord	55
R. Kida, M. Barcikowska, E. Joachimowicz, T. Michalska, A. Siekierzyńska, A. Walasik, K. Roszkowski, E. Figura: Paraneoplastic subacute sensory neuronopathy. Clinical-pathological study	63
H. Kroh, J. Bidziński: Glial differentiation in medulloblastoma. Case report	75
P. Nowacki, B. Zdziarska: Intravascular coagulation in the central nervous system in patients with acute myeloblastic leukemias	83
A. Kapuściński: Effect of clinical death on inositol 1, 4, 5-trisphosphate in the rat brain	91
M. Dąbska, I. Kuchna, M. Wróblewska-Kałużewska: Cerebral infarcts in newborns and infants with cyanotic cardiac anomalies	97